Diss. ETH No. 21621

The impact of climate change on groundwater temperature and oxygen concentration in Swiss aquifers

A thesis submitted to attain the degree of

DOCTOR OF SCIENCES of ETH ZURICH
(Dr. sc. ETH Zurich)

presented by
SIMON FIGURA

MSc in Statistics, ETH Zurich
born 26.09.1984
citizen of Hochfelden/ZH

accepted on the recommendation of:

Prof. Dr. Rolf Kipfer, examiner
Dr. David M. Livingstone, co-examiner
Prof. Dr. Bernhard Wehrli, co-examiner
Prof. Dr. Masaki Hayashi, co-examiner

2013

Danksagung

An erster Stelle möchte ich mich bei meiner Freundin *Mirjam* bedanken. Obwohl man eine Freundin während der Dissertation durchaus mal als zeitfressenden Störfaktor betrachten könnte, war *Mirjam* wahrscheinlich der Grund, dass ich während den vergangenen Jahren ein einigermassen soziales Wesen geblieben bin. Ausserdem hat sie mich zusammen mit meiner *Familie*, welcher ich an dieser Stelle auch herzlich danken möchte, bei meinem Entschluss, eine Diss zu machen unterstützt. Meine *Familie* hat mich auch während der Disszeit immer unterstützt, auch wenn ich nie genau erklären konnte, was ich den ganzen Tag so mache.

Bei meinen Betreuern *RoKi* und *David* möchte ich mich dafür bedanken, dass sie mir überhaupt ermöglicht haben, eine Diss zu machen, mich bei Allem immer tatkräftig unterstützt haben (ein spezielles Dankeschön an dieser Stelle an *David* für seine Korrekturarbeiten an meinen Texten) und mich, sei es in Edinburgh, Calgary oder Berlin, bei vielen Gelegenheiten gastfreundlich aufgenommen haben. Einfach war die Zusammenarbeit nicht immer. Manchmal stiessen *RoKis* überbordender Optimismus und *Davids* nüchterne Skepsis den jungen, sensiblen Autor in einen Strudel der Unentschlossenheit. Andere Male kujonierten mich die beiden mit Zynismus oder wortklauberischer Spitzfindigkeit bei der Formulierung von Texten. Doch das waren nur Episoden, und so lassen die Warmherzigkeit und Fairness von *RoKi* und *David* die positiven Gefühle klar überwiegen.

Ich möchte mich auch bei den aktuellen und vergangen Mitgliedern der *ui-Gruppe* bedanken. *Nadias* Fröhlichkeit war ansteckend und sie hat meinen Klagen und Magengeräuschen immer ein offenes Ohr geliehen. *Yamas* penible Organisation war mir ein Vorbild und sein Fachwissen bei Wein und Kaffee garantierte für die Qualitätssicherung dieser beiden während einer Diss so wichtigen Suchtmittel. *Matthias'* beruhigende Worte, wenn ich meinte das Edelgaslabor würde wegen mir in die Luft fliegen waren immer hilfreich. Seine Sucht nach Zucker beunruhigt mich aber, für eine Schwarzwälder Torte hatte er in der Kanalisation von Zürich sogar mal einen Vertreter der taxonomischen Familie der Ranidae geküsst. *Lina* möchte ich danken, weil sie mit ihrer Unbekümmertheit ein lebendes Beispiel ist, dass am Ende doch alles gut kommt. Auch hat sie mir die Vorzüge einer Bootsfahrt mit einem ratternden Stromgenerator an Bord nähergebracht. Mit ihrem gemeinsamen Abschluss vor einem Jahr haben mir *Ryan*, *Stephan* und *Lars* zwar in dreifacher Dosis vor Augen gehalten, dass ich zu diesem Zeitpunkt mit meiner Diss noch lange nicht fertig war. Ich bin aber auch froh, dass mir niemand anders die Zeit

Summary

Groundwater is an important drinking water resource in Switzerland and throughout the world. Despite the importance of groundwater, research on the impact of climate change on groundwater has attracted interest only recently. However, most of the research studies on this topic have focused on the potential impact of a changing climate on groundwater quantity rather than quality. The basic research task of this thesis was to determine past and future impacts of climatic forcing and climate change on some aspects of groundwater quality in Switzerland. To accomplish this task, time-series of historical records measured in the groundwater of several Swiss aquifers were analyzed. The best available data with regard to length and temporal resolution consisted of time-series of groundwater temperature and groundwater dissolved oxygen (DO) concentration in aquifers recharged by riverbank infiltration (RBF). Both groundwater temperature and DO concentration are important determinants of groundwater quality, in particular at RBF sites. The time-series were used to analyze the impact of the 1980s climate regime shift on groundwater temperature, to build models which enabled forecasts of groundwater temperature up to the end of the current century to be modeled, and to estimate the impact of a changing climate on groundwater DO concentration.

To investigate the impact of climate variability on groundwater temperature in five aquifers recharged by RBF, the impact of the late 1980s climate regime shift on groundwater temperature was revealed using three statistical methods. The late 1980s climate regime shift is associated with a shift in the Arctic Oscillation to a strong positive phase. This shift led to an abrupt, strong increase in air and river-water temperatures in Switzerland in spring and summer from 1987 to 1988. In groundwater, the temperature increase was found in all seasons because the climate signal was damped and delayed. Although the size of the abrupt temperature shift as well as the behavior of groundwater temperature after the late 1980s climate regime shift were not homogeneous from aquifer to aquifer, the study confirmed that groundwater temperature at RBF sites responds strongly to large-scale climatic phenomena.

Forecasts of groundwater temperature, which were calculated using two linear regression models for seven Swiss aquifers, indicated that groundwater in aquifers recharged by RBF is likely to undergo substantial warming by the end of the current century. Depending on the greenhouse-gas emissions scenario employed, groundwater at these sites is predicted to warm by 1 to 3.5 K with respect to the reference period 1980-2009. For aquifers which are not

recharged by RBF but by the percolation of precipitation only, the models predicted a maximum increase of 1 K but the performance of the models was comparatively poor. With regard to these aquifers, however, the time-series used as training data for the calibration of the regression models started later and were therefore shorter than those available from the RBF sites. Because the model performance depends strongly on the training data, it is not clear whether the poor performance of the linear regression models and the small predicted increase for aquifers recharged by the percolation of precipitation resulted from a weak response to climatic forcing or from the inadequate length of the training data set.

The strong warming of groundwater and river water observed in the past probably led to an increase in microbial respiration and reduced oxygen solubility, resulting in multi-annual periods of decreasing groundwater DO concentration at the five RBF sites analyzed. By contrast, the DO concentration also underwent some large, abrupt increases, which were caused presumably by strong changes in local hydrological conditions related to river discharge, groundwater pumping rates or riverbed clogging. Taking into account these findings and the groundwater temperature projections, it can be concluded that groundwater DO concentrations at RBF sites will undergo a further decrease in the future, but that the occasional occurrence of strong changes in hydrological conditions will result in increases in DO concentration that will prevent the groundwater from turning permanently anoxic.

The main conclusions of this thesis are that climate change will affect groundwater temperature and DO concentration at RBF sites, and that this will have negative consequences for groundwater quality. These consequences will not be so grave as to render groundwater from these sites unusable as a source of raw drinking water; nevertheless, under certain conditions groundwater quality in aquifers recharged by RBF is likely to be reduced periodically, making it necessary to take counter-measures. To further examine the impacts of climate change on groundwater quality at Swiss RBF sites, further co-ordinated research and long-term monitoring will be necessary.

Zusammenfassung

Grundwasser ist weltweit und insbesondere in der Schweiz eine wichtige Trinkwasserressource. Ungeachtet dessen wurde erst in letzter Zeit damit begonnen, mögliche Einflüsse des Klimawandels auf das Grundwasser wissenschaftlich zu untersuchen. Die meisten Studien haben dabei lediglich den Einfluss des Klimawandels auf die Verfügbarkeit des Grundwassers untersucht, während der Einfluss auf die Qualität nur marginal behandelt wurde. Das Hauptziel der vorliegenden Arbeit war es, vergangene und zukünftige, durch den Klimawandel verursachte Einflüsse auf die Grundwasserqualität in der Schweiz zu beurteilen. Zu diesem Zweck wurde auf historische Aufzeichnungen zurückgegriffen, die in verschiedenen Aquiferen der Schweiz gemacht wurden. Die bezüglich Länge und zeitlicher Auflösung besten Daten sind Zeitreihen von Temperatur und Sauerstoffkonzentration im Grundwasser von Aquiferen, die vornehmlich von Flüssen gespeist werden. Sowohl die Temperatur als auch die Sauerstoffkonzentration sind wichtige Kenngrössen für die Grundwasserqualität. Die Zeitreihen wurden verwendet, um den Einfluss des abrupten Klimasprungs Ende der 1980er-Jahre auf die Grundwassertemperatur nachzuweisen, um mit statistischen Modellen die Grundwassertemperatur bis zum Ende des Jahrhunderts vorherzusagen, sowie um den Einfluss der Klimaänderung auf die Sauerstoffkonzentration im Grundwasser abzuschätzen.

Mittels drei statistischen Methoden wurde der Klimasprung Ende der 1980er-Jahre (die sprunghafte Änderung des Klimas auf der Nordhemisphäre Ende der 1980er-Jahre) in der Grundwassertemperatur nachgewiesen. Der Klimasprung Ende der 1980er-Jahre wird mit einem Wechsel zu einer stark positiven Phase im Index der Arktischen Oszillation assoziiert und führte in der Schweiz zu einem abrupten und starken Anstieg der Lufttemperatur und der Flusswassertemperaturen im Frühling und Sommer zwischen 1987 und 1988. Im Grundwasser wurde dieser Temperaturanstieg in allen Jahreszeiten beobachtet, weil das atmosphärische Signal nur gedämpft und zeitlich verschoben ins Grundwasser eindringt. Ausserdem wurde festgestellt, dass sich die einzelnen Aquifere bezüglich des Ausmasses des Temperaturanstieges und des Verhaltens der Grundwassertemperatur nach dem sprungartigen Anstieg der Lufttemperatur unterscheiden. Nichtsdestotrotz belegt die Studie, dass die Grundwassertemperatur in flussgespeisten Aquiferen stark auf grossräumige Klimaschwankungen, in diesem Fall die atmosphärische Zirkulation im Nordatlantik, reagiert.

Mit zwei linearen Regressionsmodellen wurde die Grundwassertemperatur für sieben Aquifere basierend auf Klimaprognosen für die Schweiz vorhergesagt. Die Vorhersagen zeigen, dass in flussgespeisten Aquiferen mit einem starken Anstieg der Grundwassertemperatur bis zum Ende dieses Jahrhunderts zu rechnen ist. Abhängig vom zugrundeliegenden Emissionsszenario für Treibhausgase wird sich die Temperatur in diesen Aquiferen im Vergleich zur Referenzperiode 1980-2009 um 1 bis 3.5 K erwärmen. Für Aquifere, die ausschliesslich durch Niederschlag und nicht von Flüssen gespeist werden, beträgt die Erwärmung maximal 1 K. Allerdings zeigte sich, dass die Länge der Zeitreihen, die für die Kalibrierung der Grundwassertemperaturmodelle verwendet wurden, die Güte der Modellierung beeinflusst. Bei den niederschlagsgespeisten Aquiferen beginnen die zur Kalibrierung verwendeten Temperaturzeitreihen erst 1989. Somit sind sie deutlich kürzer als die Zeitreihen, die für die flussgespeisten Aquifere verwendet werden konnten. Entsprechend lassen sich für die kleine vorhergesagte Erwärmung niederschlagsgespeister Aquifere zwei mögliche Erklärungen finden. Entweder verhindern die kurzen Zeitreihen bei niederschlagsgespeisten Aquiferen eine gute Modellierung der Temperatur oder die Grundwassertemperatur niederschlagsgespeister Aquifere reagiert schwach auf atmosphärische Bedingungen.

Die Auswertung der Sauerstoffkonzentration im Grundwasser von fünf flussgespeisten Aquiferen ergab, dass die Sauerstoffkonzentration in diesen Aquiferen über Zeiträume von mehreren Jahrzehnten kontinuierlich zurückgegangen ist. Dieser Rückgang der Sauerstoffkonzentration war vermutlich eine Folge der erhöhten Grundwassertemperaturen, die die Sauerstofflöslichkeit im Grundwasser verringerten und einen Anstieg der mikrobiellen Aktivität verursachten. Der Rückgang der Sauerstoffkonzentration im Grundwasser wurde aber an fast allen Standorten durch starke, abrupte Anstiege der Sauerstoffkonzentration unterbrochen. Die Anstiege traten infolge hoher Abflussmengen der Flüsse, hoher Grundwasserpumpmengen und einzelner Hochwasserereignisse auf. Diese extremen hydrologischen Ereignisse erhöhten den Eintrag sauerstoffreichen Flusswassers ins Grundwasser und führten zu den beobachteten Anstiegen der Sauerstoffkonzentration. Die Erkenntnisse dieser Studie lassen vermuten, dass die Sauerstoffkonzentration im Grundwasser von flussgespeisten Aquiferen durch die zukünftige Zunahme der Grundwassertemperaturen weiter abnehmen wird. Diese Abnahme wird aber durch Hochwasserereignisse, mit welchen in Zukunft wahrscheinlich vermehrt zu rechnen ist, unterbrochen werden. Permanent anoxische Bedingungen im Grundwasser werden dadurch verhindert werden.

Die zentrale Schlussfolgerung dieser Arbeit ist, dass der Klimawandel die Temperatur und Sauerstoffkonzentration im Grundwasser von flussgespeisten Aquiferen stark beeinflussen wird. Dies wird Auswirkungen auf die Grundwasserqualität nach sich ziehen, die jedoch nicht so gravierend sein werden, dass das Grundwasser von solchen Standorten nicht mehr für die Trinkwasserproduktion herangezogen werden kann. Allerdings muss bei flussgespeisten Aquiferen in Zukunft vermehrt damit gerechnet werden, dass die Grundwasserqualität während kurzen Perioden beeinträchtigt sein wird. Entsprechend sind dann Massnahmen zu treffen, um die Trinkwasserversorgung sicherzustellen, z. B. die Aufbereitung des gepumpten Grundwassers oder die Beschaffung von Grundwasser von anderen Standorten. Um mögliche Auswirkungen des Klimawandels auf die Grundwasserqualität in flussgespeisten Aquiferen weitergehend zu untersuchen, ist eine Koordination weiterer Forschungstätigkeiten mit kontinuierlichen, langfristigen Beobachtungen zwingend notwendig.

Contents

<div align="right">

1

</div>

Introduction

1.1 Introduction and scope of the work

Groundwater accounts for approximately 50% of the world's drinking-water production (Connor et al., 2009) and an even higher proportion – fully 80% – in Switzerland (Tripet, 2005; SVGW, 2008). Current knowledge of the effects of climatic forcing on groundwater suggests that groundwater will potentially be affected strongly by climate change (Bates et al., 2008; Green et al., 2011; Taylor et al., 2013). However, despite the importance of groundwater as a vital resource, Kundzewicz et al. (2007) noted in the 4th report of the Intergovernmental Panel on Climate Change (IPCC) that "There has been very little research on the impact of climate change on groundwater, including the question of how climate change will affect the relationship between surface waters and aquifers that are hydraulically connected." Furthermore, Kundzewicz et al. (2007) found that it was not possible to distinguish between anthropogenic and climate-induced impacts on groundwater because of a lack of relevant long-term data. In recent years, the number of published scientific studies on groundwater and climate change has been increasing (Green et al., 2011), but most of these studies have focused on processes affecting groundwater quantity (i.e., recharge, discharge, flow). With respect to groundwater quality, which will also be affected by climate change, there is still a large knowledge gap, which is again due largely to a lack of relevant long-term data (Aureli and Taniguchi, 2006; Dragoni and Sukhija, 2008; Green et al., 2011).

The central goal of the work at hand was to determine the potential impact of climate change on groundwater quality in Switzerland through the use of long-term historical data that were collected in the run-up to this thesis by a transdisciplinary working group set up jointly by the Swiss Federal Institute of Aquatic Science and Technology (Eawag), the Swiss Federal Office for the Environment, and the Swiss Hydrogeological Society (Schürch, 2011). To be considered for this study, the data were required to cover a period of at least 20 years with a resolution of at least one measurement per month. Moreover, to be able to focus on the climatic impact only, data from urban areas or from aquifers subject to direct anthropogenic intervention (e.g., heat pump operation, building construction, changes in river or groundwater management) were excluded. Most of the data were obtained from drinking-water suppliers and thus consisted of measurements made in groundwater pumping wells or spring captures.

Because of the crucial importance of groundwater for drinking-water production, groundwater quality is often defined in terms of the standards applied to drinking-water. In most cases, these standards apply to a large number of physico-chemical variables (Bouwer, 1978; FOPH, 2003). This work, though, focuses only on the impacts of climate change on groundwater temperature and dissolved oxygen (DO) concentration, both of which are highly relevant to groundwater quality. The restriction of the scope of this study to these two variables was a practical consequence of the lack of availability of other relevant data. The time-series of groundwater temperature and DO concentration were the most common and the quality of these time-series with respect to length and temporal resolution was best (Figura, 2009). The relevance of groundwater temperature and DO concentration for groundwater quality and the potential effects of climatic forcing and climate change on these two variables are outlined in Chapter 2. High-quality temperature and DO concentration data were available primarily from pumping wells in aquifers that are recharged by riverbank infiltration (RBF). The results of this work are thus mainly limited to RBF sites, but are nevertheless of high practical relevance because of the great importance of aquifers recharged by RBF for the production of drinking-water in Switzerland (Tripet, 2005; SVGW, 2008) and Europe (Ray et al., 2002), and because RBF systems have been identified as being highly susceptible to climate change (Sprenger et al., 2011).

The purpose of using historical data was to determine the extent to which the impact of climatic forcing on groundwater temperature and DO concentration is regionally coherent as opposed to site-specific, and to capture long-term effects that might not be detectable in individual field studies. This is accomplished in two separate chapters on groundwater temperature (Chapter 3) and groundwater DO concentration (Chapter 5). Chapter 4 presents forecasts of groundwater temperature for the 21st Century calculated using empirical models constructed to relate groundwater temperature to regional air temperature. These models were calibrated to historical data and used recently published air temperature projections for Switzerland (CH2011, 2011) as input.

1.2 Outline

Chapter 2: Scientific background
This chapter provides scientific background on the factors influencing groundwater temperature and groundwater DO concentration, focusing particularly on RBF sites. Furthermore, the chapter describes how climate change might affect these two variables and discusses the potential implications of changes in groundwater temperature and DO concentration for groundwater quality.

Chapter 3: Regime shift in groundwater temperature triggered by the Arctic Oscillation
Three statistical methods – the Rodionov regime shift test, the Pettitt change-point test, and the Barry and Hartigan change-point test – were used to reveal the occurrence in the late 1980s of an abrupt warming of the groundwater in five Swiss aquifers that are recharged by RBF. This abrupt warming, which was also found in regional air temperatures and river-water temperatures and was associated with a shift in the behavior of the Arctic Oscillation, contributed substantially to the overall long-term groundwater temperature increase in the five

aquifers analyzed. This chapter has been published in *Geophysical Research Letters* (Figura et al., 2011).

Chapter 4: Projections of groundwater temperature with linear regression models using historical data

The groundwater temperature time-series of seven Swiss aquifers were related empirically to regional air temperatures using linear regression models. Using recently published air temperature projections for Switzerland as input, these models were then run to calculate forecasts of groundwater temperature. The study showed that the linear regression models are dependent on the training period and are appropriate for the prediction of groundwater temperature based on air temperature only in specific cases. However, for three aquifers recharged by RBF the model forecasts are trustworthy. These aquifers are expected to warm strongly by the end of the current century. This chapter is in preparation to be submitted for publication.

Chapter 5: Competing controls on groundwater oxygen concentrations revealed in multidecadal time-series from riverbank filtration sites

Time-series of DO concentration measured in the pumping wells of four aquifers recharged by RBF all showed temporal features such as long-term trends and abrupt increases. The study showed that DO concentrations are likely to have undergone a long-term decrease in response to groundwater and river-water warming. However, changes in hydrological conditions – e.g., high pumping rates and river discharge events, as well as individual extreme discharge events which unclogged the riverbed – led to abrupt increases in DO concentrations that prevented the occurrence of hypoxia in the groundwater. This chapter has been published in *Water Resources Research* (Figura et al., 2013a).

Chapter 6: Conclusions and outlook

This chapter summarizes the key findings of this work and discusses recommendations for future related work.

Appendix

The appendix describes the statistical methods used most frequently in this work. It includes the Supplementary Information belonging to Chapter 3. The appendix also gives a brief summary of additional publications that originated during the thesis.

Scientific background

This chapter discusses the most important factors and processes affecting groundwater temperature and DO concentration (illustrated in Fig. 2.1). Possible responses of these two variables to climate change, and the implications of these responses for groundwater quality, are discussed. Special attention is given to processes occurring in aquifers recharged by RBF, which are the main focus of this work (see Section 1.1). More general information on groundwater is obtainable in various textbooks, for example Bouwer (1978) or Freeze and Cherry (1979). For more background knowledge on the processes discussed below, see Anderson (2005) for a review of processes of heat transport in groundwater, Malard and Hervant (1999) for a review of processes affecting groundwater oxygen concentration, and Chapelle (1993) for detailed information on groundwater microbiology and geochemistry. Articles by Green et al. (2011) and Sprenger et al. (2011) provide the most comprehensive reviews of the potential impacts of climate change on groundwater and on RBF systems, respectively.

2.1 Controls on groundwater temperature

According to Parsons (1970), aquifers can be divided into a deeper, geothermal zone and an upper, surficial zone. If there is no substantial vertical groundwater flow or lateral inflow of groundwater of a different temperature, the groundwater temperature in the geothermal zone below a depth of ~10-20 m shows no seasonal fluctuations and follows the geothermal gradient with increasing depth, increasing by approximately 1 K per 20-40 m. In the surficial zone and in aquifers closely connected to surface water, however, groundwater temperature is subject to seasonal fluctuations and is driven mainly by the flux of heat through the ground surface. Heat transport through the ground surface can be diffusive or advective (with the moving water). The seasonal fluctuations in groundwater temperature are damped and lagged in time with increasing depth or with increasing distance from the location where recharge occurs or surface water infiltrates (Anderson, 2005). In the surficial zone the annual mean groundwater temperature lies approximately 1 - 2 K above annual mean surface temperature (Anderson, 2005). Groundwater temperature might also be affected by direct anthropogenic intervention;

e.g., by the operation of heat pumps for cooling and heating (Lee and Hahn, 2005; Shin et al., 2010; Epting and Huggenberger, 2013) or by heat lost from urban areas ("urban heat islands"; Taniguchi et al., 1999; Ferguson and Woodbury, 2007; Taylor and Stefan, 2009).
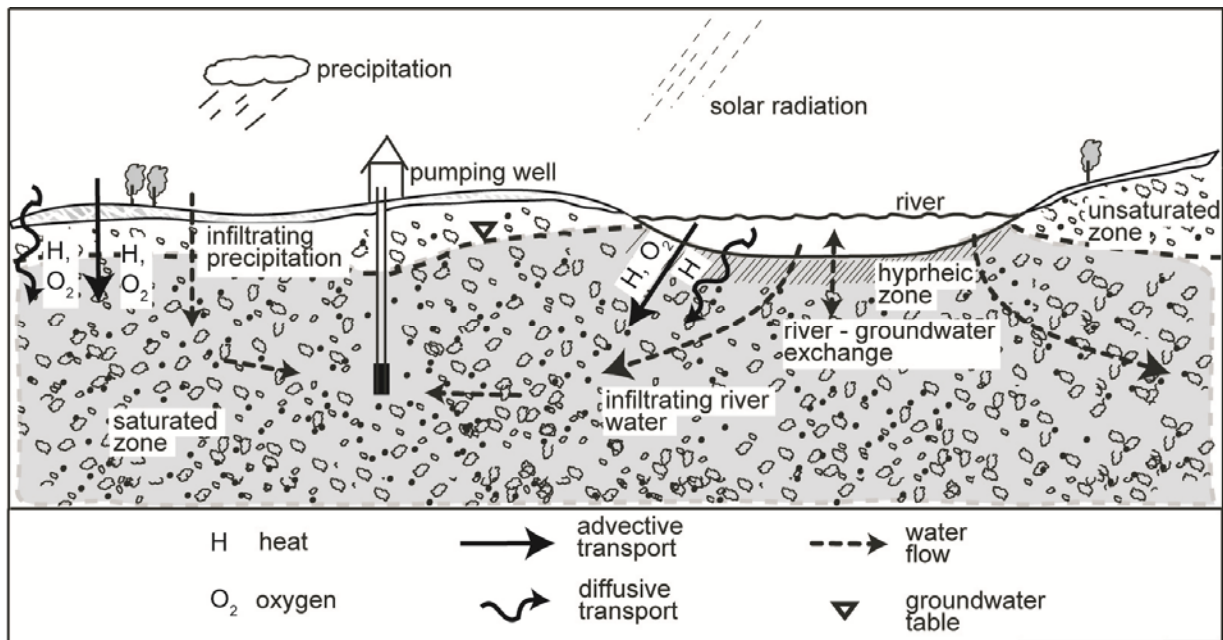
Figure 2.1: Schematic representation of an aquifer with a connected river highlighting the main processes affecting groundwater temperature and DO concentration.

The groundwater temperature measured in the pumping wells of shallow aquifers that are recharged by RBF is controlled by several factors. For the RBF sites analyzed in this work, the most important of these are related to the water temperature of the connected river and river groundwater exchange processes. Both river water temperature (Caissie, 2006) and river-groundwater exchange processes (Woessner, 2000) are themselves controlled by a large variety of factors. Among the different factors affecting river water temperature, atmospheric conditions (e.g., air temperature, solar radiation, and precipitation) are the most important (Caissie, 2006). With regard to river-groundwater exchange processes, the hydraulic head difference between the river and groundwater, and the hydraulic conductivity of the riverbed and the aquifer, are the most important factors (Woessner, 2000). Here it should be noted that the hydraulic head difference between the river and groundwater is obviously affected by the groundwater pumping rate. Despite the importance of the infiltrating river water on the groundwater temperature measured in the pumping wells of the RBF sites analyzed here, other influences cannot be neglected. Firstly, for a very shallow aquifer the diffusive and advective transport of heat through the unsaturated zone above the aquifer might affect the groundwater temperature, reducing the clarity of the temperature signal from the infiltrating river water. Secondly, geothermal heat (in the case of a very deep aquifer), or the inflow of groundwater which does not originate from RBF might attenuate the river-water temperature signal. Because special attention was paid to finding data from anthropogenically "undisturbed" sites during the data search (Section 1.1), the groundwater temperatures analyzed in this work have most probably not been influenced substantially by direct anthropogenic heat sources or sinks.

An illustrative example of some of the features found in the groundwater temperature time-series analyzed in this work is presented in Fig. 2.2, which shows data from the *Seewerben* aquifer. The *Seewerben* aquifer is recharged mainly by the River Rhine and is located in northeastern Switzerland, approximately 10 km downstream of the city of Schaffhausen. Fig. 2.2 firstly shows, as discussed in Chapter 3, that the time-series of annual mean groundwater temperature (Fig. 2.2b) is similar to that of annual mean river-water temperature and annual mean air temperature (Fig. 2.2a). Secondly, the time-series of monthly mean groundwater temperature (Fig. 2.2c) shows a clear seasonal signal. However, as also discussed in Chapter 3, the seasonal signal in groundwater temperature is damped and delayed with respect to the seasonal signal observed in the water temperature of the losing river because heat transfer is not instantaneous (Anderson, 2005). Owing to differences in the intrinsic properties of the aquifers (e.g., in flow velocity or in the specific heat capacity of the aquifer matrix), the damping and delaying effects vary from aquifer to aquifer.
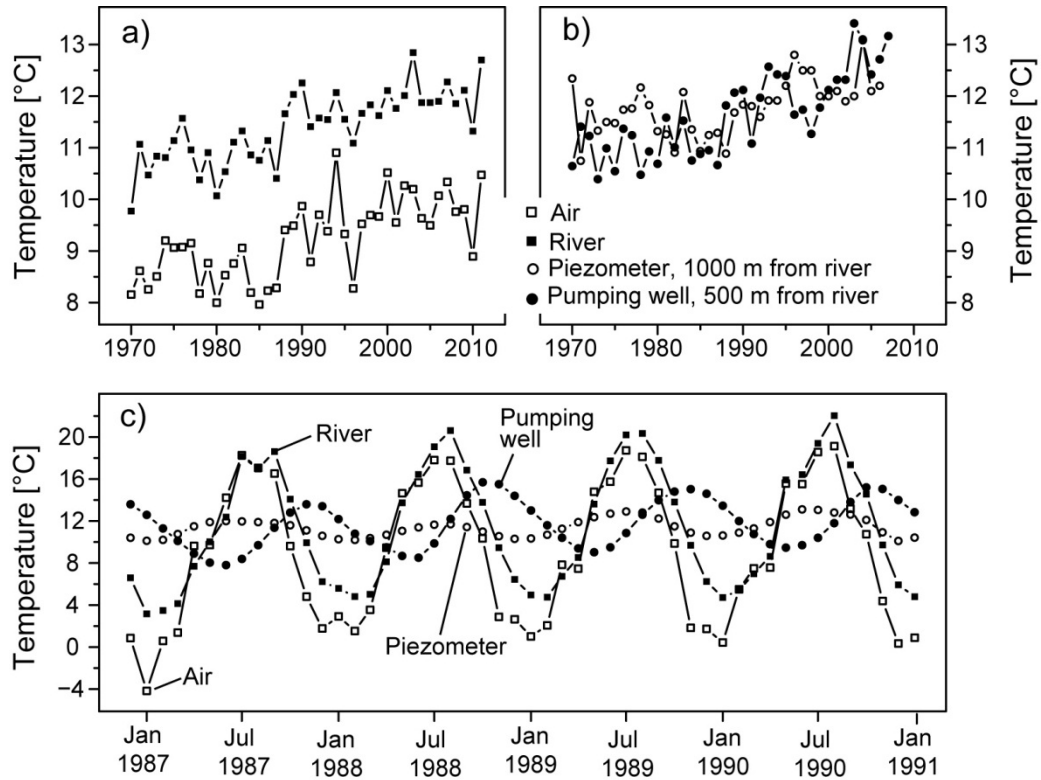
Figure 2.2: Time-series of air temperature, river-water temperature and groundwater temperature at the *Seewerben* aquifer. (a) Annual mean time-series of air temperature at Schaffhausen (open squares) and river-water temperature of the River Rhine (filled squares). (b) Annual mean groundwater temperature measured in a pumping well (filled circles) and a piezometer (open circles). (c) Corresponding monthly mean time-series. The pumping well and piezometer are 500 m and 1000 m, respectively, from the bank of the losing river. The figure illustrates the similarity of the annual mean regional air temperature, river-water temperature, and groundwater temperature and the damping and delay of the seasonal signal in groundwater temperature with respect to the seasonal signal in air temperature and river-water temperature.

2.2 Controls on groundwater oxygen concentration

Because there is no oxygen production in groundwater[1] the DO concentration in groundwater is determined by the rates of transport of oxygen from the atmosphere into the groundwater and by the oxygen consumption rates in the groundwater (Chapelle, 1993). The oxygen input from the atmosphere to groundwater occurs in two ways: firstly by advective transport via the infiltration of precipitation or surface water (Malard and Hervant, 1999), and secondly by the diffusion of gaseous oxygen through the soil and the pore spaces of the unsaturated zone adjacent to the aquifer. Compared to the advective transport of oxygen, the diffusion of oxygen in the water phase is negligible (Refsgaard et al., 1988), making the diffusive input of oxygen across the interface between surface water and groundwater irrelevant. Oxygen is consumed in groundwater by the microbial respiration of organic matter (Chapelle, 1993). The rate of oxygen consumption depends on various factors; e.g., on the bacterial biomass, the amount and composition of organic matter, groundwater flow velocity, and temperature (Malard and Hervant, 1999). With respect to the effect of temperature, a warming of 10 °C will increase the respiration rate by a factor of 2-4 according to the van't Hoff equation (Sprenger et al., 2011). Temperature also affects the solubility of oxygen. At the standard atmospheric pressure of 1013.25 hPa, the solubility of oxygen in water is 10.9 mg O_2 l^{-1} at 10 °C, but only 8.8 mg O_2 l^{-1} at 20 °C.

The DO concentrations analyzed in this study are thus also the result of several factors. The oxygen input rate might be controlled primarily by the DO concentration in the river water and by the rate of infiltration of river water. Although DO concentrations in river water can fluctuate greatly, the rivers analyzed in this study were in the main either saturated or close to saturation with respect to DO (see Chapter 5). The factors determining the infiltration rate of river water have been defined in the previous section (see Section 2.1). In addition to the direct effect of advective transport in the infiltrating river water, the infiltration rate of river water might affect groundwater DO concentration via the phenomenon of "excess air". "Excess air" in groundwater results when entrapped air bubbles dissolve in groundwater after abrupt rises in groundwater level. This dissolution of air bubbles, and hence of the oxygen enclosed in these bubbles, has been shown to have an impact on groundwater DO concentration in various studies (e.g., Kohfahl et al., 2009; Mächler et al., 2013). Regarding the oxygen sinks, the microbial oxygen consumption occurring in the hyporheic zone is probably of crucial importance. The hyporheic zone – the transition zone between river and groundwater (White, 1993; Findlay, 1995) – plays a key role in the hydrology and biogeochemical cycles of RBF systems (Brunke and Gonser, 1997). Because oxygen consumption rates in the hyporheic zone are substantially higher than in groundwater, oxygen consumption there often dominates the total oxygen consumption in RBF systems (Beyerle et al., 1999; Malard and Hervant, 1999). Compared to processes affecting the oxygen consumption in groundwater, the oxygen consumption in the hyporheic zone seems to depend to a greater extent on flow velocity; i.e., on the residence time of infiltrating water in the hyporheic zone during infiltration (Malard and Hervant, 1999).

---

[1] The only exception is oxygen production through the radiolysis of water by alpha emissions at depths of 2000 - 3000 m (Gutsalo, 1971).

2.3 Potential impacts of climate change on groundwater temperature and oxygen concentration

Detailed climate projections recently published for Switzerland (CH2011, 2011) specify the likely future change in air temperature and precipitation under three greenhouse-gas emissions scenarios (A2, A1B, and RCP3PD) for three future time periods (2020-2049, 2045-2074, and 2070-2099; Fig. 2.3). Compared to the reference period 1980d-2009, the CH2011 air temperature projections for northeastern Switzerland, which are the ones used here, estimate a medium warming of 1.3 – 3.6 K in winter and 1.6 – 4.4 K in summer, depending on the emissions scenario employed. The projections for precipitation are less clear. In winter an increase of 1.2 – 3.4 % in precipitation is expected, but the error bars extend over the line of zero change. In summer, however, a clear change in precipitation of -7.8 to -21.4 % is projected. Theoretical considerations also suggest that the frequency of extreme precipitation events will increase (CH2011, 2011).
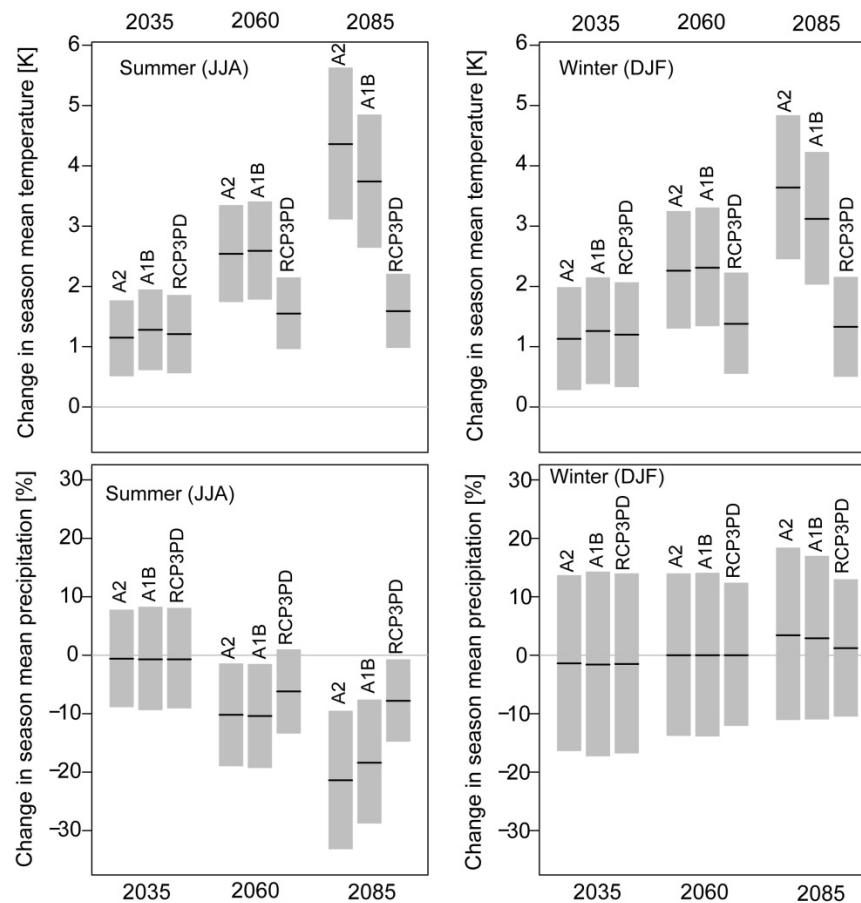
Figure 2.3: CH2011 climate projections for air temperature (top panels) and precipitation (bottom panels) in summer (left-hand panels) and winter (right-hand panels) in northeastern Switzerland for the three emissions scenarios A2, A1B, and RCP3PD and the three scenario periods 2020-2049 (designated by 2035), 2045-2074 (2060), and 2070-2099 (2085) with respect to the reference period 1980-2009.

Extrapolating the results of studies on the impact of past climatic forcing on the water temperatures of Swiss lakes (e.g., Livingstone, 2003) and rivers (e.g., Hari et al., 2006) suggests that these will increase in the future. Especially during longer periods of low-flow conditions during summer, rivers might warm excessively (FOEN, 2012). The study by FOEN (2012) also

calculated the impacts of changes in air temperature and precipitation on river discharge in Switzerland based on the CH2011 climate projections. While the annual mean runoff of rivers is unlikely to change strongly, the seasonal distribution of discharge will be altered significantly. Particularly in the second half of this century, low-flow conditions in summer will be more pronounced, discharge in winter will increase slightly, and high discharge events will probably occur more frequently (FOEN, 2012).

Taking into account what has already been said in Sections 2.1 and 2.2, future climatic conditions and changes in river discharge rates will affect groundwater temperature and DO concentration. These changes will have implications for groundwater quality (see Section 2.4). The most obvious effect that can be expected (which will be discussed in Chapter 4) is the warming of groundwater in response to the warming of the atmosphere. In recent years a few studies have calculated the potential warming of groundwater likely to result from climate change. Compared to 2004 conditions, Taylor and Stefan (2009) forecast that a doubling of CO_2 emissions would result in an increase of 2.0 – 5.2 K in shallow aquifers around St. Paul, Minnesota, USA. Gunawardhana and Kazama (2011) and Gunawardhana et al. (2011) made several predictions of groundwater temperature in the Sendai plain, Japan. Depending on the greenhouse-gas emissions scenario employed, they estimated a warming of 1.0 - 4.3 K at 8 m depth by 2080 with respect to the reference period 1967-2006. For the groundwater in a small, forested catchment in New Brunswick, Canada, the most recent study by Kurylyk et al. (2013) forecasted an increase of 1.0 - 3.5 K by 2046-2065, depending on depth and month, with respect to the reference period 1961-2000. None of the aquifers analyzed in the studies mentioned above are recharged by RBF. However, a strong warming can be expected in aquifers recharged by RBF because of the high probability that river water temperatures will increase (FOEN, 2012).

The increase in river-water and groundwater temperatures will presumably cause a decline in groundwater DO concentrations by increasing microbial respiration rates and reducing the solubility of oxygen (Section 2.2). At RBF sites hydrological conditions might also negatively affect groundwater DO concentrations. Longer periods of low-flow conditions in summer will result in a prolongation of the residence time of infiltrating water in the hyporheic zone and in the aquifer, and will increase the concentration of organic material in the river water, additionally fostering microbial respiration (Sprenger et al., 2011; Diem et al., 2013). In addition, a higher frequency of extreme precipitation and river discharge events might increase the load of organic material in river water (Diem et al., 2013).

Changes in air temperature and precipitation will also affect groundwater recharge directly (e.g., changes in evapotranspiration and precipitation) or indirectly (e.g., higher pumping rates). Although it is not clear whether recharge amounts will change, the seasonal distribution of groundwater recharge will change (Green et al, 2011; Sprenger et al., 2011; Taylor et al., 2013). These seasonal shifts in recharge will also affect groundwater temperature and DO concentration.

2.4 Importance of groundwater temperature and oxygen concentration for groundwater quality

Temperature is an important physical variable which affects chemical and biological processes that are relevant for groundwater quality. Higher temperatures might affect groundwater quality directly by accelerating geochemical processes (e.g., the dissolution of salts) or indirectly by increasing microbial respiration rates (Chapelle, 1993), the effect of which can be positive or negative. Enhanced microbial activity favors the degradation of pollutants in groundwater (Sprenger et al., 2011) and the removal of pathogens (Schijven and de Roda Husman, 2005), but might also lead to the formation of unwanted byproducts by reducing DO concentration and altering redox conditions (see below). In addition, temperature also affects physical processes that are important for groundwater quality. Increasing temperatures affect groundwater DO concentration by reducing the solubility of oxygen in water. The viscosity and hydraulic conductivity of water are also influenced by temperature. Particularly at RBF sites, where surface water temperature is subject to large fluctuations, a change in hydraulic conductivity due to a change in water temperature alters infiltration rates (Constantz et al., 1994) potentially affecting groundwater quality.

Groundwater DO concentration is a crucial determinant of groundwater quality, as oxygen represents the most preferred electron acceptor in microbial respiration processes (Chapelle, 1993). The presence of DO thus ensures the microbial degradation of organic pollutants in groundwater. However, if groundwater turns hypoxic (i.e., low in DO) or even anoxic (i.e., DO-free), other dissolved or solid terminal electron acceptors such as nitrate, iron and manganese (hydr)oxides, and sulfate are used. As a result of the reduction of iron and manganese (hydr)oxides, iron and manganese go into solution, which is of concern for the operation of the pumping well. As a result of re-aeration in the pumping well, iron and manganese precipitate out, which can cause clogging in the pumping well (Hunt et al., 2002) and lead to an unwanted organoleptic alteration of the pumped groundwater. Pumping wells at RBF sites are particularly susceptible to changes in redox conditions resulting from enhanced microbial respiration because the connection to the surface water ensures that the organic material that sustains microbial respiration is replenished (Sprenger et al., 2011). In recent studies, anoxic conditions at RBF sites have been documented in Germany (Rohns et al., 2006) and Switzerland (Hoehn and Scholtis, 2011) during the summer of 2003, during which Europe experienced extraordinarily hot, dry conditions (Schär et al., 2004). At the Swiss study site, the anoxic conditions led to a reductive dissolution of iron and manganese (hydr)oxides and the consequent precipitation of iron and manganese (hydr)oxides in the pumping well (A. Scholtis, unpublished data). Using historical groundwater DO concentrations, the risk of RBF aquifers turning anoxic in response to future climatic conditions is discussed in Chapter 5.

Regime shift in groundwater temperature triggered by the Arctic Oscillation

This chapter has been published in *Geophysical Research Letters* (Figura et al., 2011)[2]. The Supplementary Information which was published with this chapter can be found in Appendix A and B.

Abstract. Groundwater is the world's most important source of raw drinking water. However, the potential impact of climate change on this vital resource is unclear because of a lack of relevant long-term data. Here we statistically analyze over 20 years of groundwater temperature data from five Swiss aquifers fed predominantly by river-bank infiltration. The results reveal an abrupt increase in annual mean groundwater temperature centered on 1987-1988 that can also be observed in air and river temperatures. We associate this temperature increase with the Northern Hemisphere late 1980s climate regime shift (CRS), which itself is related to an abrupt change in the behavior of the Arctic Oscillation. Because temperature affects redox conditions in groundwater, groundwater biogeochemistry in aquifers fed by river-bank infiltration is likely to depend on large-scale climatic forcing and will be affected by climate change.

3.1 Introduction

Climate change is expected to have a strong impact on the hydrological cycle (Bates et al., 2008). However, owing to the paucity of relevant long-term data, little is known about its effects on groundwater (Bates et al., 2008), which accounts for about half of global drinking

---

water production (Connor et al., 2009). In a recent review paper, Green et al. (2011) emphasize that existing studies on this topic focus on variables that are associated primarily with groundwater quantity, such as water table levels and recharge rates. Scarcely anything is known about the impact of climate change on groundwater quality (Bates et al., 2008; Green et al., 2011).

Temperature is an important determinant of groundwater quality. Based on current knowledge of heat transport in groundwater (Anderson, 2005), an increase in groundwater temperature driven by climate change is likely. A few studies on this topic have tried to describe and predict the magnitude of the groundwater temperature increase by applying simple heat transport models (e.g., Taylor and Stephan, 2009; Gunawardhana and Kazama, 2011) or by analyzing vertical borehole temperatures (Taniguchi et al. 1999, 2007). However, to the best of our knowledge no empirical studies exist which demonstrate in detail the direct effect of recent climate change on groundwater temperature. Higher groundwater temperatures may affect biogeochemical processes such that groundwater is rendered less suitable as a source of raw drinking water (von Gunten et al., 1991; Sprenger et al., 2011; Green et al., 2011). During the heat wave that occurred during summer 2003 in much of Europe (Schär et al., 2004), reducing conditions in groundwater were reported at study sites in Germany (Eckert et al., 2008) and Switzerland (Hoehn and Scholtis, 2011). At the Swiss study site, the reducing conditions led to the precipitation of iron and manganese in the pumping wells in response to re-aeration in the open pumping station (Hoehn and Scholtis, 2011). Knowledge of the response of groundwater temperature to climatic forcing may therefore be crucial for future groundwater resource quality management.

Large-scale climate modes, such as the El Niño Southern Oscillation, the North Atlantic Oscillation, and the Pacific Decadal Oscillation, appear to affect groundwater level and recharge (Hanson et al., 2006; Gurdak et al., 2007; Holman et al., 2011), suggesting that large-scale climatic forcing might also affect groundwater temperatures. Here, we analyze statistically several long time-series (at least 20 years of regular measurements) of Swiss groundwater temperatures with a view to detecting the impact of one clear, recent feature of large-scale climate change. This feature is the now well-documented climate regime shift (CRS) that occurred over large areas of the Northern Hemisphere in the late 1980s as a result of an alteration in atmospheric circulation patterns associated with an abrupt change in the behavior of the Arctic Oscillation (Rodionov and Overland, 2005). The late 1980s CRS is known to have had a substantial effect on physical and biological processes in seas (Hare and Mantua, 2000; Reid et al. 2001; Alheit et al., 2005; Rodionov and Overland, 2005; Tian et al., 2008; Conversi et al., 2010), lakes (Gerten and Adrian, 2000; Anneville et al., 2004; Temnerud and Weyhenmeyer, 2008), and rivers (Hari et al., 2006), but an effect on groundwater has not yet been demonstrated.

3.2 Data and Methods

We analyzed time-series of water temperatures measured in the pumping wells of five granular, unconsolidated aquifers on the Swiss Plateau (Fig. 3.1). These aquifers have thicknesses of 15-30 m and are recharged predominantly from four rivers by river-bank infiltration (Appendix B). The temperatures were measured in tubes within the pumping wells before the water came in

contact with the atmosphere and are likely to be broadly representative of groundwater temperatures in the aquifers. The rivers feeding the aquifers are the Rhine (Rh), Emme (Em), Aare (Aa), and Toess (To). The aquifers are abbreviated here as *RhSe*, *RhNe*, *EmSi*, *AaKi*, and *ToLi*, where the first two letters designate the river feeding the aquifer. For the first four of these aquifers, groundwater temperature time-series were available from one pumping well per aquifer. For the fifth aquifer (*ToLi*), a groundwater temperature time series was obtained by combining the temperature time-series from five individual pumping wells (Appendix B). Time-series of the water temperatures of the four rivers feeding the aquifers were also analyzed, as was the time-series of the Swiss Plateau regional air temperature (Appendix B).

The air and river water temperature data had been sampled at intervals of at least one day and did not require interpolation; the daily data were aggregated to obtain monthly and annual means. The groundwater temperature data had been sampled at irregular intervals. The raw data were first interpolated at daily intervals using a cubic spline, and the interpolated data were then aggregated to yield estimates of monthly and annual means (Appendix A).

Rodionov's sequential t-test analysis of regime shifts (STARS) (Rodionov, 2004) was employed to identify abrupt shifts in the time-series. The STARS results were cross-checked using the non-parametric Pettitt change-point test (Pettitt, 1979) and the parametric Bayesian change-point test of Barry and Hartigan (1993). The former computes the location of a change-point and assigns it a significance value; the latter computes the posterior probability that any given point in the time-series is a change-point. Whilst STARS and the Barry-Hartigan test can detect multiple change-points in a time-series, the Pettitt test can detect only one change-point (see Appendix A for a more detailed description of the tests). The period covered by the analysis is 1978-2000, for which the density of available data was optimal. All three tests are commonly used to detect abrupt shifts in climatic and environmental time-series (Rodionov and Overland, 2005; Hari et al., 2006; Metsaranta and Lieffers, 2010).

Cross-correlation functions between time-series of monthly mean air, river, and groundwater temperatures were computed to estimate temperature travel time during the river-bank infiltration process. Trend and seasonality were removed from all time-series prior to computation using the seasonal-trend decomposition procedure of Cleveland et al. (1990).

3.3 Results

3.3.1 The late 1980s regime shift in the time-series of annual means

In the late 1980s, regional air temperature, river water temperatures, and groundwater temperatures all exhibited an abrupt regime shift (Fig. 3.1). Application of STARS to the time-series of the respective annual means provided objective confirmation of this (Table 3.1a). In regional air temperature and river water temperatures an abrupt regime shift ($p < 0.01$) occurred from 1987 to 1988, with the means for the period 1988-2000 (henceforth Regime II) exceeding those for the period 1978-1987 (henceforth Regime I) by 0.7 to 1.4 K (the To river temperature time-series was excluded from this part of the analysis because of its shortness). The groundwater temperature time-series behaved similarly: in all five aquifers, a statistically significant regime shift ($p < 0.01$) was detected from 1987 to 1988, with the Regime II mean exceeding the Regime I mean by 0.7 to 1.1 K. In all cases analyzed, the difference between the two regimes in the groundwater temperature time-series was comparable to that in the relevant

river water temperature time-series (Fig. 3.2, left-hand panels). Note that in three of the aquifers (*EmSi*, *AaKi*, *ToLi*), an additional regime shift was detected in the mid-1990s (Table 3.1a).
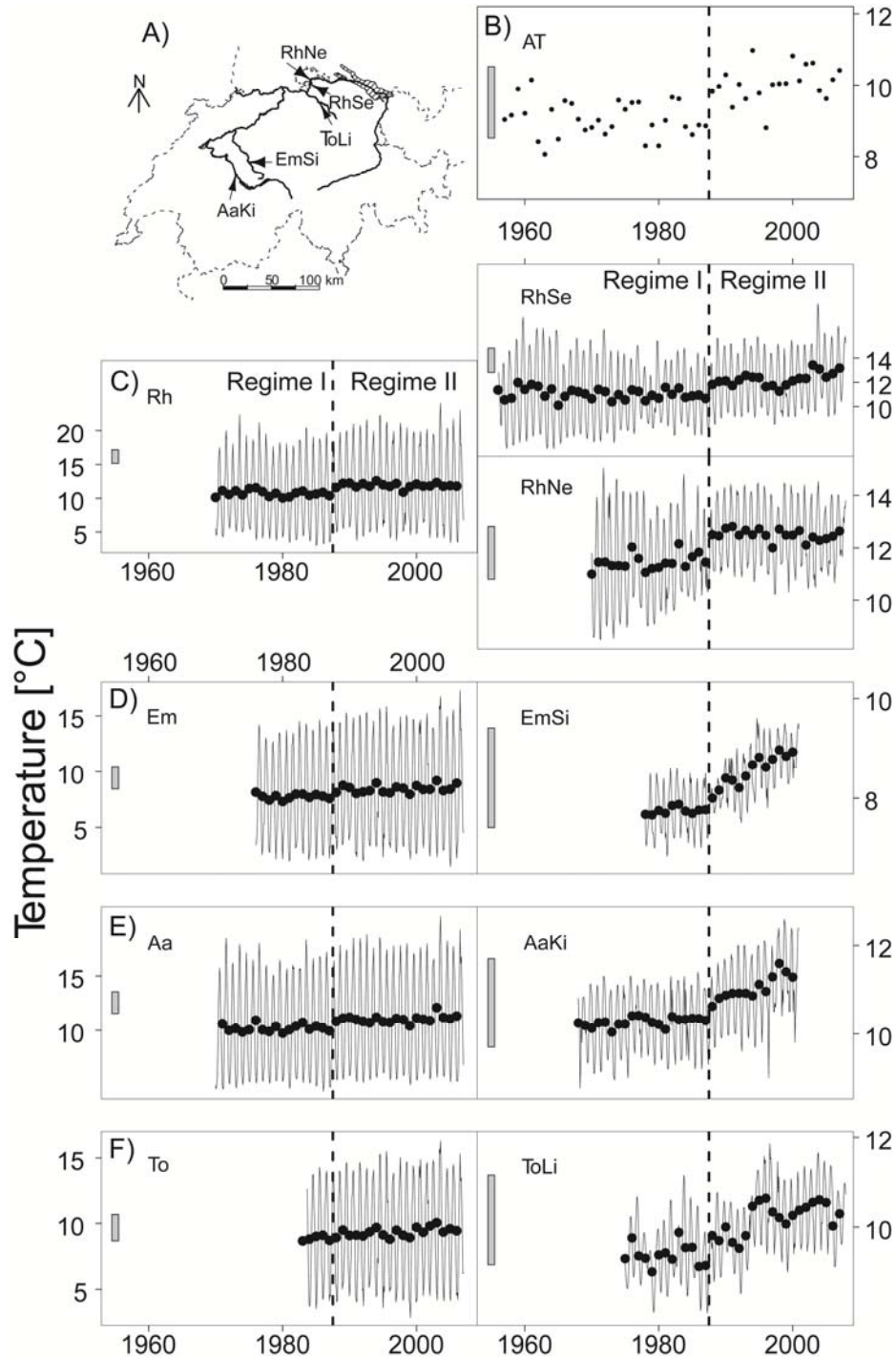
Figure 3.1: A) Map of Switzerland showing locations of rivers and aquifers. B) Annual mean regional air temperature. C-F) Monthly means (lines) and annual means (dots) of measured river water temperatures (left-hand panels) and groundwater temperatures (right-hand panels). The vertical dashed lines separate Regime I (1978-1987) from Regime II (1988-2000). Note the different scales on the y-axes. To facilitate comparison, a gray rectangle located on the left-hand side of each panel illustrates a temperature difference of 2 K.

The Pettitt (Pettitt, 1979) and Barry-Hartigan (Barry and Hartigan, 1993) change-point tests provided additional confirmation of the existence of a regime shift in the annual mean temperature time-series in the late 1980s. The change-points detected by the Pettitt test are in all

cases located between 1987 and 1989 (Table 3.1b). The locations of the most likely change-points detected by the Barry-Hartigan test (Table 3.1c) generally agree with the locations of the regime shifts detected by STARS: i.e., 1987-1989 (and, for aquifers EmSi, AaKi and ToLi, additionally the mid-1990s).

Table 3.1: Results of the regime shift and change-point tests. (a) Results of the STARS regime shift test. Listed are the temporal locations of significant ($p < 0.01$) regime shifts. (b) Results of the Pettitt change-point test. Listed are the temporal locations of change-points detected at significance levels $p < 0.1$ (*), $p < 0.05$ (**), and $p < 0.01$ (***). (c) Results of the Barry-Hartigan change-point test. Listed are the temporal locations of the highest posterior probability P of a change-point for $0.01 < P < 0.20$ (°), $0.20 < P < 0.70$ (°°), and $P > 0.70$ (°°°). All tests were applied to the time-series (1978-2000) of annual and seasonal means of regional air temperature (AT), river water temperatures (Rh, Em, Aa) and groundwater temperatures (*RhSe*, *RhNe*, *EmSi*, *AaKi*, *ToLi*) in Switzerland.

		Annual	Winter	Spring	Summer	Autumn
a) STARS	AT	87/88		87/88	89/90	
	Rh	87/88	87/88	87/88	87/88	
	Em	87/88		88/89	87/88	
	Aa	87/88		87/88	87/88	
	RhSe	87/88		88/89	87/88	87/88
	RhNe	87/88	87/88	85/86	87/88	87/88
	EmSi	87/88	86/87	87/88	88/89	
		94/95	94/95	94/95		90/91
	AaKi	87/88	87/88	87/88	87/88	87/88
		96/97	97/98	94/95	96/97	96/97
	ToLi	87/88		88/89	87/88	
		93/94	93/94			93/94
b) Pettitt	AT	87/88**		87/88***	87/88**	
	Rh	87/88***	87/88**	87/88**	87/88***	
	Em	87/88***		88/89***	88/89***	
	Aa	87/88***		87/88***	87/88*	
	RhSe	87/88***		88/89*	87/88***	87/88***
	RhNe	87/88***	88/89***	87/88***	87/88***	87/88*
	EmSi	88/89***	88/89***	87/88***	87/88***	89/90***
	AaKi	88/89***	88/89***	88/89***	88/89***	88/89***
	ToLi	87/88***	92/93*	88/89***	87/88***	93/94**
c) Barry-Hartigan	AT	87/88°	87/88°	87/88°	87/88°	
	Rh	87/88°°°		87/88°°°	87/88°	
	Em	87/88°°		88/89°°°		
	Aa	87/88°°°		87/88°°°		
	RhSe	87/88°°°			87/88°°°	87/88°
	RhNe	87/88°°°	89/90°°	85/86°°	87/88°°°	
	EmSi	88/89°°	86/87°°	87/88°°°	89/90°°	
		93/94°°°	94/95°°	94/95°°	92/93°°	93/94°°°
	AaKi	87/88°°°	89/90°°	88/89°°	87/88°°°	87/88°°
		96/97°°°	97/98°°	94/95°°	96/97°°°	96/97°°°
	ToLi	87/88°°		87/88°°	87/88°°°	87/88°
		93/94°°°	93/94°°°	92/93°°	93/94°	93/94°

3.3.2 The late 1980s regime shift in the time-series of seasonal means

To determine whether seasonal differences existed in the occurrence of the late 1980s regime shift, STARS was also applied to time-series consisting of either winter (December-February), spring (March-May), summer (June-August) or autumn (September-November) data only, focusing on the detection of shifts within the period 1985-1990 (Table 3.1a). For regional air temperature, the occurrence of the late 1980s regime shift was confined to spring and summer. This was also true for two of the rivers (Em and Aa); for the third river (Rh), the temperature regime shift was additionally detected in winter. In all five aquifers, the late 1980s groundwater temperature regime shift showed a seasonal pattern that was different and less consistent than that shown by the air and river water temperature regime shifts (Fig. 3.2). In the groundwater temperatures, the late 1980s regime shift could occur in any or all seasons. The Pettitt and Barry-Hartigan tests provided confirmation of the STARS results for the seasonal data (Table 3.1b, c).
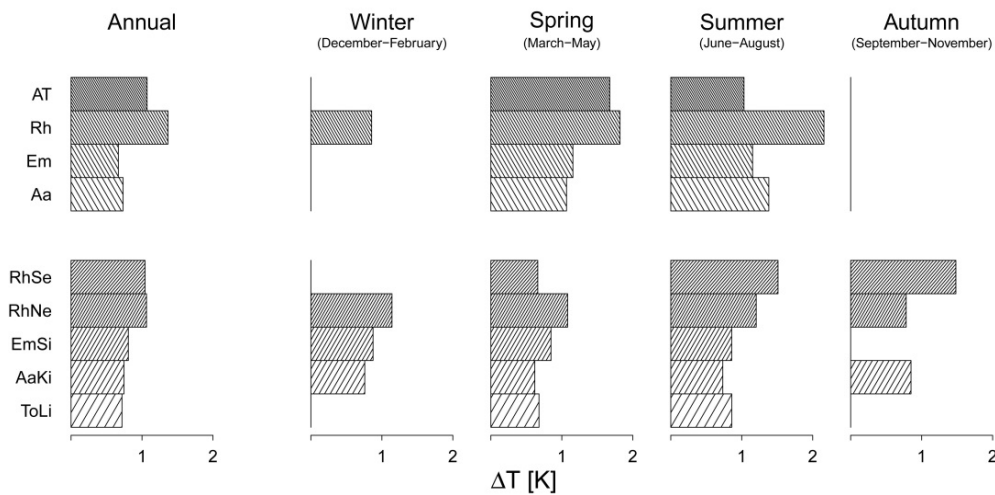
Figure 3.2: Magnitude of the late 1980s regime shift in annual and seasonal mean values of regional air temperature (AT), river water temperatures (Rh, Em, Aa), and groundwater temperatures (*RhSe, RhNe, EmSi, AaKi, ToLi*) in Switzerland. Shown is the increase ΔT in the mean of each time series from Regime I (1978-1987) to Regime II (1988-2000) for all cases when a regime shift was detected by the STARS test (Rodionov, 2004) between 1985 and 1990 (Table 3.1a); when no regime shift was detected, ΔT was assumed to be zero.

3.3.3 Time-lags between river water and groundwater temperatures

Computation of cross-correlation functions between the time-series of the monthly mean temperature data allowed the relevant time-lags between the time-series to be determined (Table 3.2). The locations of the maxima of the cross-correlation functions indicate that the water temperature in all rivers responds rapidly to fluctuations in regional air temperature. By contrast, the groundwater temperature in the pumping wells lags the water temperature of the river feeding the aquifer, and hence also the regional air temperature, by 2-4 months. The maxima of the cross-correlation functions between the regional air temperature and the river water temperatures were 2-3 times greater than the maxima of the cross-correlation functions between the regional air temperature and the respective groundwater temperatures (Table 3.2), implying that, as would be expected, the signal of the regional air temperature transmitted to the groundwater is weaker than that transmitted to the river water.

Table 3.2: Cross-correlation functions of monthly mean time series. (a) Value and lag of the maximum of each cross-correlation function computed between (a) monthly mean time-series of Swiss regional air temperature and river water temperatures (Rh, Em, Aa, To), (b) regional air temperature and groundwater temperatures (*RhSe*, *RhNe*, *EmSi*, *AaKi*, *ToLi*), and (c) river water temperatures and groundwater temperatures. The lag in months is given in parentheses, along with the estimated uncertainty associated with the sampling interval and the damping of the temperature signal. A positive lag implies groundwater temperature lags air temperature or river water temperature. All computations are based on the period 1978-2000 except for those involving the River Toess, which are based on the period 1984-2000. Trend and seasonality were removed prior to all computations using the seasonal-trend decomposition procedure of Cleveland et al. (1990). All cross-correlation coefficients listed differ significantly from zero at the p < 0.05 level. Note that the discrepancies between the lags at b) and c) for *RhSe* and *RhNe* lie within the estimated range of uncertainty.

a)	Regional air temperature and river water temperature	Rh		Em	Aa	To
		0.58		0.75	0.61	0.70
		(0)		(0)	(0)	(0)
b)	Regional air temperature and groundwater temperature	*RhSe*	*RhNe*	*EmSi*	*AaKi*	*ToLi*
		0.27	0.23	0.28	0.24	0.17
		(4±1)	(4±1)	(2±1)	(3±1)	(2±1)
c)	River water temperature and groundwater temperature	*RhSe*	*RhNe*	*EmSi*	*AaKi*	*ToLi*
		0.40	0.28	0.34	0.31	0.15
		(3±1)	(2±1)	(2±1)	(3±1)	(2±1)

3.3.4 Non-stationarity in Regime II

All the time-series illustrated in Fig. 3.1 are statistically stationary during Regime I, but not all are statistically stationary during Regime II. For regional air temperature and river water temperature, linear regression revealed no statistically significant (p < 0.05) linear trend during either Regime I or Regime II, implying that the late 1980s regime shift is able to explain the entire temperature increase that occurred during the period 1978-2000. The same was true for two groundwater temperature time-series (*RhSe*, *RhNe*). However, the other three groundwater temperature time-series (*EmSi*, *AaKi*, *ToLi*) behaved differently: although no significant linear trend was detected during Regime I, a significant linear trend (of ~0.065 K yr^{-1}) was detected during Regime II. As noted above, in these three aquifers both STARS and the Barry-Hartigan test detect not only the late 1980s regime shift, but also an additional regime shift, involving increasing temperatures, in the mid-1990s (Table 3.1a, c). Regardless of the statistical description employed (linear increase or abrupt shift), it follows that groundwater temperatures in three of the five aquifers increased during Regime II.

3.4 Discussion and conclusions

The late 1980s CRS was a large-scale atmospheric phenomenon that had substantial impacts on various environmental systems in the Northern Hemisphere. In Switzerland, most of the warming that rivers throughout the country have undergone since the 1970s is attributable to an abrupt water temperature increase of 0.1 - 1.1 K that occurred from 1987 to 1988 (Hari et al., 2006). Here we have shown that a regime shift in the late 1980s is also clearly detectable in the groundwater temperatures of Swiss aquifers that are recharged by river-bank infiltration,

providing evidence that large-scale climatic forcing can strongly affect groundwater temperatures. Although the response of river water temperature to climatic forcing is strong and almost immediate, this is not necessarily the case for groundwater temperatures, in which the climatic signal is damped and delayed. Because lag times differ from aquifer to aquifer, the effect of seasonally specific climatic forcing can manifest itself at the pumping station at different times of the year depending on the hydraulic conductivity of the aquifer, the groundwater hydraulic gradient, the pumping rate, and the distance of the pumping station from the river.

The statistical stationarity of the annual mean time-series of regional air temperature and of all river water temperatures during each of Regimes I and II implies that the only significant temperature increase that occurred during 1978-2000 was the abrupt increase associated with the late 1980s CRS. This was also the case for the two aquifers fed by the River Rhine (*RhSe* and *RhNe*). However, groundwater temperatures in the other three aquifers (*EmSi*, *AaKi* and *ToLi*) all exhibited a substantial, statistically significant increase during Regime II. Thus, as emphasized by Holman et al. (2011) for the related case of groundwater levels, the response of groundwater temperature to climatic forcing is likely to be complex and heterogeneous, varying from aquifer to aquifer (perhaps as a result of differences in pumping rates or land use, or because of differences in the intrinsic properties of the aquifers).

Nevertheless, this study strongly suggests that an abrupt change in large-scale climatic forcing, represented here by the well-documented late 1980s CRS, had a clear and substantial impact on groundwater temperature in all five aquifers analyzed. Because biogeochemical processes in groundwater are strongly temperature-dependent (von Gunten et al., 1991; Sprenger et al., 2011; Green et al., 2011), this suggests that the quality of water extracted from aquifers recharged by river-bank infiltration for drinking-water production is likely to be affected by large-scale climatic forcing, and hence by climate change. In some countries this may necessitate modifications to the current drinking-water supply infrastructure, which may not be able to cope with the adverse effects of altered redox conditions that may be encountered in the future as a result of higher groundwater temperatures.

4

Forecasting groundwater temperature with linear regression models using historical data

This chapter is in preparation for submission.

Abstract. Temperature is an important determinant of many biogeochemical processes in groundwater, but despite this, very few studies have attempted to estimate the response of groundwater temperature to future climate warming. Here we calculate empirical forecasts of groundwater temperature for seven aquifers in Switzerland based on historical groundwater temperature time-series, using two different linear regression models. Model evaluation reveals that using linear regression models to link groundwater temperature to air temperature empirically is an adequate approach if the underlying training data are sufficiently long and contain sufficient variability. The models applied in this study allowed the groundwater temperature of three aquifers recharged by riverbank filtration to be modeled adequately. To calculate future groundwater temperature, the models were fed with regional air temperature projections for Switzerland calculated for the greenhouse-gas emissions scenarios A2, A1B, and RCP3PD. The groundwater temperature forecasts indicate that with respect to the reference period 1980-2009, groundwater temperature at Swiss riverbank filtration sites is likely to increase by 1.0 K (error range: -0.9 to 2.9 K) to 3.5 K (-0.1 to 7.5 K) by the end of the current century, depending on the greenhouse-gas emissions scenario employed.

4.1 Introduction

The temperature of groundwater in shallow aquifers is controlled by the diffusive and advective transport of heat from the atmosphere to the aquifer across the ground surface and via interactions with surface water (Anderson, 2005). Long-term observations have shown that groundwater temperatures (Figura et al., 2011), subsurface temperatures (Baker and Baker, 2002), and surface-water temperatures (Webb, 1996; Livingstone 2003; Hari et al., 2006) have all responded strongly to climatic forcing in the past. An increase in groundwater temperature in response to global warming is therefore to be expected. Although groundwater is an

21

important source of drinking water globally (Connor et al., 2009) and temperature is an important factor influencing groundwater quality (Bouwer, 1978; Chapelle, 1993; Sprenger et al., 2011; Figura et al., 2013a), little is actually known about the impact of climate change on groundwater temperature (Green et al., 2011).

Most previous predictions of the impact of climate change on groundwater temperature are based on mechanistic, one-dimensional heat transport models. To estimate the impact of increasing air temperature on groundwater temperature, Taylor and Stefan (2009) modeled vertical heat transport into groundwater by employing an analytical solution to a one-dimensional heat conduction equation. Gunawardhana and Kazama (2011), Gunawardhana et al. (2011), and Kurylyk and MacQuarrie (2013) used the same approach but added advective vertical heat transport. By implementing the analytical solution of the resulting one-dimensional advection-diffusion equation, the authors modeled the impact of climate change on groundwater temperature in the Sendai plain, Japan. A follow-up study evaluating the expected groundwater temperature increase under a changing climate in the Sendai plain (Gunawardhana and Kazama, 2012) used a numerical model for groundwater flow and heat transport.

To calibrate the one-dimensional heat transport function and the numerical heat transport model, these studies relied on measurements of groundwater temperature at different depths. The aquifers analyzed can be described reasonably well in terms of vertical heat transport alone because they are not influenced substantially by horizontal groundwater flow. At study sites where measurements of groundwater temperature at different depths do not exist, or where horizontal flow is substantial – for instance at riverbank filtration sites – a one-dimensional heat transport model is clearly unsuitable. At riverbank filtration sites the modeling of heat transport mechanistically is notoriously difficult because of the complexity of groundwater flow. In such cases, empirical modeling offers a possible alternative. In a recent study, Kurylyk et al. (2013) were able to forecast groundwater temperatures in a small forested catchment in New Brunswick, Canada, by linking groundwater temperature to soil-surface temperature using an empirical transfer function calibrated on a 2-yr-long time-series of groundwater temperature measured at different depths.

Here, we use historical, long-term groundwater temperature data measured by Swiss drinking-water suppliers to predict groundwater temperature up to the end of the current century. This is accomplished by first constructing linear regression models to link groundwater temperatures directly to ambient air temperatures, and then by using recently published regional air temperature projections[3] for Switzerland (CH2011, 2011) to drive these models. For locations where sufficiently long groundwater temperature time-series are available, this approach allows groundwater temperature to be modeled simply and rapidly from commonly available air temperature data. To our knowledge, this is the first study using historical time-series to predict the future impact of climate warming on groundwater temperatures.

---

[3] Following the definitions of the IPCC and CH2011 (2011) the term "projection" is used referring to estimates of future climate or air temperature. When referring to estimates of future groundwater temperature as obtained from the linear regression models applied here, the terms "prediction" or "forecast" are used.
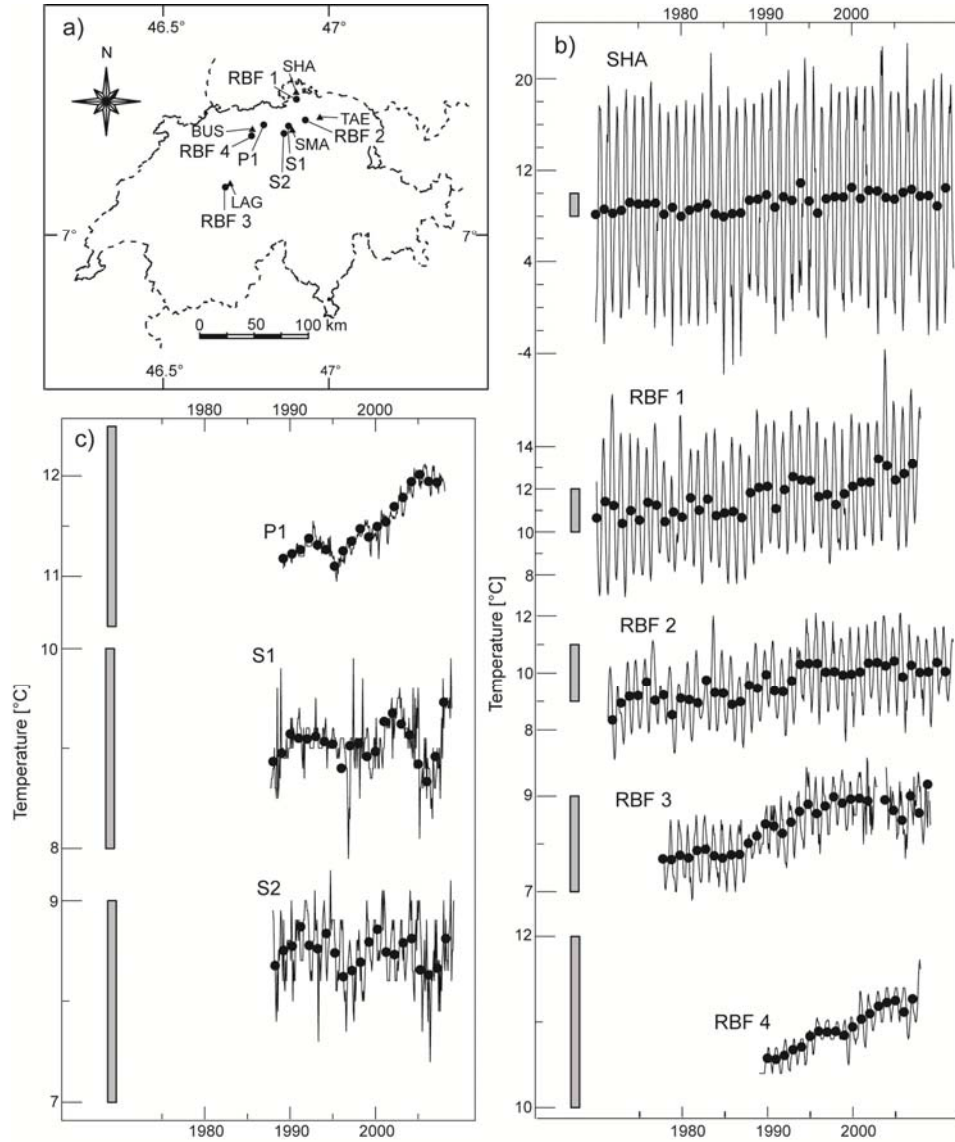
Figure 4.1: Map and temperature data. (a) Map of Switzerland showing the location of the aquifers investigated (filled circles) and SwissMeteo stations (triangles) from which data were obtained. (b) Air temperature time-series from the SHA SwissMeteo station (shown exemplarily for all air temperature data), and groundwater temperature time-series measured in the pumping wells of the 4 aquifers recharged by riverbank infiltration (*RBF 1-4*). (c) Groundwater temperature time-series measured in the pumping well of aquifer *P1* and in the well captures of aquifers *S1* and *S2*. The lines in (b) and (c) are the monthly mean time-series while the dots indicate annual mean values. Note the different scales on the y-axes. To facilitate comparison, a gray rectangle located on the left-hand side of each time-series illustrates a temperature difference of 2 K.

4.2 Data and Methods

4.2.1 Data

4.2.1.1 Groundwater temperature data

In this study we used seven groundwater temperature time-series from two different types of aquifers in Switzerland that are used for drinking-water production (Fig. 4.1a). The time-series covered periods of at least 19 years and sampling resolution was at least four measurements per year but usually better (Table 4.1). Four temperature time-series (*RBF 1-4*) were measured in the pumping wells of alluvial valley-fill aquifers that are recharged predominantly by riverbank

infiltration (Kempf et al., 1986 for *RBF1*; Kempf et al., 1986 and Beyerle et al., 1999 for *RBF2*; Blau and Muchenberger, 1997 for *RBF3*; and Jäckli, 1968 for *RBF4*). Aquifers *RBF1*, *RBF2*, and *RBF3* are identical to aquifers *RhSe*, *ToLi*, and *EmSi*, respectively, in Figura et al. (2011, 2013a). Time-series *P1* was measured in the pumping well of an aquifer that is recharged by precipitation only (Jäckli, 1968). The remaining two time-series (*S1*, S*2*) were measured in the capture points of two small depression springs. Table 4.1 contains general information on the aquifers. The annual mean and monthly mean groundwater temperature time-series are shown in Figs. 4.1b,c.
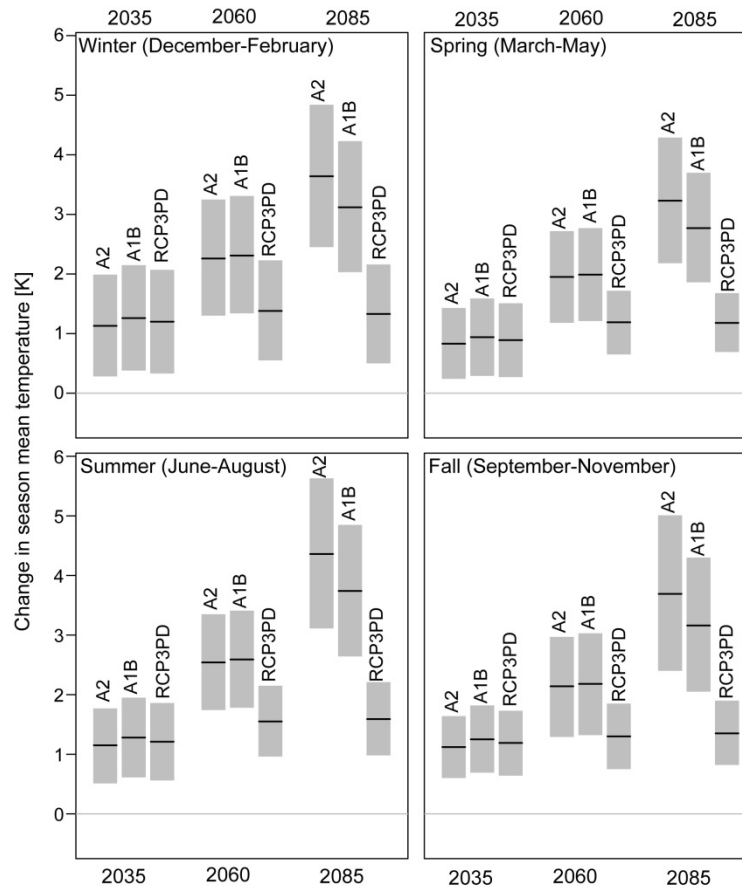
Figure 4.2: *CH2011* seasonal air temperature projections for northeastern Switzerland. Changes in seasonal mean temperature in northeastern Switzerland with respect to the reference period 1980-2009 for the three emission scenarios A2, A1B, and RCP3PD and three scenario periods 2035, 2060, and 2085. Data provided by the *CH2011* initiative (CH2011, 2011) and obtained from the *Center for Climate Systems Modeling* (C2SM; www.c2sm.ethz.ch).

4.2.1.2 Air temperature data

Monthly mean air temperatures measured 2 m above ground were obtained from the Federal Office for Meteorology and Climatology (MeteoSwiss) for the meteorological stations located closest to the aquifers (Fig. 4.1a). These stations were: Schaffhausen (SHA); Aadorf-Tänikon (TAE); Langnau im Emmental (LAG); Zürich-Fluntern (SMA); and Buchs-Aarau (BUS). All air temperature time-series covered the period 1950-2012 at least.

The groundwater temperature forecasts were based on the air temperature projections (Fig. 4.2) compiled within the framework of the *CH2011* initiative (CH2011, 2011) and obtained from the *Center for Climate Systems Modeling* (C2SM; www.c2sm.ethz.ch). In the *CH2011*

initiative, eight global climate models (GCM) were combined with 14 regional climate models (RCM) to obtain 20 projections of air temperature and precipitation for three regions in Switzerland (northeastern, western, and southern Switzerland). The calculations of the 20 GCM-RCM model chains were processed for the three scenario periods 2020-2049 (denoted in *CH2011* (2011) as 2035), 2045-2074 (2060), and 2070-2099 (2085), and for three different global greenhouse-gas emissions scenarios, respectively. Emissions scenario A2 assumes a regionally diverse economic growth under which the global population continuously increases and the introduction of efficient technologies is slow. Under this scenario greenhouse-gas emissions continue to increase until the end of the century. Emissions scenario A1B assumes very rapid economic growth worldwide, with an increase in global population until the middle of the century and a decline thereafter. Furthermore, the fast implementation of more efficient technologies is assumed, such that emissions reach a mid-century maximum before decreasing slightly. The RCP3PD scenario assumes a drastic reduction in greenhouse-gas emissions that allows the increase in global mean surface air temperature to be limited to 2 K with respect to the pre-industrial period (CH2011, 2011).

4.2.2 Methods

4.2.2.1 Processing of groundwater temperature data

Values that were suspected to be outliers by visual inspection were checked in more detail. If the difference between the suspect value and the mean of a 5-yr window around this value exceeded 3 standard deviations, the value was deleted. To make the data recorded at different and irregular time intervals better comparable, all data were interpolated at daily intervals using a cubic spline as long as gaps in the data did not exceed 3 months. In a next step the data were aggregated to monthly mean and annual mean values and a cubic regression model was fitted to the monthly mean data. To interpolate over gaps longer than 3 months, the deviations of the measured data from the cubic regression model were averaged for each month and added to the value modeled by the cubic regression model to obtain a monthly time-series, which was then used to fill the gaps. No gaps were longer than 4 months.

4.2.2.2 Processing of air temperature data

The historical air temperature data obtained from MeteoSwiss were already available as monthly mean values and required no further processing. The *CH2011* regional air temperature projections, however, were in the form of "lower", "medium", and "upper" estimates of the annual cycle of the change in air temperature relative to the 30-yr reference period 1980-2009, at daily resolution. To obtain air temperature projections for each of the five meteorological stations SHA, TAE, LAG, SMA, and BUS, the annual cycle of predicted changes (with respect to the reference period) in the regional air temperature of northeastern Switzerland was added to the mean annual cycle of daily mean air temperature at the relevant meteorological station for the 30-yr reference period. Thus absolute values of "lower", "medium", and "upper" air temperature projections were obtained at daily resolution for each emissions scenario (A1B, A2, RCP3PD), each scenario period (2035, 2060, 2085), and each meteorological station (SHA, TAE, LAG, SMA, BUS). The daily data were then aggregated to yield projections of monthly mean air temperature.

Table 4.1: Properties of the aquifers investigated. Descriptive characteristics of each aquifer investigated, including the approximate elevation of the ground surface; depth to the water table; thickness of the aquifer; amount of groundwater pumped from the wells or collected in the spring capture points; name of the losing river; duration and (in parentheses) measurement frequency of the available data; and the official abbreviation and elevation of the adjacent meteorological station. With regard to the measurement frequencies, the upper-case letters in parentheses specify the temporal resolution: bi-weekly (BW), monthly (M), or quarterly (Q). The lower-case letters in parentheses indicate whether the data consist of individual spot measurements (s) or are the mean of several measurements (m). (For example, Ms stands for one measured spot value per month and Mm for monthly mean values.)

ID	Elevation	Depth to water table	Thickness of aquifer	Pumping amount or spring discharge	Losing river	Available groundwater temperature data	Meteorological station (MeteoSwiss notation)	Elevation of the meteorological station
	[m a.s.l.]	[m]	[m]	$[10^6 \text{ m}^3 \text{ yr}^{-1}]$				[m a.s.l.]
RBF 1	374-385	10-20	10-15	0.4	Rhine	1971-2007 (Ms)	SHA	438
RBF 2	456-475	2.5-4	10-20	0.3	Toess	1972-2011 (Ms, Qs)	TAE	539
RBF 3	685-693	2-4	15-20	7	Emme	1980-2009 (Ms)	LAG	745
RBF 4	400-401	5-6	20-25	0.7	Suhr	1989-2007 (BWs)	BUS	387
P1	406-408	32-34	25-30	0.65	-	1989-2007 (BWs)	BUS	387
S1	540-542	-	2-5	0.01	-	1989-2010 (Mm)	SMA	556
S2	500-550	-	4-8	0.03	-	1989-2010 (Mm)	SMA	556

4.2.2.3 Linear regression models

As a first step in predicting groundwater temperature from air temperature, linear regression models were constructed to relate the two. This required some knowledge of the temporal delay up to which air temperature affects groundwater temperature. To obtain this knowledge we analyzed the cross-correlation functions between the time-series of air temperature and groundwater temperature. Prior to calculating the cross-correlation functions, the trend and the seasonality of the monthly mean time-series were removed using the seasonal-trend decomposition procedure of Cleveland et al. (1990) as implemented in the package *stl* of the statistical software *R* (R Development Core Team, 2011). The cross-correlation functions of the monthly mean time-series were in most cases significant ($P < 0.05$) up to lags of at most 12 months. The cross-correlation functions of the annual mean time-series were significant at lags of 0 to 2 yr.

Two linear regression models, Linear Model 1 (LM1) and Linear Model 2 (LM2), were built that differed slightly with regard to their main focus: whereas LM1 was focused on modeling the trend component in the annual mean groundwater temperature time-series, LM2 was formulated to capture the seasonal structure of each time-series more accurately by modeling the groundwater temperature for each month separately.

LM1 consisted of two separate multiple linear regression models, one for the annual mean target variable (eq. 4.1) and one for the monthly mean target variable (eq. 4.2), to account both for the significant correlations at lags of 0-2 years, and at lags of 0-12 months, respectively. The linear regression model for the annual mean values was intended to capture long-term trends, whereas the model for the monthly mean values accounted for seasonality. In the latter case the monthly mean time-series was first detrended using the seasonal-trend decomposition procedure of Cleveland et al. (1990).

To model the annual mean groundwater temperature, the following equation was used:

$$T(J) = \alpha + \sum \beta_k T_{in}(J - k) + \varepsilon(J) \qquad (4.1)$$

where *T(J)* is the annual mean target variable for year *J*, α and β_k are the regression coefficients, and $\varepsilon(J)$ is an error term. $T_{in}(J - k)$ denotes annual mean air temperature for year *J - k*, with $k = 0 \ldots 2$ yr.

Eq. 4.1 was also used in a first attempt to model the detrended monthly mean groundwater temperature. However, residual analysis for this approach revealed significant ($P < 0.05$) autocorrelations. To obtain adequate error estimates for the coefficients of the model for monthly mean values, we therefore added an autoregressive term and a moving average term (Box and Jenkins, 1970) to the regression model as follows:

$$T(M) = \alpha + \sum \beta_k T_{in}(M - k) + \sum \gamma_p T(M - p) + \sum \delta_q E(M - q) + \varepsilon(M) \quad (4.2)$$

where *T(M)* is the monthly mean target variable in month *M*, α and β_k are the regression coefficients, and $\varepsilon(M)$ is an error term. $T_{in}(M - k)$ is the monthly mean air temperature in month *M - k* with $k = 0 \ldots 12$ months. The number of variables was further reduced by stepwise elimination using the *R* function *step* (R Development Core Team, 2011). The autoregressive

term is described by γ_p (the p-th autoregressive parameter) and $T(M - p)$ (the monthly mean target variable in month $M - p$). Here, $p = 0$ or $p = 1$ or $p = 2$; when seasonality was strong, an additional term with $p = 12$ was added. The moving average term is defined by δ_q (the q-th moving-average parameter), and $E(M - q)$ (the white-noise error term for month $M - q$), with q taking on the same range of values as p. To obtain the final fitted temperature time-series of LM1 for each monthly mean value, $T(M)$ was then added to the annual mean value of the corresponding year, $T(J)$.

LM2 consisted of 12 multiple linear regressions, one for each month of the year (i.e., January, February,…, December), as follows:

$$T(M) = \alpha_c + \sum \beta_{c,k} T_{in}(M - k) + \varepsilon(M) \qquad (4.3)$$

where α_c and $\beta_{c,k}$ are again the regression coefficients for month M but are specific to the month of the year being modeled. $\varepsilon(M)$ is again the error term. To avoid over-parameterization, the maximum value of k was set to 12 months. The number of parameters in the 12 models was again reduced using *step*. The data for the LM2 model were detrended, and no autoregressive or moving average terms to account for auto-correlation were added. Each of the 12 separate regressions comprising LM2 described the long-term development of the groundwater temperature in one month only. LM2 was assumed to capture the seasonal structure of the data better than LM1.

LM1 and LM2 thus differed with respect to two major points. Firstly, LM1 took into account the relationship between annual mean groundwater temperature and annual mean air temperature for lags of up to 2 yr, while LM2, which was confined to monthly means, was able to take into account the relationship between the two variables only for lags of up to 12 months. Secondly, in LM1 the regression coefficients (β_k) in the model for monthly means (eq. 4.2) are the same for each month (e.g., the coefficients used to model the groundwater temperature in December from the air temperature in the previous few months are the same as the coefficients used to model the groundwater temperature in May). By contrast, the regression coefficients (β_k) in LM2 are unique; i.e., they are different for each month.

For each time-series, models LM1 and LM2 were calibrated on the data covering the period from the beginning of the time-series (which varied from time-series to time-series) to 2007. The calibrated models were then fed with *CH2011* air temperature projections to yield forecasts of monthly mean groundwater temperature. The use of the "lower", "medium", and "upper" estimates of air temperature projections resulted in three corresponding output time-series, which we will call here the "lower medium", "medium medium" and "upper medium" time-series (Fig. 4.3). Each of these time-series of groundwater temperature predictions had an error given by the corresponding prediction interval *PI* of the linear regression model (eq. 4.4), so that six further time-series resulted: a "lower lower", "lower upper", "medium lower", "medium upper", " upper lower", and "upper upper" time-series (Fig. 4.3):

$$PI(\hat{y}_t) = \hat{y}_t \pm q_{0.975}^{t_{n-2}} \sqrt{\sigma^2 + (s.e.(\hat{y}_t))^2} \qquad (4.4)$$

where $\hat{y}_t$ is the estimated value of the target variable at time t, $q_{0.975}^{t_{n-2}}$ is the respective quantile of the t-distribution, n is the number of data points, σ is the standard error of the residuals, and $s.e.(\hat{y}_t)$ is the standard error of $\hat{y}_t$. The standard error $s.e.(\hat{y}_t)$ is itself a combination of σ and the sum of squares of the independent variable. For LM1 the errors of the linear regression model for the annual mean values and monthly mean values were added to obtain the total error. It should be noted here that the structure of the *CH2011* air temperature projections leads to asymmetric errors in the groundwater temperature predictions. The interannual variability of the "upper" estimates of the *CH2011* air temperature projections is greater than that of the "lower" estimates. This fact leads to the last term of eq. 4.4, and thus also *PI*, being greater when the "upper" estimates of monthly mean air temperature projections are fed into the models than when the "lower" estimates are used.

Of the nine groundwater temperature time-series that result from each emissions scenario (Fig. 4.3), five are relevant here: the "medium medium" time-series, which represents the most probable forecast of groundwater temperature; the "lower medium" and "upper medium" time-series, which represent the error in the groundwater temperature forecast caused by the uncertainty inherent in the climate projections (i.e., the error associated with the range of the air temperature projections); and the "lower lower" and "upper upper" time-series, which are obtained from the combination of the error caused by the uncertainty in the air temperature projections and the model error (Fig. 4.3). Henceforth, the total error is defined as the difference between the "upper upper" and "lower lower" estimates; the error caused by the uncertainty of the air temperature projections is defined as the difference between the "upper medium" and "lower medium" estimates; and the model error is defined as the difference between the total error and the error caused by the uncertainty of the air temperature projections (Fig. 4.3).
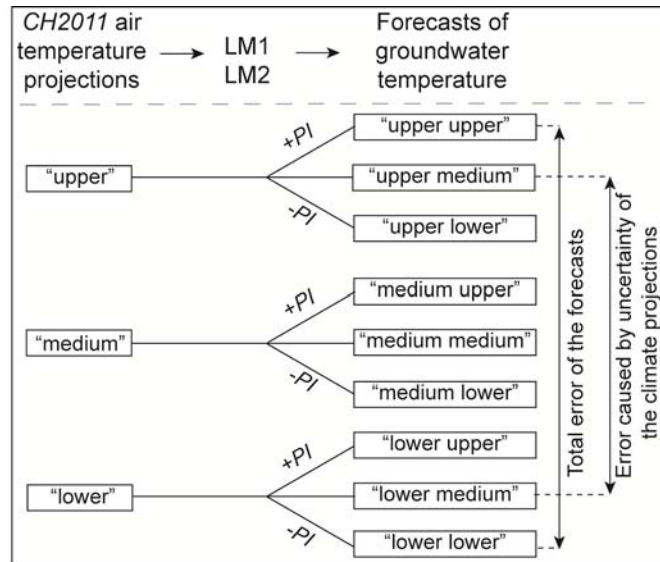
Figure 4.3: Explanation of the groundwater temperature prediction procedure. For every emissions scenario (A2, A1B, RCP3PD) and every scenario period (2035, 2060, 2085) the linear regression models LM1 and LM2 were fed with the "lower", "medium", and "upper" *CH2011* air temperature projections to yield forecasts of groundwater temperature ("lower medium", "medium medium", "upper medium", etc.). The errors associated with each of these forecasts were calculated using eq. 4.4. The arrows on the right-hand side indicate the total error of the groundwater temperature predictions and the error attributable to the uncertainty in the climate projections. The model error (not shown in the figure) was defined as the difference between the two.

4.2.2.4 Evaluation of the models

A model evaluation based on the forecasts of groundwater temperature was conducted to compare LM1 with LM2 and, for each model, to partition the total prediction error into two error components: one attributable to the uncertainty inherent in the climate projections and one to the model error. Additionally, the goodness of fit of both models and their robustness with respect to the underlying data used for calibration were assessed. To accomplish this, the groundwater temperature data were split into a variety of training periods and evaluation periods that were required to fulfill the following three criteria: the ratio of training period to evaluation period had to be at least 2:1; the length of the evaluation period had to be at least 3 yr; and the training period had to start no later than 1989. The data from the training periods were used to calibrate the linear regression models, which were then used to model the groundwater temperature during the evaluation periods. The models were used only for forecasting; i.e., no hindcasting was performed. The goodness of fit of the models was evaluated based on the ratio of the root mean square error to the standard deviation (*RSR*, nomenclature from *Moriasi et al.*, 2007; eq. 4.5) and on the mean bias (*BIAS*; eq. 4.6). *RSR* and *BIAS* were calculated for the modeled and measured groundwater temperature data during the evaluation periods as follows:

$$RSR = \frac{\sqrt{\sum_{i=1}^{n}(\hat{y}_i - y_i)^2}}{\sqrt{\sum_{i=1}^{n}(y_i - \bar{y})^2}} \tag{4.5}$$

$$BIAS = \frac{\sum_{i=1}^{n}(\hat{y}_i - y_i)}{n} \tag{4.6}$$

where $\hat{y}_i$ and y_i denote the modeled and measured groundwater temperatures, respectively, in the evaluation period, and $\bar{y}$ is the mean value of the n groundwater temperatures measured during the evaluation period. A comparison of the predictions calculated with models that were calibrated on different training periods allowed the sensitivity of the model predictions to the choice of training period to be evaluated.

4.3 Results

4.3.1 Forecasts based on models calibrated on the whole length of the time series

For each aquifer, models LM1 and LM2 were fitted to data covering the period from the start of the relevant time-series to a common end point, 2007. Thus, the data used for calibrating the models were from 1971-2007 for *RBF1*; 1972-2007 for *RBF2*; 1979-2007 for *RBF3*; and 1989-2007 for *RBF4*, *P1*, *S1*, and *S2*. The following two sections present forecasts of the annual and seasonal means of groundwater temperature calculated using the models calibrated on these training periods and fed with the *CH2011* air temperature projections for northeastern Switzerland.

Fig. 4.4 shows the predicted changes in annual mean groundwater temperature with respect to the reference period 1980-2009. In all aquifers the "medium medium" predictions indicate an increase in groundwater temperature by the end of the century. However, the predicted changes

in annual mean groundwater temperature differ strongly among the aquifers, especially under emissions scenarios A2 and A1B (Fig. 4.4a,b). Under emissions scenario RCP3PD, however, groundwater temperatures are predicted to remain approximately constant after the 2035 scenario period (Fig. 4.4c), and the differences in the "medium medium" groundwater temperature predictions among the aquifers are less accentuated.
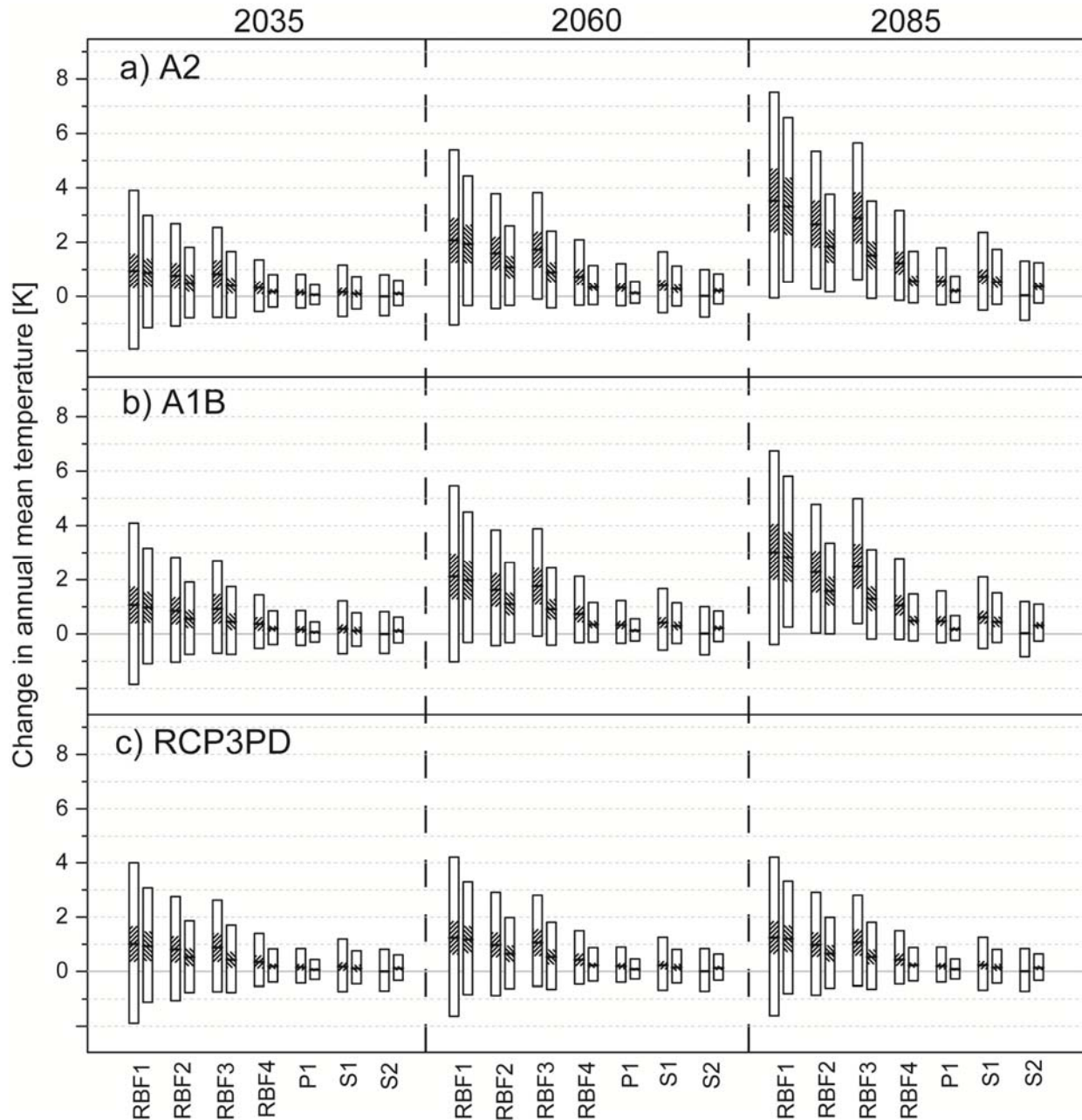
Figure 4.4: Forecasts of groundwater temperature. Model predictions of the change in mean annual groundwater temperature with respect to the reference period 1980-2009 for the three emission scenarios (a) A2, (b) A1B, and (c) RCP3PD. Shown are the forecasts of the two linear regression models (LM1, LM2) for each aquifer (*RBF1 - RBF4, P1, S1 - S2*) and scenario period (2035, 2060, 2085). For each aquifer the LM1 model prediction is shown in the left-hand bar (hatching from lower left to upper right), and the LM2 model prediction in the right-hand bar (hatching from upper left to lower right). The bars indicate the total error of the prediction, the bold horizontal lines within each bar show the "medium medium" prediction, and the hatched areas indicate the error attributable to the uncertainty in the climate projections (see text and Fig. 4.3).

The differences among the aquifers mentioned above allow the seven aquifers to be divided roughly into two groups. The first group consists of aquifers *RBF1, RBF2*, and *RBF3* for which a very strong, continuous warming is forecast. In the 2085 scenario period the "medium medium" predictions for aquifers *RBF1, RBF2*, and *RBF3* range from a warming of 0.5 K under emissions scenario RCP3PD (calculated for *RBF3* with LM2; range of the total error: -0.6 to 1.8 K) to a warming of 3.5 K under emissions scenario A2 (*RBF1*; LM1; -0.1 to 7.5 K) (Fig. 4.4). In the second group, consisting of the four aquifers *RBF4, P1, S1*, and *S2*, groundwater temperatures are predicted to rise only slightly under all emissions scenarios, and the "medium medium" predictions do not exceed a maximum of 1.2 K, which occurs under scenario A2 (*RBF4*; LM1; -0.1 to 3.2 K) (Fig. 4.4).

The "lower lower" values of the forecasts for the 2035 and 2060 scenario periods are negative for all emissions scenarios, implying that the predictions do not exclude a situation in which no warming or even a slight cooling might take place. Under emissions scenarios A2 and A1B in the 2085 scenario period, however, the ranges of the total error for *RBF1* with LM2, *RBF2* with both models (LM1 and LM2), and *RBF3* with LM1 contain no negative values (Fig. 4.4a,b) implying that in these cases warming is expected.

Forecasts of seasonal means, which were obtained by aggregating the monthly mean forecasts, indicate no clear differences in the expected warming among the seasons (Fig. 4.5).
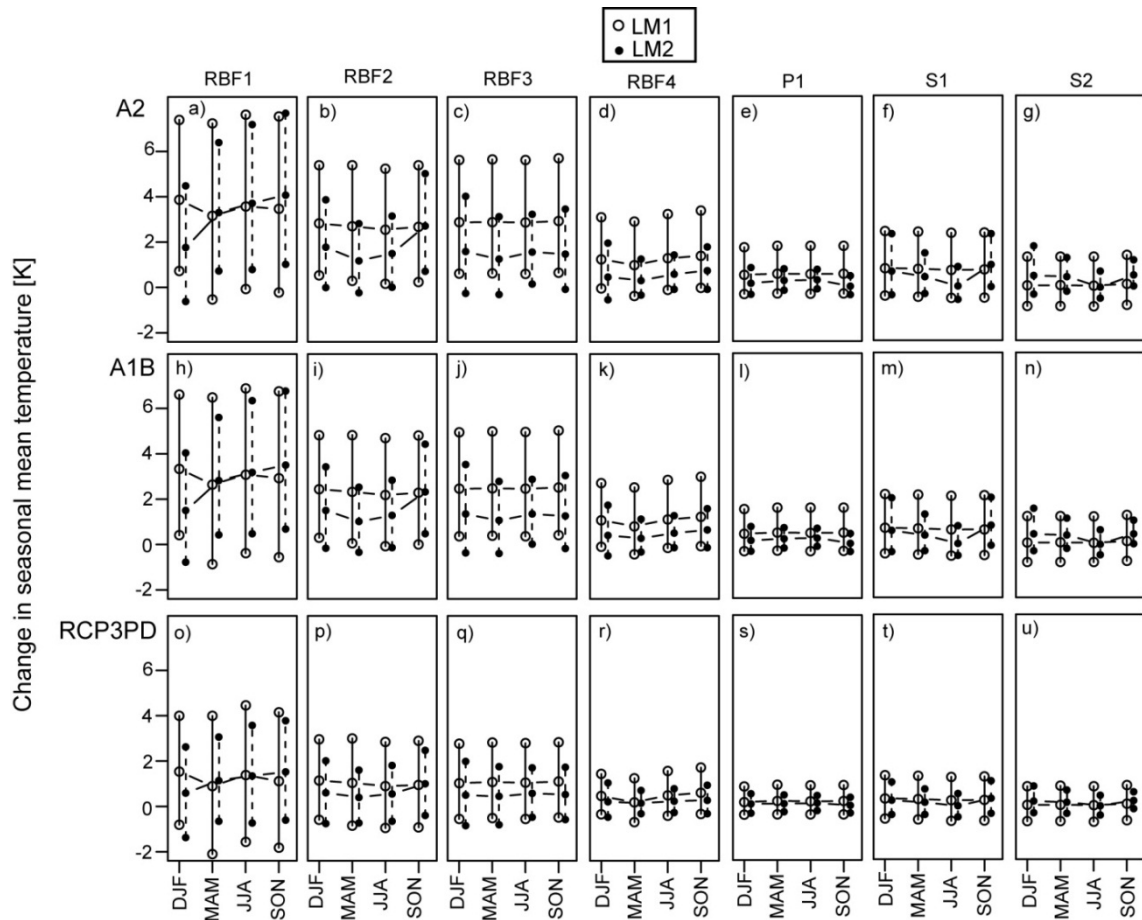
Figure 4.5: Forecasts of seasonal groundwater temperature for the 2085 scenario period. Model predictions of the change in seasonal groundwater temperature for the 2085 scenario period (2070-2099) using models LM1 (open circles) and LM2 (full circles) for each aquifer (columns: *RBF1 - RBF4, P1, S1 - S2*) and emission scenario (rows: A2, A1B, RCP3PD). The change in each season is described with respect to the seasonal mean of the reference period 1980-2009. Unlike Fig. 4.4, only the total error of each prediction is shown.

4.3.2 Model evaluation

4.3.2.1 Model evaluation based on the forecasts

4.3.2.1.1 Models calibrated on the whole length of the time-series
A comparison of the model forecasts from LM1 and LM2 reveals clear differences between the two. Except for the case of *S2*, the "medium medium" predictions of LM1 forecast a stronger warming than those of LM2 (Fig. 4.4). For example, the difference between the "medium medium" predictions of LM1 and LM2 at *RBF3* reaches a value of 1.4 K under emissions scenario A2 in the 2085 scenario period. These findings are reflected in the forecasts of seasonal mean groundwater temperatures (Fig. 4.5). In addition, the variability among the seasonal predictions is greater for LM2 than for LM1 (Fig. 4.5).

An evaluation of the errors in the predictions shows that the model error accounts for most of the total error, with the share attributable to the uncertainty in the climate projections being clearly smaller. The largest contribution of the model error to the total error (99%) is found in the LM1 predictions for the 2085 scenario period using emissions scenario A2 at aquifer *S2*. However, in most cases the contribution of the model error to the total error ranges between 63% and 85% (Fig. 4.4). The errors in the forecasts further show that the error range for LM1 is greater than that for LM2, and that the error range is greater in aquifers recharged by RBF than in the other aquifers.

4.3.2.1.2 Models calibrated to different training periods
At *RBF4*, *P1*, *S1*, and *S2* the models were calibrated on the training periods 1989-2001 to 1989-2004, which represent all training periods that fulfill the above-mentioned training-period criteria. For *RBF2* and *RBF3* only training periods 1972-2001 to 1972-2004 and 1980-2001 to 1980-2004 were chosen, which represented the longest possible training periods of the *RBF2* and *RBF3* aquifers that had the same evaluation periods as the *RBF4*, *P1*, *S1*, and *S2* aquifers.

The forecasts of the models calibrated on different training periods are shown in Fig. 4.6 for the 2085 scenario period under emission scenario A2. For aquifers *RBF1* - *RBF4* (Fig. 4.6a-d) the models generally forecast a stronger warming the longer the training period is. At *RBF1* (Fig. 4.6a, only for training periods 1989-2001 and 1989-2002), *RBF2* (Fig. 4.6b) and *RBF3* (Fig. 4.6c) the mean predictions of the regression models that were calibrated on training periods starting in 1989 are lower than those of the models calibrated on training periods starting in either 1980 (Fig. 4.6a,b,c) or 1972 (4.6a,b). At *RBF1* - *RBF3* it should also be noted that for training periods starting in 1989 a larger proportion of the total error is attributable to model error than for other training periods. The predictions of models calibrated on different training data for aquifers *S1*, *S2*, and *P1* (Fig. 4.6e-g) show no evident general features. However, some model predictions are notable because only a very slight warming is predicted and their errors are attributable almost entirely to the model error (Fig. 4.6e-g).
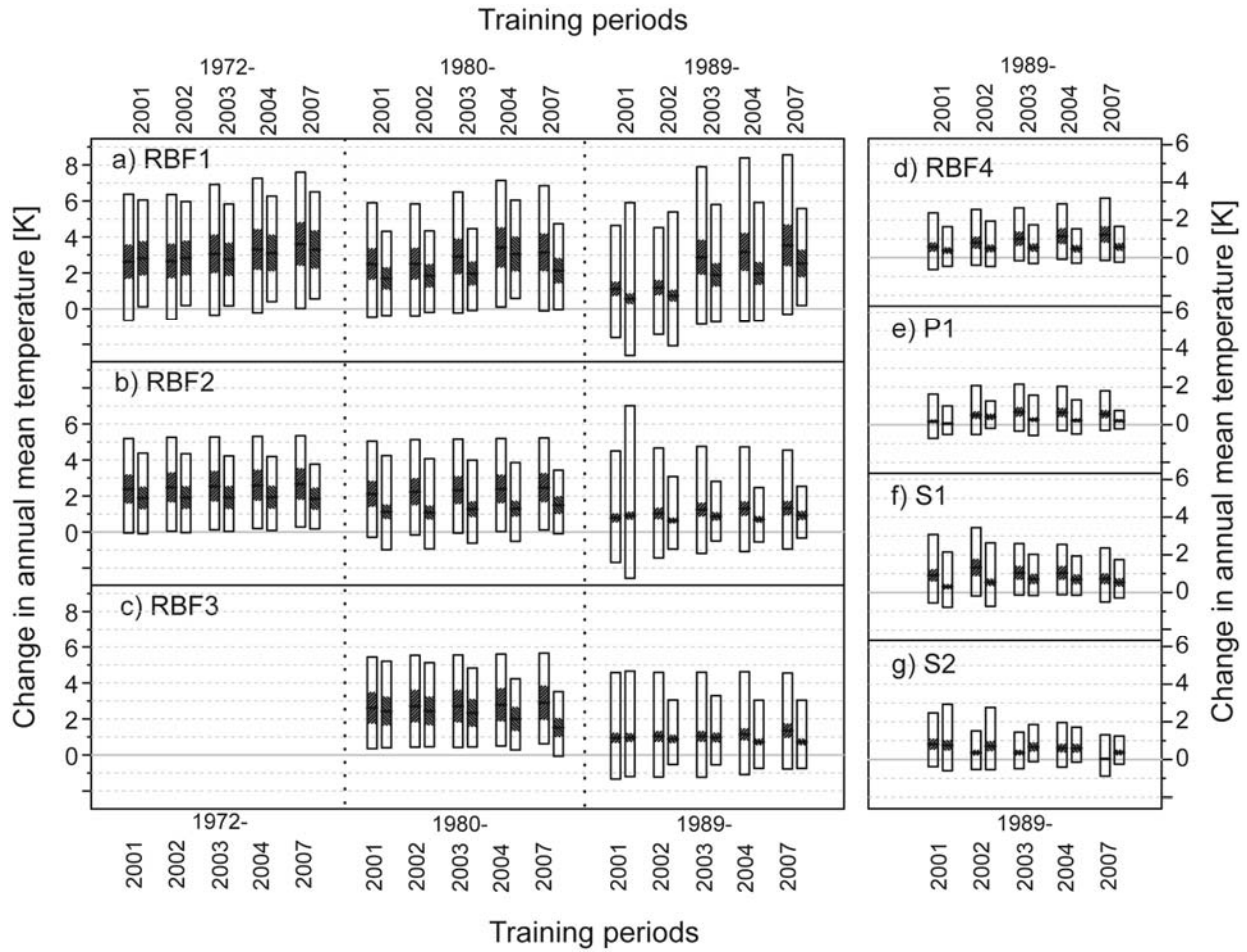
Figure 4.6: Forecasts of groundwater temperature made by models LM1 and LM2, calibrated on different training periods, for emissions scenario A2 and the 2085 scenario period. Model predictions of the change in mean annual groundwater temperature with respect to the reference period 1980-2009 in aquifers *RBF1 - RBF4*, *P1*, and *S1 - S2* for the 2085 scenario period based on emissions scenario A2. The two linear regression models (LM1, LM2) were calibrated to different training periods, which are shown in the x-axis of each panel. For each training period the LM1 prediction is shown in the left-hand bar, the LM2 prediction in the right-hand bar. The bars indicate the total error of the predictions, the bold horizontal lines in each bar show the "medium medium" prediction, and the shaded areas indicate the error attributable to the uncertainty in the climate projections (see text).

4.3.2.2 RSR and BIAS of models calibrated to different training periods

4.3.2.2.1 RBF1 aquifer

Because the groundwater temperature time-series at the *RBF1* aquifer was longest, the regression models for this aquifer were calibrated to all training periods that fulfilled the above-mentioned three training-period requirements. Figure 4.7a shows that RSR can vary strongly depending on the choice of training period. This is especially true for LM2, for which *RSR* varies up to a maximum value of 0.46 (difference between RSR for the training period 1974-2001 and the training period 1989-2001). By contrast, for LM1 the maximum difference between RSR values in an evaluation period is 0.1 (difference between *RSR* values for the training period 1981-1998 and the training period 1974-1998). Also, *RSR* values for LM1 are in most cases below 0.5, indicating a good model performance [*Moriasi et al.*, 2007]. The RSR values for LM1 and LM2 are approximately the same in the evaluation periods 1995-2007, 1996-2007, 1997-2007, 1998-2007, and 1999-2007 (evaluation periods i-iv in Fig. 4.7a). In the

evaluation periods starting in the year 2000 or later (evaluation periods v-x in Fig. 4.7a), the *RSR* values indicate, however, that LM1 performed better than LM2 when the models were calibrated to the same training period.

The *BIAS* values are in most cases negative, and show that in general the models underestimate the measured groundwater temperatures in the evaluation periods by approximately 0.5 K to 1 K (Fig. 4.7b). The exception is LM2 for the evaluation periods 1996-2007, 1997-2007, and 1998-2007, where the model overestimates the measured values. Some features of the *BIAS* values are similar to those found for the *RSR* values. For instance, the *BIAS* values show a much higher variability for LM2 than for LM1, and with decreasing length of the training period the *BIAS* of LM2 increases, while the *BIAS* of LM1 slightly decreases.

Figure 4.7: *RSR* and *BIAS* of models LM1 and LM2 for aquifer *RBF1* calibrated to different training periods. Values of (a) *RSR* and (b) *BIAS* for groundwater temperature models LM1 (open circles) and LM2 (full circles) applied to aquifer *RBF1*. To evaluate the models, they were calibrated to different training periods and employed to forecast the groundwater temperature during ten evaluation periods (segments i - x). The x-axis shows the starting years of each training period that ends in the year immediately previous to the start of the respective evaluation period. For example, the values of *RSR* and *BIAS* given for 1977 in segment vii (= evaluation period 2002-2007) refer to the training period 1977-2001 (where 2001 is the year immediately preceding 2002).

4.3.2.2.2 All aquifers

As mentioned above, the models for *RBF2, RBF3, RBF4, P1, S1,* and *S2* were also calibrated to different training periods. Based on the RSR values, the goodness of fit of the LM1 models for the groundwater temperature at *RBF2* (Fig. 4.8b) is similar to that at *RBF1* (Figs. 4.7a, 4.8a).

The increase in the *RSR* of LM2 with decreasing length of the training period, however, is more pronounced at *RBF2* (Figs. 4.8a,b). At *RBF3* (Fig. 4.8c) the RSR values are higher than at *RBF1* and *RBF2*. The RSR values at *RBF4* (Fig. 4.8d), *P1* (Fig. 4.8e), *S1* (Fig. 8f), and *S2* (Fig. 4.8g) are higher than at the other three aquifers. Note that the *RSR* for aquifers *RBF4*, *P1*, *S1*, and *S2* and some *RSR* values of LM2 at *RBF2* and *RBF3* are larger than 1, implying that the mean groundwater temperature would fit better than the regression model. At *S1* and *S2* the difference between LM1 and LM2 is substantial (Figs. 4.8f,g).

Figures 4.8i-n show that the model predictions at *RBF2*, *RBF3*, *RBF4*, *P1*, *S1*, and *S2* deviate less from the measured values than the model predictions at *RBF1* (Fig. 4.7b, 4.8h). The predictions of both models at *RBF2* (Fig. 4.8i) and *RBF4* (Fig. 4.8k), and the predictions of LM2 at *RBF3* (Fig. 4.8j), slightly underestimate the measured values in the evaluation period. At *P1* (Fig. 4.8l) and *S1* (Fig. 4.8m) the models overestimate the measured values. The *BIAS* of both models at *S2* is small (Fig. 4.8l) and the bias of LM2 at *RBF3* is scattered around zero (Fig. 4.8j).
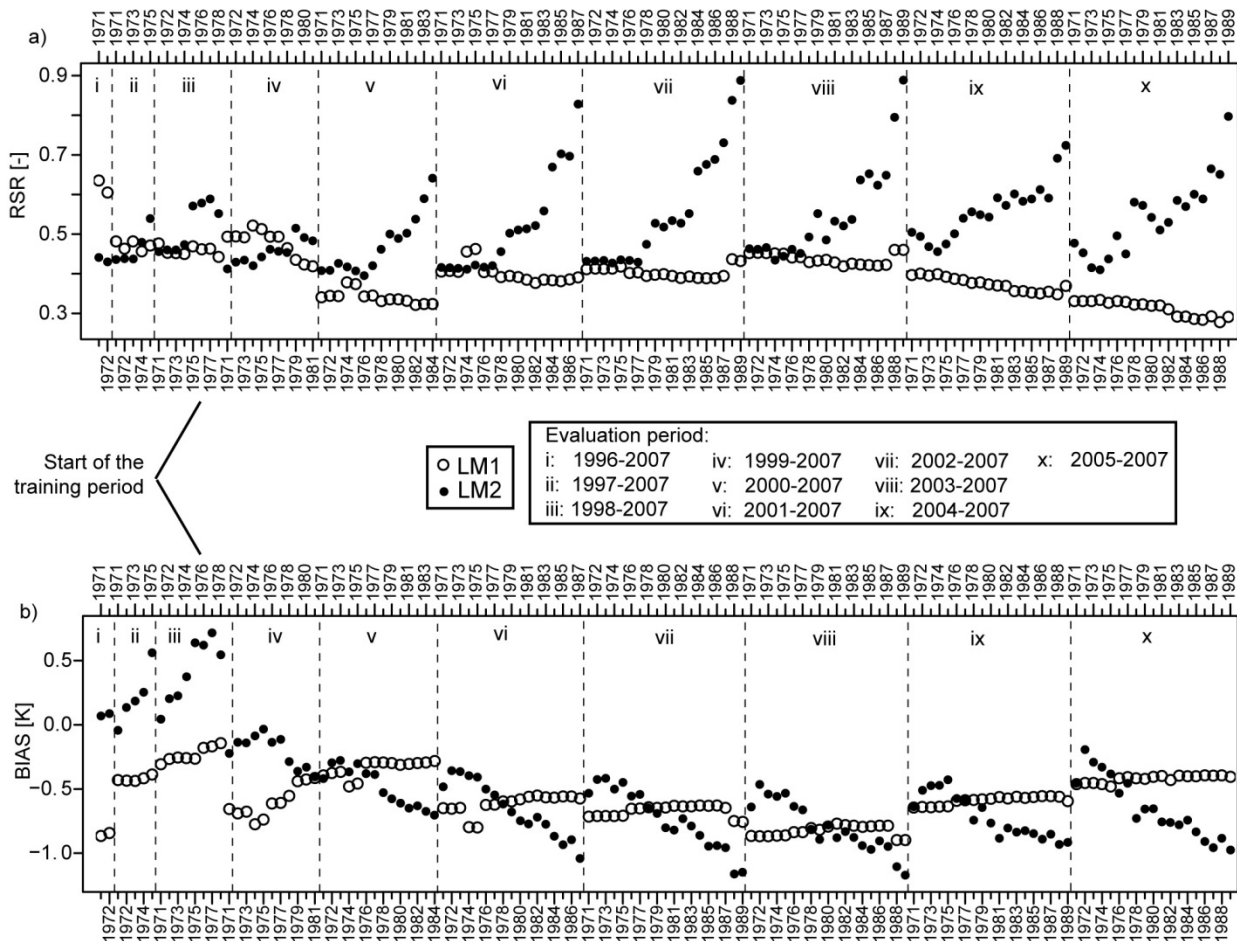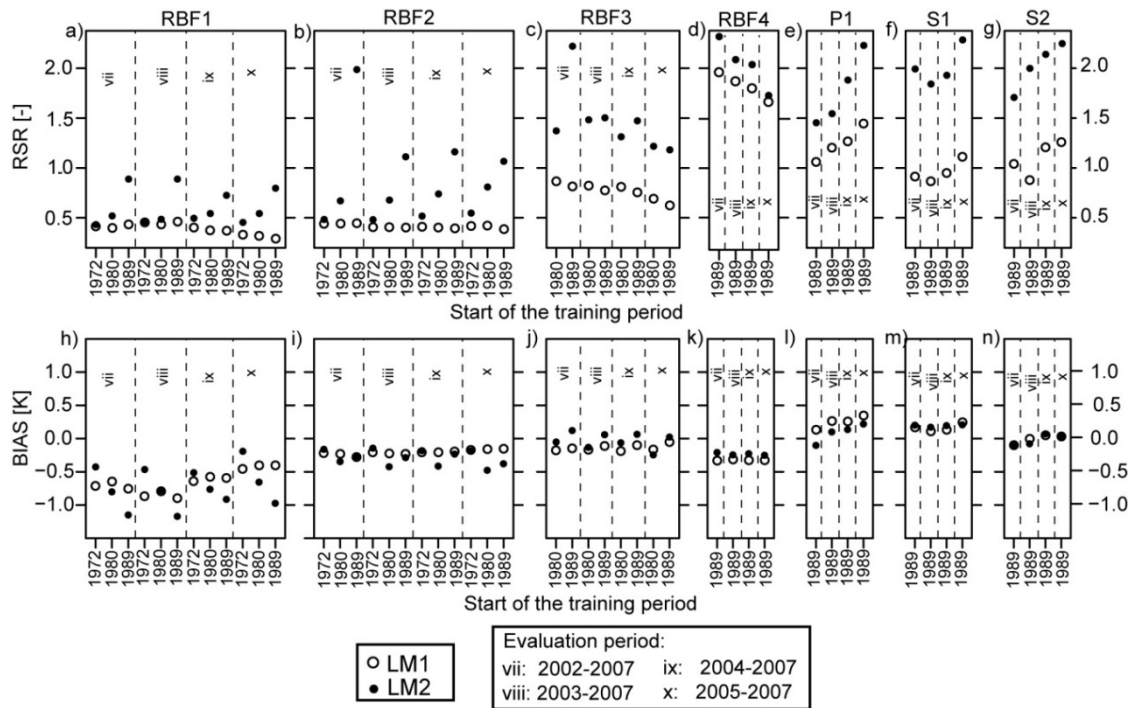

Figure 4.8: *RSR* and *BIAS* of models LM1 and LM2 for all aquifers calibrated to different training periods. Values of (a) *RSR* and (b) *BIAS* for groundwater temperature models LM1 (open circles) and LM2 (full circles) applied to all aquifers. To evaluate the models, they were calibrated to different training periods and employed to forecast the groundwater temperature during ten evaluation periods (segments i - x). The x-axis shows the starting years of each training period that ends in the year immediately previous to the start of the respective evaluation period. For example, the values of *RSR* and *BIAS* given for 1989 in segment viii (= evaluation period 2003-2007) refer to the training period 1989-2002 (where 2002 is the year immediately preceding 2003).

4.4 Discussion

When discussing the results of empirical models, such as the linear regression models employed here, it has to be kept in mind that the validity of any empirical model is limited to the range of

data used in its construction. Our forecasts are thus valid only if it can be assumed that the empirical relationship linking groundwater temperature to air temperature remains the same even under different environmental conditions. By calibrating our models to different training periods we attempted to simulate a variety of environmental conditions, which allowed the reliability of the model predictions to be evaluated.

The model evaluation shows that the choice (or availability) of training period data has an impact on the goodness of fit of the models in the evaluation periods and, consequently, on the outcome of the groundwater temperature forecasts. Three features highlight this dependence. Firstly, the computed *RSR* and *BIAS* values show that the goodness of fit of the models depends strongly on the choice of training period (Figs. 4.7, 4.8). Secondly, this finding is confirmed by the groundwater temperature predictions at *RBF1*, *RBF2*, and *RBF3* produced by models calibrated on different training periods (Figs. 4.6a,b,c). The groundwater temperature predictions are distinctly lower when the start of the training period is moved for instance from 1980 to 1989 or from 1972 to 1980 (Figs. 4.6a,b,c). Thirdly, the analysis of the share of the total error that is attributable to the uncertainty in the model predictions as opposed to the uncertainty in the climate projections gives a further indication of the influence of the training period on the goodness of fit of the models. When the contribution of the error attributable to the model prediction is relatively high, this indicates a rather poor model performance. If the model fits poorly, the regression coefficients (the βs in eqs. 1-3) are small and the model prediction is more or less constant. As a consequence, the difference between the "lower medium" and "upper medium" groundwater temperature prediction is small. Figs. 4.6a,b,c show that the error attributable to the model is noticeably greater when the models were calibrated to training data that did not begin until 1989. The likely reason for this is that the variability of the groundwater temperature time-series after 1989 is not sufficiently large to establish a good empirical relationship between the groundwater temperature and air temperature data.

The abrupt increase in groundwater temperature from 1987 to 1988 (Figura et al., 2011) represents a potentially important source of variability in the training data. To test the hypothesis that the inclusion of this abrupt increase was essential to establishing a good empirical relationship between groundwater temperature and air temperature, we modified the groundwater temperature data from aquifers *RBF1 - RBF3* and the corresponding air temperature data by removing the late 1980s regime shift from all time-series. For each time-series, this was accomplished by calculating the difference between the mean temperature measured before 1988 and after 1988, and subtracting this difference from that part of the time-series that covered the period from 1988 onward. The resulting modified time-series were used to recalibrate the models. We hypothesized that calibration of the groundwater temperature models to the modified time-series would result not only in lower "medium medium" predictions, but also in an increase in the share of the total prediction error attributable to the model error. For aquifers *RBF1 - RBF3* the model predictions calibrated to the modified data are shown in Fig. 4.9 for the example of emissions scenario A2 and the 2085 scenario period. The groundwater temperature forecasts of the models that were calibrated to the modified data were lower than those of the models calibrated to the unmodified data by 0.9 to 2.4 K, and the share of the total error attributable to the model error was clearly higher (Fig. 4.9). The impact of the removal of the late 1980s regime shift on the forecasts suggests that the linear regression

models are unlikely to be capable of capturing the variability in the groundwater temperature data sufficiently well, if the data do not contain a pronounced pattern such as the late 1980s regime shift.

To test additionally whether the existence of a single year with extraordinary temperatures might affect model performance in the same way as the occurrence of the late 1980s regime shift, the data were modified in a further way. In the year 2003, Switzerland experienced an extremely hot, dry summer (Schär et al., 2004) that affected groundwater temperatures and other aspects of groundwater behavior (BUWAL, 2004). The 2003 data were removed from the time-series by replacing them (month by month) with the mean of the corresponding values observed in 2002 and 2004. However, removal of the 2003 data had essentially no effect on the model performance (Fig. 4.9). Removing the 2003 data from the time-series that had already been modified by removing the late 1980s regime shift also had no effect on the model performance (Fig. 4.9). Thus, although the presence in the training data of the abrupt shift in the late 1980s had a substantial effect on model performance, it is unlikely that the presence of one individual extreme year, such as 2003, in the training data will suffice to affect model performance to any noticeable degree.
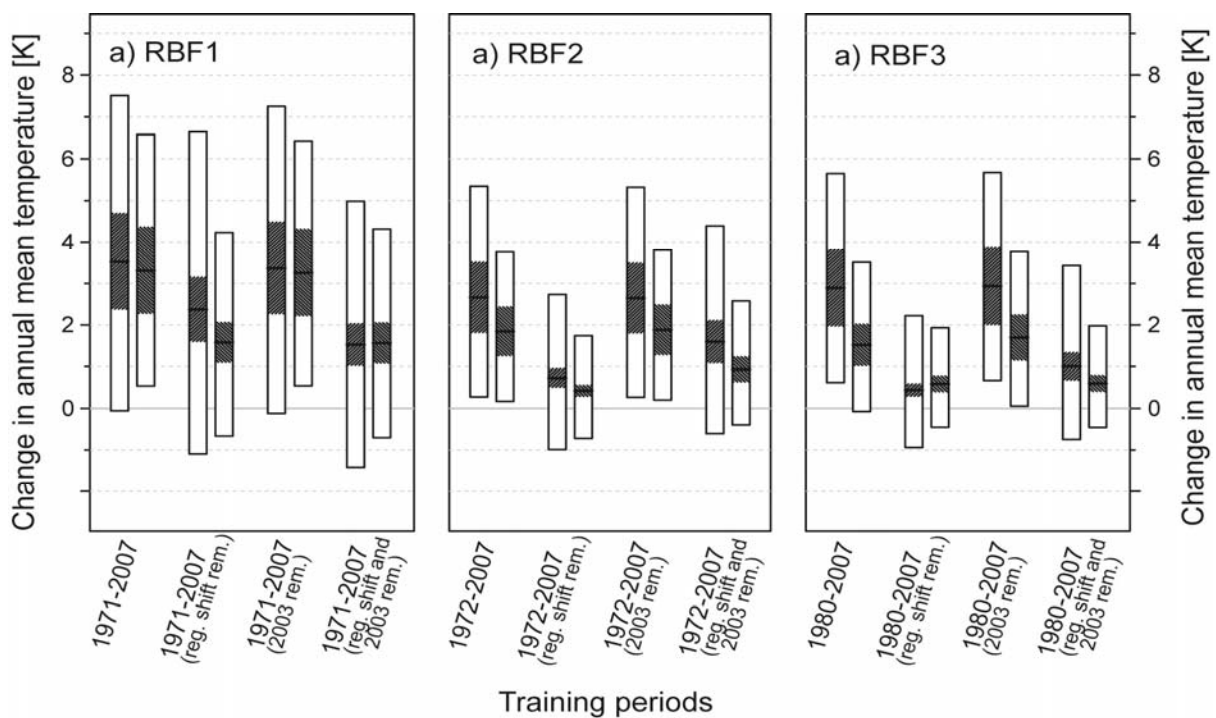
Figure 4.9: Forecasts of groundwater temperature for aquifers *RBF1 - RBF3*, emissions scenario A2, and the 2085 scenario period made by models LM1 and LM2 calibrated on modified training data. Model predictions of the change in mean annual groundwater temperature with respect to the reference period 1980-2009 in aquifers *RBF1 - RBF3* for the 2085 scenario period based on emissions scenario A2. The two linear regression models (LM1, LM2) were calibrated to the data used for the predictions illustrated in Fig. 4.4 and to modified data. The modified data were created (i) by removing the shift in groundwater temperature from 1987 to 1988 (3rd and 4th bars in each panel, denoted by reg. shift rem.); (ii) by replacing the values of the year 2003 with the mean value of the years 2001 and 2002 (5th and 6th bars in each panel, denoted by 2003 rem.); or (iii) by making both modifications (7th and 8th bars in each panel, denoted by reg. shift and 2003 rem). For each data set the LM1 prediction is shown in the left-hand bar and the LM2 prediction in the right-hand bar. The bars indicate the total error in the predictions, the bold horizontal lines in each bar show the "medium medium" prediction, and the shaded areas indicate the error attributable to the uncertainty in the climate projections (see text).

Two important aspects of the errors of the forecasts need to be noted here. Firstly, the error range of the predictions for the aquifers recharged by RBF exceeds that for the aquifers recharged by precipitation only. The reason for this is presumably that fluctuations in the annual mean groundwater temperature are greater for aquifers recharged by RBF than for aquifers recharged by precipitation only (Fig. 4.1). These larger interannual fluctuations are reflected in the larger error ranges. Secondly, it should be noted that the error ranges in the LM1 predictions exceed those of the LM2 predictions because in LM1 the errors of the annual mean (eq. 4.1) and monthly mean (eq. 4.2) models are added.

Based on our findings, it is not possible to determine whether the forecasts for the aquifers *RBF4*, *P1*, *S1*, and *S2* (Fig. 4.4) are low because the models are not able to capture the variability of the groundwater temperature, or because groundwater temperature in these aquifers does not respond to changes in air temperature as strongly as in the aquifers *RBF1* - *RBF3*. The groundwater temperature predictions for aquifers *RBF4*, *P1*, *S1*, and *S2* (Figs. 4.4, 4.6d,e,f,g) might thus be too low, and should be regarded as minimum estimates.

While the groundwater temperature forecasts might not be strictly robust for aquifers *RBF4*, *P1*, *S1*, and *S2*, they most probably are for aquifers *RBF1* - *RBF3*. Because there is a large discrepancy between the LM1 and LM2 predictions at *RBF2* and *RBF3*, the range of warming to be expected in these two aquifers is large. However, Figs. 4.6a,b,c, 4.7, and 4.8 show that for LM1, the goodness of fit and the predictions at *RBF1* - *RBF3* are more robust than for LM2. These differences in the forecasts and performance of the two models are clearly related to their structure. Because mean annual air temperature is often reflected well in annual mean groundwater temperature (Anderson, 2005), LM1 is able to capture the long-term trend in groundwater temperature quite well. If LM2 fails to describe groundwater temperature sufficiently in all months or in a subset of months, it will consequently also fail to model the long-term trend in the annual mean groundwater temperature adequately. The possibility of LM2 failing in a certain month appears to be rather high, presumably because short-term variability in various external forcing factors besides air temperature (e.g., changes in flow conditions resulting from extreme precipitation events, changes in discharge rate, changes in pumping rate) can strongly affect the monthly mean groundwater temperature. As a consequence, the behavior of the time-series of groundwater temperature in any given month would be extremely difficult to predict.

Based on the discussions in the previous paragraph, it can be assumed that the LM1 predictions are better than the LM2 predictions. Depending on the emissions scenario, the "medium medium" LM1 predictions for the 2085 scenario period (Table 4.2) indicate an increase of 1 K (found at *RBF2*; error range: -0.9 to 2.9 K; emissions scenario RCP3PD) to 3.5 K (*RBF1*; -0.1 to 7.5 K; A2). With respect to the values for aquifer *RBF1* it should be borne in mind that the model evaluation revealed a bias of approximately 0.5 K (Fig. 4.7), and that the error of LM1 is compiled by adding the prediction interval (eq. 4.4) of the model for the annual means (eq. 4.1) and monthly means (eq. 4.2). This suggests that the increase calculated for *RBF1* is significant, although the error range overlaps the value of zero change. However, with regard to the seasonal predictions, LM1 gives no indications whether the changes in groundwater temperature will be seasonally diverse.

4.5 Conclusion

This study has shown that groundwater temperature in Swiss aquifers that are recharged by riverbank infiltration are likely to increase by 1 to 3.5 K on average by the end of the current century, depending on the greenhouse-gas emissions scenario assumed. In aquifers recharged by riverbank infiltration, such a temperature increase could have negative consequences for groundwater quality; e.g., by affecting groundwater DO concentration and redox conditions (Sprenger et al., 2011; Figura et al., 2013a).

The approach taken – that of using historical data to build linear regression models linking groundwater temperature to air temperature – proved to be useful in specific cases. This approach is potentially useful if long time-series are available from aquifers in which groundwater temperature responds strongly to air temperature. The models perform better if the time-series contain a pronounced pattern, which in our case was the late 1980s regime shift observed both in air temperature and in groundwater temperature. Given the availability of such data for model calibration, linear regression models such as those used here might provide a good tool to provide a rapid estimate of potential future changes in groundwater temperature without requiring extensive process-based modeling or field measurements.

Table 4.2: Forecasts of groundwater temperature for aquifers *RBF1*, *RBF2*, and *RBF3* using model LM1 for the 2085 scenario period. Model predictions of the change in mean annual groundwater temperature with respect to the reference period 1980-2009 in aquifers *RBF1*, *RBF2*, and *RBF3* as modeled with LM1. Shown are the values for the scenario period 2085 (i.e., 2070-2099) and the three emission scenarios A2, A1B, and RCP3PD. The "medium medium" prediction represents the most probable prediction of groundwater temperature in each case; the "lower lower" prediction represents the lower range of the total error, which was calculated by subtracting the prediction interval from the "lower medium" prediction; and the "upper upper" prediction represents the upper range of the total error, which was calculated by adding the prediction interval to the "upper medium" prediction. See Fig. 4.3 and text for a detailed description of the nomenclature of the predictions.

	"medium medium" [K]	"lower lower" [K]	"upper upper" [K]	"lower medium" [K]	"upper medium" [K]
RBF1					
A2	3.53	-0.06	7.51	2.38	4.69
A1B	3.01	-0.39	6.74	2.01	4.04
RCP3PD	1.24	-1.62	4.21	0.66	1.84
RBF2					
A2	2.66	0.28	5.34	1.82	3.52
A1B	2.28	0.04	4.78	1.54	3.04
RCP3PD	0.98	-0.86	2.91	0.55	1.42
RBF3					
A2	2.89	0.62	5.65	1.98	3.82
A1B	2.48	0.39	4.99	1.68	3.30
RCP3PD	1.07	-0.52	2.80	0.60	1.54

<div style="text-align: right;">

5

</div>

Competing controls on groundwater oxygen concentrations revealed in multidecadal time-series from riverbank filtration sites

This chapter has been published in *Water Resources Research* (Figura et al., 2013a)[4].

Abstract. Dissolved oxygen (DO) is an important indicator of groundwater quality, but long time-series of groundwater DO concentration are rare. Here we describe and analyze multidecadal time-series of groundwater DO data from five Swiss aquifers that are recharged by riverbank filtration (RBF), and relate temporal features of the DO time-series to potential forcing factors. Features found in the DO time-series include long-term decreases and abrupt increases. Some features occur simultaneously in hydrologically unconnected aquifers, suggesting that external forcing partially determines DO concentrations at RBF sites. The data indicate that: (i) the DO concentration in the losing river is not a critical determinant of groundwater DO concentration; (ii) increasing river-water and groundwater temperatures, by affecting both the physical solubility of oxygen and DO consumption in the hyporheic zone, probably cause the long-term decline in DO concentration observed in most aquifers investigated; and (iii) a complex interaction between hydrological factors such as groundwater pumping rate and river discharge results in abrupt changes in groundwater DO concentration. Climate models predict higher temperatures and more frequent flood events in central Europe, implying that groundwater DO concentrations at many RBF sites will continue to decrease in the long term, but that irregular high-discharge events, by scouring and unclogging riverbeds, will probably prevent the occurrence of long periods of hypoxia. Nonetheless, the risk of short periods of hypoxia at RBF sites is likely to increase.

5.1 Introduction

Riverbank filtration (RBF) is of great importance for the production of drinking water, particularly in Europe (Ray et al., 2002). One crucial factor affecting groundwater quality and pumping-well management at RBF sites is the concentration of dissolved oxygen (DO). With regard to groundwater quality, a decrease in DO concentration is likely to lower the rates of microbial degradation of contaminants (Chapelle, 1993; Sprenger et al., 2011). The reduction and dissolution of iron and manganese oxides under anaerobic conditions (von Gunten et al., 1991; Bourg and Bertin, 1993; Hoehn and Scholtis, 2011; Sprenger et al., 2011), and the subsequent formation of precipitates in the pumping wells as a result of reaeration, are of relevance for the maintenance of pumping wells (Hunt et al., 2002).

The major oxygen input into groundwater at RBF sites results from the advective transport of DO in the infiltrating river water, although in some cases the input of atmospheric oxygen through the unsaturated zone can also be important (Malard and Hervant, 1999). On the other hand, oxygen is consumed by microbial respiration in the aquifer and in the hyporheic zone (the transition zone between river and groundwater; Chapelle, 1993; Malard and Hervant, 1999). In RBF systems in which the residence time of groundwater in the aquifer is short, most of the oxygen consumption takes place in the hyporheic zone (Beyerle et al., 1999; Malard and Hervant, 1999) and is controlled by the residence time of the water in the hyporheic zone and by the respiration rates of the microbial community located there (Brunke and Gonser, 1997; Malard and Hervant, 1999). These two factors are themselves affected by a variety of factors. The residence time of water in the hyporheic zone is governed by the hydraulic conductivity of the riverbed, the stream velocity, and the hydraulic head between river and groundwater (Brunke and Gonser, 1997; Boulton et al., 1998). Respiration rates within the microbial community of the hyporheic zone are affected by the water temperature and by the availability and composition of organic material (Chapelle, 1993; Brunke and Gonser, 1997; Malard and Hervant, 1999; Sprenger et al., 2011).

Climate change is likely to lead to an increase in groundwater temperature (Kundzewicz et al., 2007; Figura et al., 2011) and to changes in hydrological conditions (Green et al., 2011), and will thus potentially affect oxygen consumption in the hyporheic zone and DO concentrations in groundwater. In 2003, central Europe experienced an extremely hot, dry summer. Regional climate model simulations suggest that by the end of the current century, about every second summer in central Europe could be as warm or warmer, and as dry or dryer, than that of 2003 (Schär et al., 2004). During the summer of 2003, anaerobic conditions were observed at study sites in Germany (Rohns et al., 2006) and Switzerland (Hoehn and Scholtis, 2011). At the Swiss study site, the dissolution of iron and manganese in the groundwater (Hoehn and Scholtis, 2011) was followed by the formation of precipitates in the pumping wells (A. Scholtis, unpubl. data), suggesting that future increases in groundwater temperature may have undesirable effects on groundwater pumping well infrastructure.

In view of the above, it is apparent that an analysis of long time-series of historical groundwater DO data would be useful to reveal any temporal features (e.g., long-term trends, short-term changes, or fluctuations) that might be related to external driving factors. Such data are rare. However, an extensive search revealed the existence of relevant data from several RBF sites in Switzerland. These multidecadal data were collected and collated, and the time-series of these data are here described statistically. To identify the processes affecting the long-term

behavior of the groundwater DO concentrations, simultaneous time-series of groundwater temperature, groundwater level, groundwater pumping rate, river-water DO concentration, river-water temperature, and river discharge rate were also analyzed. The available long-term data allowed us to investigate three possible factors that might control groundwater DO concentrations in the aquifers analyzed: (i) DO concentrations in the losing river; (ii) river-water and groundwater temperatures, which affect the physical solubility of oxygen and microbial respiration in the hyporheic zone, and which have undergone a strong parallel warming in the past (Hari et al., 2006; Figura et al., 2011); and (iii) changes in hydrological factors, such as groundwater pumping rate, river discharge rate or groundwater level, which might affect the residence time of the water in the hyporheic zone.

To our knowledge, this is the first time that time-series of groundwater DO concentration of this length and temporal resolution have been published and statistically described.

5.2 Data and Methods

5.2.1 Data

The data presented in this study resulted from a search for long time-series of groundwater data (at least 25 yr) with good temporal resolution (at least four measurements per year) from aquifers in Switzerland that had been affected as little as possible by direct anthropogenic intervention. All time-series presented here fulfill these criteria. The data originated from the drinking-water pumping wells of five granular, unconsolidated aquifers on the Swiss Plateau that are recharged predominantly by RBF from four rivers (Fig. 5.1a; Table 5.1). The aquifers are abbreviated here as *EmSi*, *AaKi*, *RhSe*, *ToLi*, and *ToZe*, where the first two letters designate the river feeding the aquifer: the Emme (Em), Aare (Aa), Rhine (Rh), or Toess (To). Time-series of groundwater DO concentration in these aquifers covered periods ranging from 29 to 41 yr (Table 5.2). Data on groundwater temperature and groundwater level were available from the same aquifers with comparable duration and resolution. Data on pumping rates were available for four of the five aquifers, but mostly for periods of substantially shorter duration (Table 5.2).

Groundwater temperature and DO concentration were measured directly at the outlets of the pumping wells according to the methods outlined in the Swiss Foodstuffs Handbook (FOPH, 2003). Groundwater temperature was measured with a precision of ± 0.1 °C and DO concentration was determined using the Winkler method with a precision of ± 0.1 mg O_2 l^{-1}. If not stated otherwise, groundwater levels were measured in piezometers in the immediate proximity of the pumping wells with an estimated precision of ± 0.05 m. Although the operators of some of the pumping wells have installed automatic loggers in the last few years, parallel measurements were continued using the methods described above.

From the rivers, the available data on DO concentration, water temperature and discharge rate covered periods ranging from 20 to 46 yr with a resolution of at least 12 measurements per year (Table 5.2). The river gauging stations that supplied the data are operated by Swiss cantonal or federal authorities. The stations are equipped with automatic samplers that take mixed samples over a cross-section of the river. Unless stated otherwise, DO concentrations in the rivers were determined weekly or monthly, while river-water temperature and discharge were available as daily means. Because the river gauging stations did not always lie in close proximity to the aquifer infiltration sites, the river-water data might not exactly represent the

conditions prevailing at the infiltration sites. However, a comparative analysis of DO data from several gauging stations on the four rivers showed that stations less than ~30 km apart were broadly similar with respect both to the DO concentrations measured and to the long-term behavior of the DO time-series.
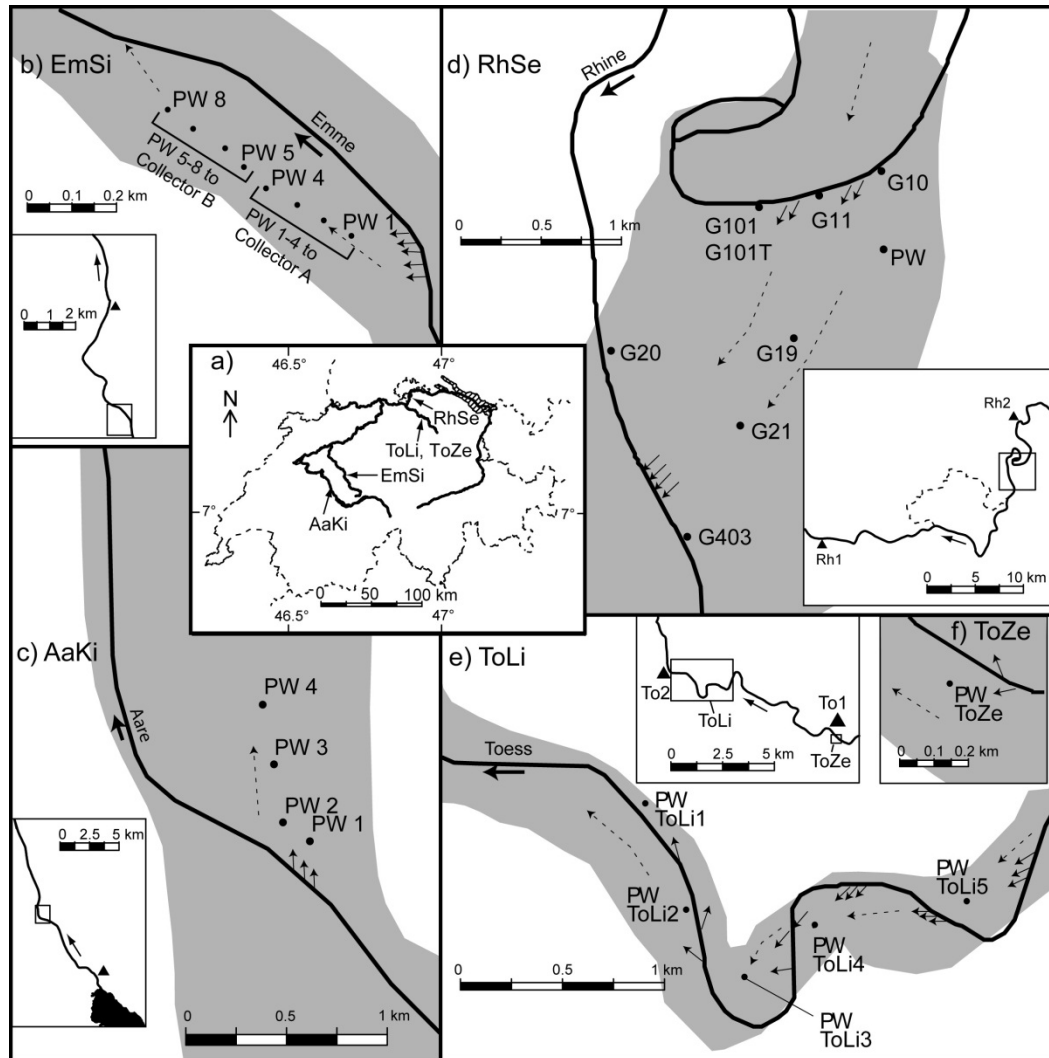
Figure 5.1: Maps showing the locations of the aquifers and pumping wells. (a) Map of Switzerland showing the locations of the aquifers analyzed in this study and their losing rivers. (b)-(f) Approximate extent of each of the aquifers (shaded areas); locations of pumping wells and piezometers (points); infiltration and exfiltration sites (solid arrows); and estimated groundwater flow direction (dashed arrows). The insets in panels (b)-(e) show the locations of the river gauging stations (triangles) with respect to the aquifers.

5.2.1.1 *EmSi*

The *EmSi* aquifer is recharged by the River Emme (Blau and Muchenberger, 1997). Groundwater has been abstracted from the *EmSi* aquifer since the 1920s. Neither the river, the pumping well, nor the surroundings of the pumping well have been subject to changes in water management or infrastructure. Groundwater is pumped out of the aquifer at eight wells (PW1-PW8, Fig. 5.1b). Measurements of groundwater temperature and DO concentration were made at the outlets of two collectors (A and B), each of which collects water from four of the eight pumping wells (Fig. 5.1b). Groundwater levels were determined in PW1 (representing Collector A) and PW6 (representing Collector B). Pumping-rate data from Collector A were available at a

resolution of one record per month. The data from Collector A comprised two independent sets of measurements covering the periods 1979-2000 and 1997-2007. Annual mean values of DO concentration, temperature, and groundwater level for the two data sets during the overlapping period 1997-2000 differed by less than the respective measurement errors, allowing the two data sets to be combined to cover the 29-yr period 1979-2007. Data from Collector B were available only for the period 1997-2007 (Table 5.2). The overall similarity of the DO concentrations measured at collectors A and B (Fig. 5.2a) indicates that the DO concentration measured at Collector A can be assumed to be representative of the whole aquifer. Data from the River Emme were available from a river gauging station 6 km downstream of the site (Fig. 5.1b, inset; Table 5.2).

Table 5.1: Characteristics of aquifers investigated. Descriptive characteristics of each aquifer investigated, including the elevation of the pumping stations, name of the losing river, hydraulic conductivity, depth of the groundwater table, and thickness of the aquifer. The locations of the aquifers and pumping stations are shown in Fig. 5.1. Hydraulic conductivity values for *EmSi* are from Blau and Muchenberger (1997), and for *RhSe*, *ToLi* and *ToZe* from Kempf et al. (1986). For *AaKi*, individual hydraulic conductivities were 3.2×10^{-3}, 2.5×10^{-3}, 4.3×10^{-3}, and 4.2×10^{-3} m s^{-1} measured at pumping wells PW1 to PW4, respectively (Kellerhals et al., 1981). For *EmSi*, *RhSe*, and *ToZe* the hydraulic conductivity was determined at many different points within the aquifer; for *AaKi* and *ToLi* it was determined only from pumping tests at each pumping well.

Name	Elevation [m a.s.l.]	Losing river	Hydraulic conductivity [m s^{-1}]	Depth of water table [m]	Thickness of aquifer [m]
EmSi	685-693	Emme	$2\text{-}4 \times 10^{-3}$	2-4	15-20
AaKi	539-545	Aare	$2.5\text{-}4.3 \times 10^{-3}$	4-5	15-20
RhSe	374-385	Rhine	$1\text{-}5 \times 10^{-3}$	10-20	10-15
ToLi	456-475	Toess	$1\text{-}15 \times 10^{-3}$	2.5-4	10-20
ToZe	520-524	Toess	$1\text{-}8 \times 10^{-3}$	2-5	35-45

5.2.1.2 *AaKi*

The *AaKi* aquifer is approximately 1.5 km wide and is recharged mainly by the River Aare (Kellerhals et al., 1981). Since construction of the *AaKi* pumping wells between 1947 and 1950, there have been no changes in river-water or groundwater management. Groundwater abstraction occurs at four pumping wells (PW1-PW4; Fig. 5.1c), but long-term measurements (1968-2000) were available from only one of these (PW4; Table 5.2). Groundwater DO concentration and temperature were measured at the outlets of the pumping wells, while groundwater level was determined in a piezometer located approximately 10 m from PW4. Monthly pumping-rate data from PW4 were available for the period 1997-2005. An additional data set comprising monthly measurements of DO concentration, temperature, and groundwater level was available for 1997-2009 at PW1, PW2, and PW3, and for 1997-2005 at PW4. At PW4, the annual mean values of the two data sets measured during the overlapping period 1997-2000 differed by less than the respective measurement errors for all variables. As in the case of *EmSi*, this allowed the two data sets to be combined, yielding time-series that covered the 38-yr period 1968-2005. The overall similarity of the DO concentrations measured at pumping wells PW1,

PW2, PW3, and PW4 from 1997-2005 (Fig. 5.3a) indicates that the DO concentration measured at PW4 can be assumed to be representative of the whole aquifer. Data from the River Aare were obtained from a gauging station 9 km upstream of the site (Fig. 5.1c, inset; Table 5.2).

Table 5.2: Available data. Overview of data measured (i) in groundwater and (ii) in the respective losing river. The upper-case letters in parentheses specify the temporal resolution: daily (D), weekly (W), bi-weekly (BW), monthly (M), quarterly (Q), or annual (A). The lower-case letters in parentheses indicate whether individual spot measurements (s), the mean of several measurements (m), or sums of measurements (sum) were available. (For example, Ms stands for one measured spot value per month and Dm for daily mean values.) At *EmSi*, data from Collector A were used for the long-term analysis and at *AaKi*, data from PW4 were used for the long-term analysis. From piezometer G101 at *RhSe* only data from 1970-1983 were available.

(i) Groundwater data

	DO concentration	Temperature	Groundwater level	Pumping rate
EmSi				
Collector A	1979-2007 (Qs, Ms)	1979-2007 (Qs, Ms)	1992-2007 (Qs, Ms)	1978-2007 (Ms)
Collector B	1997-2007 (Ms)	1997-2007 (Ms)	1997-2007 (Ms)	-
AaKi				
PW4	1968-2005 (Qs, Ms)	1968-2005 (Qs, Ms)	1968-2005 (Ms)	1997-2005 (Ms)
PW1-3	1997-2009 (Ms)	1997-2009 (Ms)	1997-2009 (Ms)	-
RhSe				
PW	1970-2007 (Ms)	1970-2007 (Ms)	1970-2007 (Ms)	1993-2010 (Msum)
Piezometers	1970-1994 (Ms), 1995-2006 (Am)	1970-1994 (Ms), 1995-2006 (Am)	1970-1994 (Ms), 1995-2006 (Am)	-
ToLi	1971-2011 (Qs)	1971-2011 (Qs)	1971-2011 (Ms)	2000-2012 (Asum)
ToZe	1971-2011 (Qs)	1971-2011 (Qs)	-	-

(ii) River data

	DO concentration	Temperature	Discharge rate
River Emme	1983-2010 (Ms)	1976-2010 (Dm)	1976-2010 (Dm)
River Aare	1966-2011 (Ms)	1962-2007 (Dm)	1970-2010 (Dm)
River Rhine Rh1	1970-2010 (BWs)	1970-2010 (BWs)	-
River Rhine Rh2	-	-	1970-2010 (Dm)
River Toess To1	1992-2011 (Ws)	1984-2011 (Dm)	-
River Toess To2	-	-	1970-2011 (Dm)

5.2.1.3 *RhSe*

Monitoring of the *RhSe* aquifer was started in the 1950s because of the construction of a hydroelectric power plant that led to the impoundment of the River Rhine in the infiltration area. The *RhSe* aquifer is recharged mainly by the infiltration of river water (Kempf et al., 1986) along the riverbank between piezometers G10 and G101 (Fig. 5.1d). A small proportion of the groundwater infiltrates into the aquifer from the river 2 km upstream of this site (Kempf et al., 1986). The pumping well (PW) in the *RhSe* aquifer was built in 1957. Neither the stretch of river between Lake Constance and the *RhSe* aquifer nor the surroundings of the *RhSe* aquifer have been subject to anthropogenic interventions that might have affected the groundwater of the *RhSe* aquifer.

Groundwater data were available from the pumping well (PW) and eight piezometers (G10, G11, G19, G20, G21, G101, G101T, and G403; Fig. 5.1d, Table 5.2). Note that piezometers G101 and G101T were set in the same location but sampled water from different depths (G101, 1-4 m; G101T, 15-20 m). Monthly pumping-rate data were available for the period 1993–2010. Data from the River Rhine at bi-weekly resolution or better were obtained from two river gauging stations, one (Rh1) approximately 30 km downstream of the site and one (Rh2) 3 km upstream of the site (Fig. 5.1d, inset).
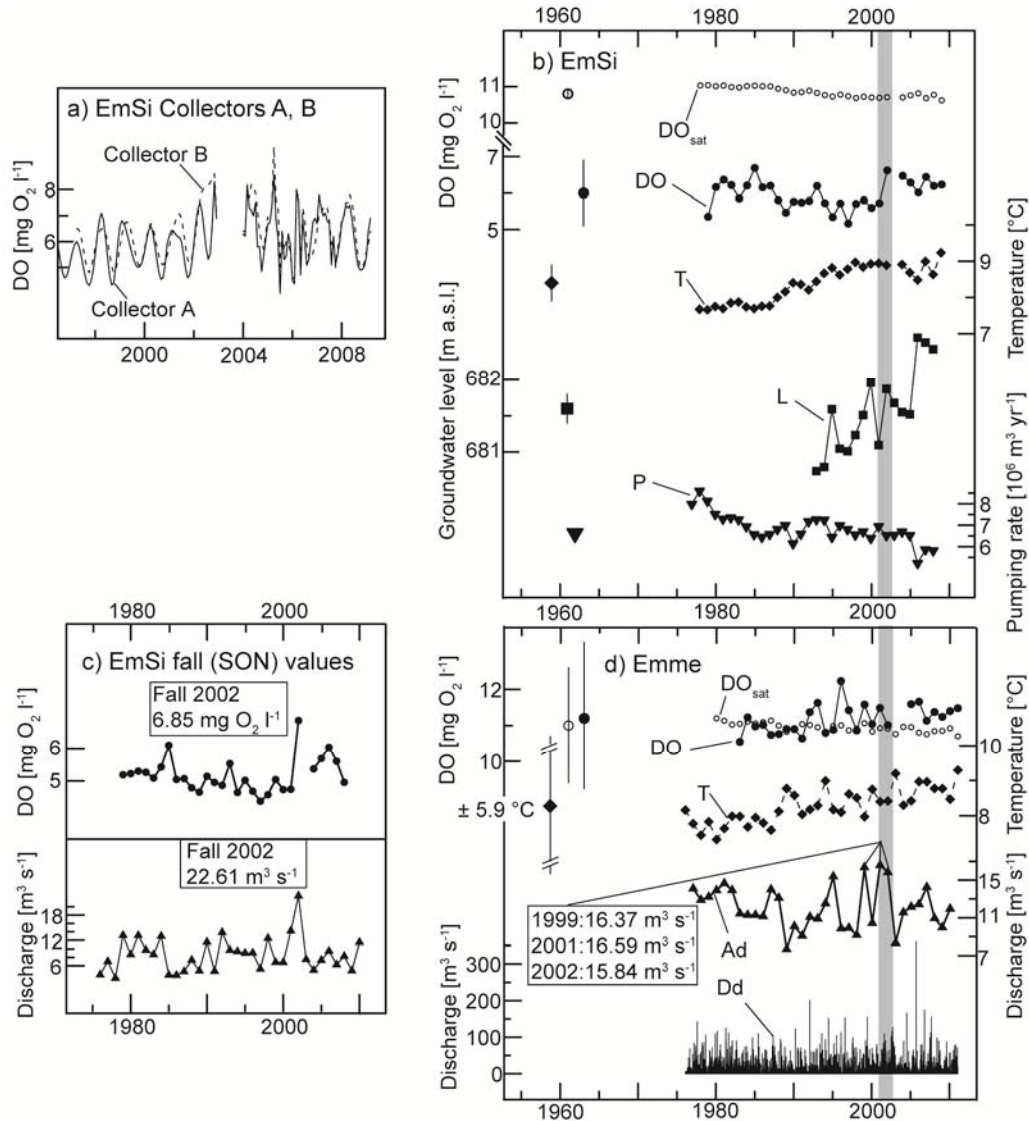
Figure 5.2: *EmSi* aquifer and River Emme. (a) Comparison of monthly mean DO concentrations in the *EmSi* aquifer as measured at Collectors A and B from 1997-2009. (b) Annual mean DO concentration (DO), groundwater temperature (T), DO saturation concentration (DO_{sat}), groundwater level (L), and annual pumping rate (P) at Collector A of the *EmSi* aquifer. (c) Comparison of the mean fall (September-November) DO concentration at the *EmSi* aquifer (upper panel) with the mean fall discharge of the River Emme (lower panel). (d) Annual mean DO concentration (DO), water temperature (T), DO saturation concentration (DO_{sat}), annual mean discharge (Ad), and daily mean discharge (Dd) for the River Emme. The symbols and vertical lines on the left-hand side of (b) and (d) illustrate the mean value of each time series and its amplitude as determined from a trigonometric regression. The interrupted vertical line illustrating the amplitude of the River Emme water temperature (panel d) was too large to fit on the plot, so the value is given explicitly. The shaded areas highlight the abrupt increase in groundwater DO concentration from 2001 to 2002.
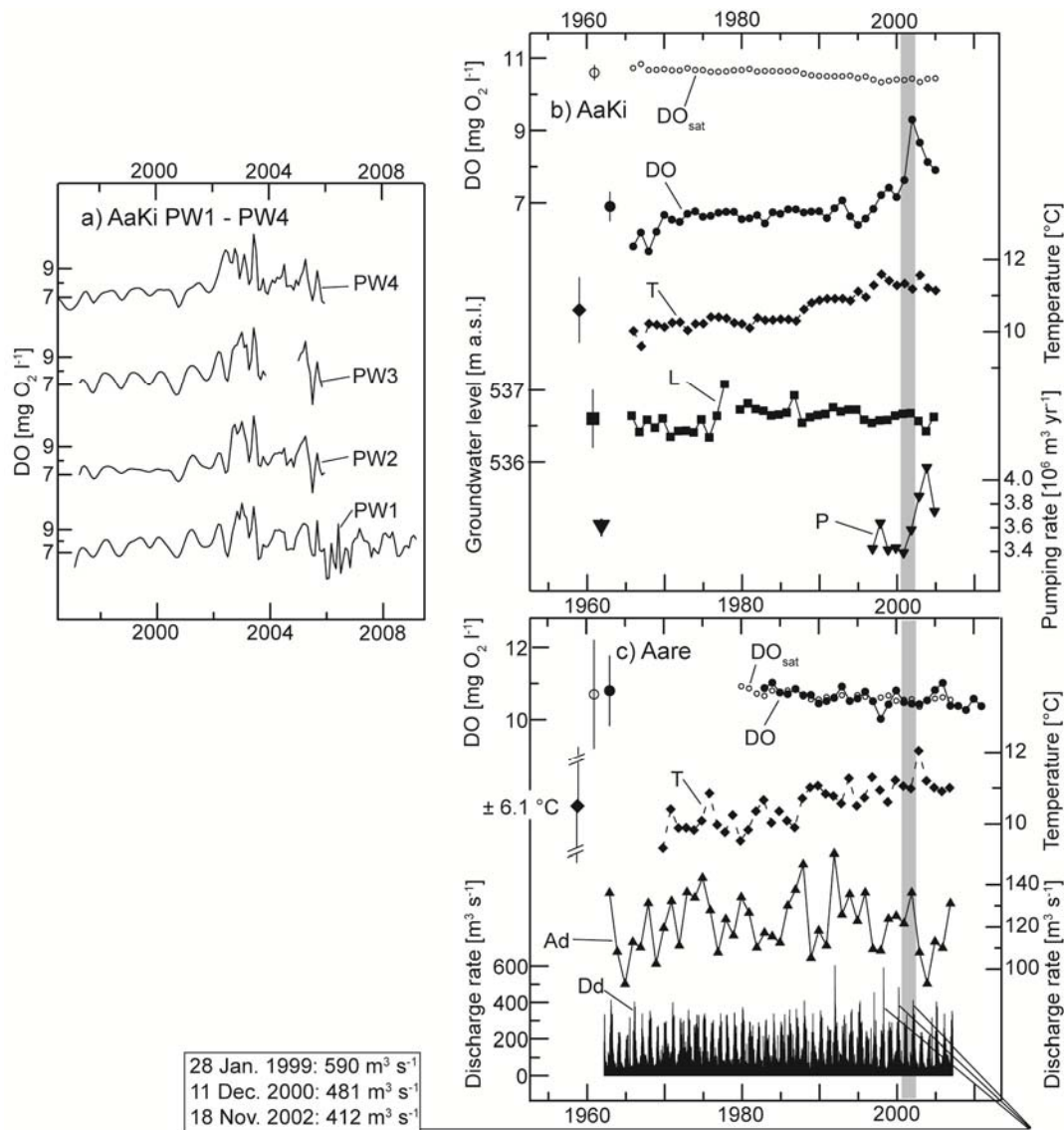
Figure 5.3: *AaKi* aquifer and River Aare. (a) Comparison of monthly mean DO concentrations measured at *AaKi* pumping wells PW1, PW2, PW3, and PW4 from 1997-2009. (b) Annual mean DO concentration (DO), groundwater temperature (T), DO saturation concentration (DO$_{sat}$), groundwater level (L), and annual pumping rate (P) measured in pumping well PW4 of the *AaKi* aquifer. (c) Annual mean DO concentration (DO), water temperature (T), DO saturation concentration (DO$_{sat}$), annual mean discharge (Ad), and daily mean discharge (Dd) for the River Aare. The symbols and vertical lines on the left-hand side of (b) and (c) illustrate the mean value of each time series and its amplitude as determined from a trigonometric regression. The interrupted vertical line illustrating the amplitude of the River Aare water temperature (panel c) was too large to fit on the plot, so the value is given explicitly. The shaded areas highlight the abrupt increase in groundwater DO concentration from 2001 to 2002.

5.2.1.4 *ToLi* and *ToZe*

The *ToLi* and *ToZe* aquifers (Fig. 5.1e,f) are part of the 45-km-long Toess Valley aquifer, which is recharged by infiltration from the River Toess (Kempf et al., 1986). Groundwater flow in the area between *ToLi3* and *ToLi4* was extensively studied by Beyerle et al. (1999) and Mattle et al. (2001). The pumping wells in both aquifers were built in the 1960s. The River Toess has not been subject to any changes in water management upstream of pumping well *ToLi2*. However, 200 m of the river between *ToLi1* and *ToLi2* was revitalized in 2001. For the revitalization, linings on the riverbank were removed and an artificial gravel island was built in

the middle of the river, leading to erosion of the riverbank and enlargement of the river and the riparian zone from ~20 m to ~50 m.

Groundwater data were available from five pumping wells in the *ToLi* aquifer (*ToLi1* - *ToLi5*) and one pumping well in the *ToZe* aquifer (Table 5.2). Pumping rate data available from the five pumping wells in the *ToLi* aquifer consisted of annual sums of pumped groundwater. Data from the River Toess at weekly resolution or better were obtained at two stations, one (To1) approximately 6 km upstream of the *ToLi* site and 0.5 km downstream of the *ToZe* site, and one (To2) 1 km downstream of the *ToLi* site and 10 km downstream of the *ToZe* site (Fig. 5.1e, inset; Table 5.2).

5.2.2 Methods

The data were checked for outliers by visual inspection. If a value was suspected to be an outlier, the mean and standard deviation of the data within a 5-yr window centered on the suspect value were calculated. If the difference between the suspect value and the calculated 5-yr mean exceeded three standard deviations, the value was identified as an outlier and deleted (over all data sets, a total of 7 outliers were deleted). Data sampling intervals were generally irregular and inconsistent, necessitating standardization. This was accomplished by first interpolating the data at consistent daily intervals using a cubic spline (except over gaps longer than 3 months), then aggregating the interpolated data to yield estimates of monthly and annual means. Interpolation over gaps of 3–6 months was accomplished by fitting a cubic regression model to the monthly mean data. The deviations of the measured data from the cubic regression model were averaged for each month and added to the modeled value to obtain a monthly time-series, which was then used to fill the gaps. No interpolation was performed over gaps longer than 6 months. Because the pumping-rate data from the *ToLi* aquifer consisted of annual sums only, the pumping rates of the *EmSi*, *AaKi*, and *RhSe* aquifers were also aggregated to annual sums. This was accomplished at *EmSi* and *AaKi* by summing the interpolated daily mean pumping rates, and at *RhSe* by summing the monthly sums of the pumping rates.

The data were described and analyzed using standard statistical methods. Temporal trends in the data were assessed using the nonparametric Theil-Sen method (Theil, 1950; Sen, 1968) and tested for statistical significance at the $p < 0.05$ level using the nonparametric Kendall τ statistic (Helsel and Hirsch, 1992). Spearman rank correlation coefficients for lags of 0 - 2 yr were calculated between the time-series of annual means of groundwater DO concentration and time-series of the annual means of potential driving variables after first removing the trends in the time-series, which were determined using the seasonal-trend decomposition procedure of Cleveland et al. (1990) as implemented in function *stl* of the statistical software *R* (R Development Core Team, 2011). For each time-series, the amplitude of the seasonal variation was estimated by fitting a trigonometric regression model to the monthly mean data. Oxygen saturation concentrations were calculated from the water temperature data and the elevation of the measurement site using the empirical relationship given by Bührer (1975):

$$S_h = 10^{log(760)-h/18400}(14.60307 - 0.4021469T +$$
$$0.00768703T^2 - 0.0000692575T^3 \tag{5.1}$$

where h is the elevation of the measuring site in m a.s.l., T is the water temperature in °C, and S_h is the oxygen saturation concentration in mg O_2 l^{-1} at elevation h.

We also conducted an event-based comparison of the time-series to investigate the possible nonlinear forcing of groundwater DO concentration by extreme river discharge rates. After checking subjectively whether the occurrence of extreme river discharge rates (either annual or daily) was followed by the occurrence of abrupt, strong changes in groundwater DO concentration, intervention analysis was employed to obtain objective confirmation of any potential relationship found. Intervention analysis is an extension of the autoregressive integrated moving average (ARIMA) time-series model to describe the impact of an event on the time-series at a specific point in time (Box and Tiao, 1975; Cryer and Chan, 2008). For the purposes of this analysis, the five highest values of river discharge rate were defined as extreme events. Binary intervention time-series were constructed, in which an intervention was defined to take place in the year in which such an extreme river discharge event was observed. One to five interventions were allowed to take place in the intervention time-series, which resulted in 31 binary intervention time-series (five intervention time-series containing only one intervention, ten containing two interventions, ten containing three interventions, five containing four interventions, and one containing all five interventions). In a next step, 31 intervention models were constructed as follows (using the notation of Cryer and Chan (2008)):

$$Y_t = N_t + m_t, \tag{5.2}$$

where Y_t is the modeled groundwater DO concentration, N_t is an ARIMA model for groundwater DO concentration that is determined before the intervention model is calibrated, and m_t is a pulse function that represents the change in the mean caused by the intervention (with $m_t = 0$ before the intervention takes place). Under the assumption that the impact of an extreme river discharge event on groundwater DO concentration dies out gradually, we used a first-order autoregressive model to represent m_t, as recommended by Cryer and Chan (2008), which results in m_t taking on the form of an exponentially decaying pulse function. The best ARIMA representation of N_t was determined by fitting all possible ARIMA models up to an order of (2,1,2). The model with the lowest value of the Akaike information criterion (Akaike, 1974) was the one selected. The model that fitted the DO concentration data best was determined by comparing the root mean square deviations (RMSD) associated with each of the 31 intervention models. The interventions (i.e., the extreme river discharge events) identified by this model were assumed to be responsible for the nonlinear response in the groundwater DO concentration.

5.3 Results and Discussion

5.3.1 Observed features in the time-series of groundwater DO concentration

Time-series plots (Figs. 5.2-5.7) suggest that the groundwater DO concentrations in the aquifers analyzed are not statistically stationary, but undergo long-term trends and abrupt changes. In the next two sections, these two features in the historical data will be discussed in more detail.
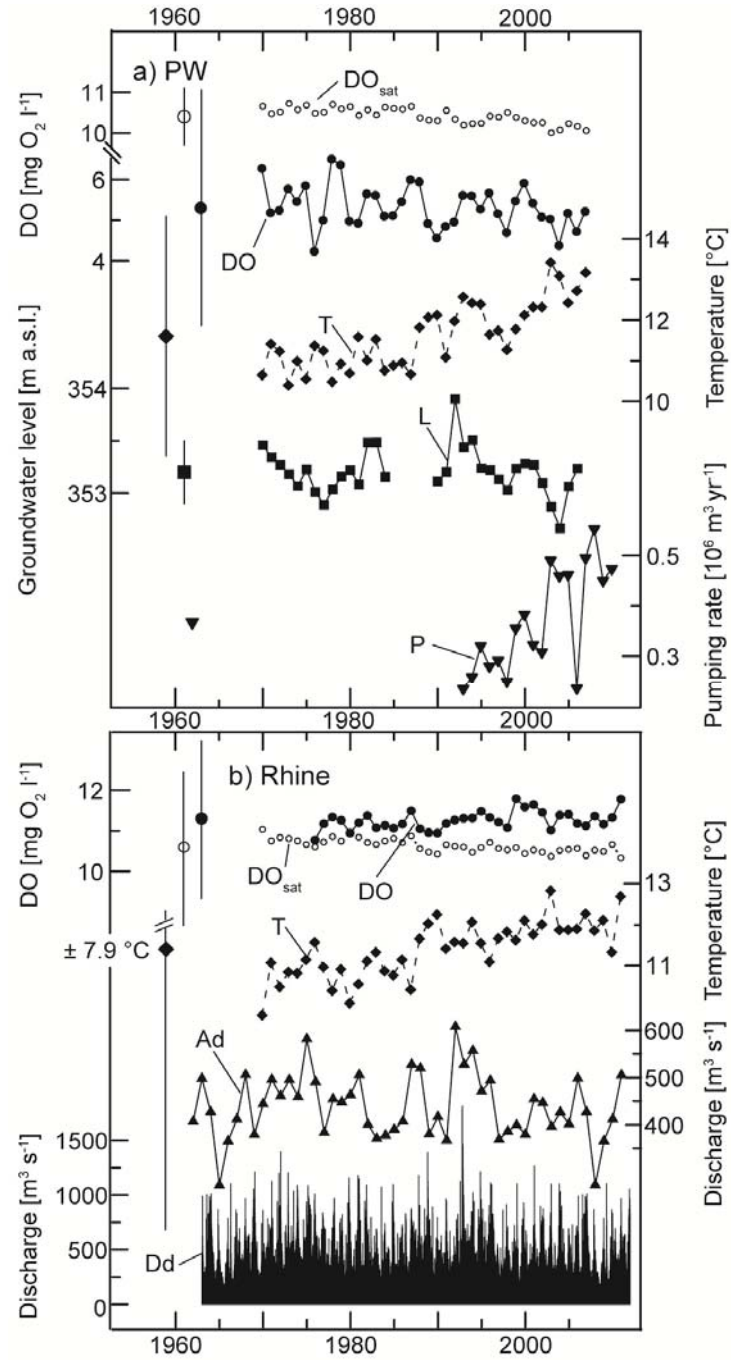
Figure 5.4: *RhSe* aquifer (PW) and River Rhine. (a) Annual mean DO concentration (DO), groundwater temperature (T), DO saturation concentration (DO$_{sat}$), groundwater level (L), and annual pumping rate (P) measured in the pumping well of the *RhSe* aquifer. (b) Annual mean DO concentration (DO), water temperature (T), DO saturation concentration (DO$_{sat}$), annual mean discharge (Ad), and daily mean discharge (Dd) of the River Rhine. The symbols and vertical lines on the left-hand side of the panels illustrate the mean value of each time series and its amplitude as determined from a trigonometric regression. The interrupted vertical line illustrating the amplitude of the River Rhine water temperature (panel b) was too large to fit on the plot, so the value is given explicitly.

51
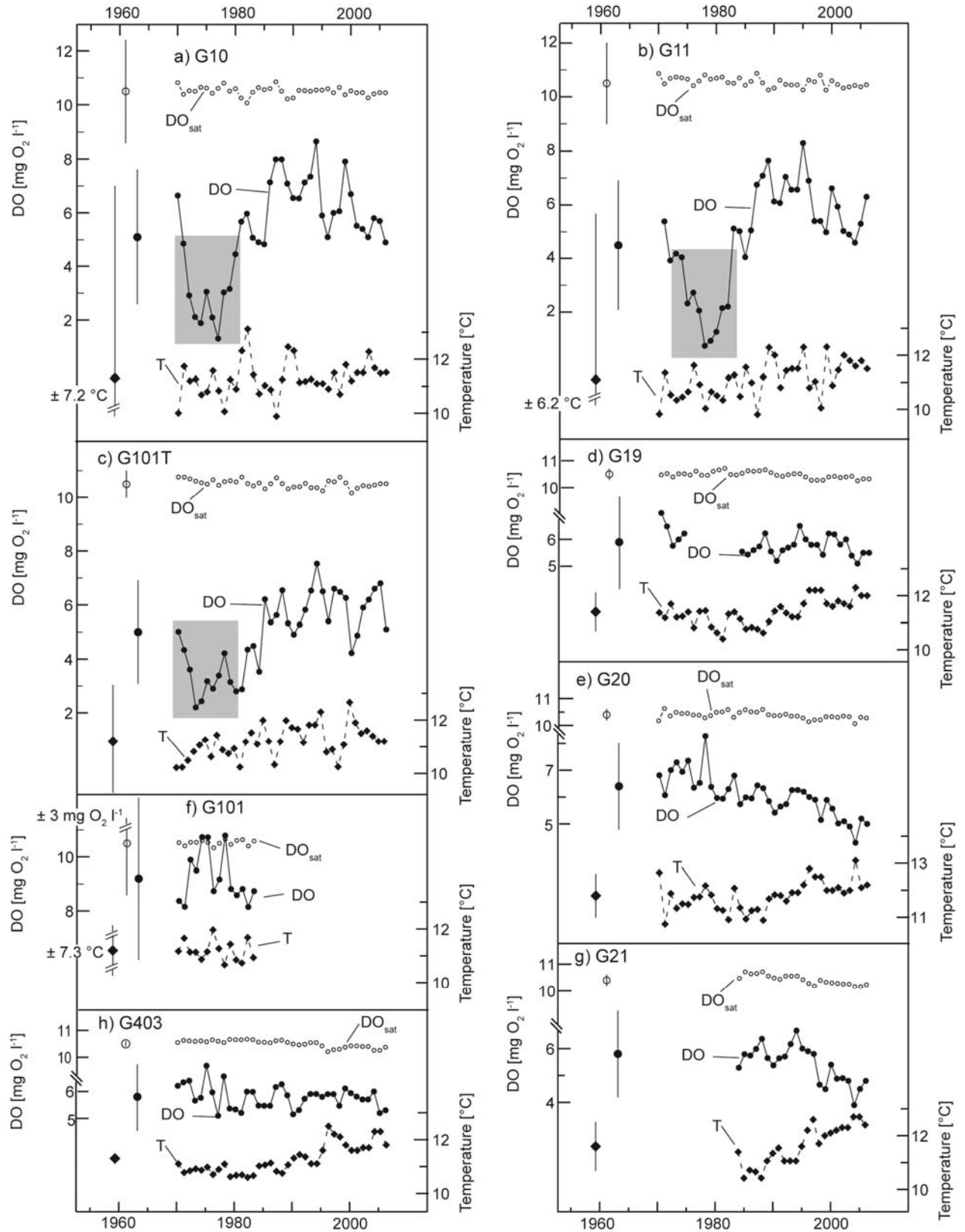
Figure 5.5: *RhSe* aquifer (piezometers). Annual mean DO concentrations (DO), groundwater temperatures (T), and DO saturation concentrations (DO$_{sat}$) measured at the eight piezometers (G10, G11, G101, G101T, G19, G20, G21, G403) of the *RhSe* aquifer. The symbols and vertical lines on the left-hand side of each panel illustrate the mean value of each time-series and its amplitude as determined from a trigonometric regression. The interrupted vertical lines illustrating the amplitudes of the groundwater temperatures at G10, G11, G101, and of the DO saturation concentration at G101, were too large to fit on the plot, so their values are given explicitly (panels a,b,f). The shaded areas highlight the unusually low groundwater DO concentrations that occurred when the riverbed was clogged by zebra mussels (see text).

52
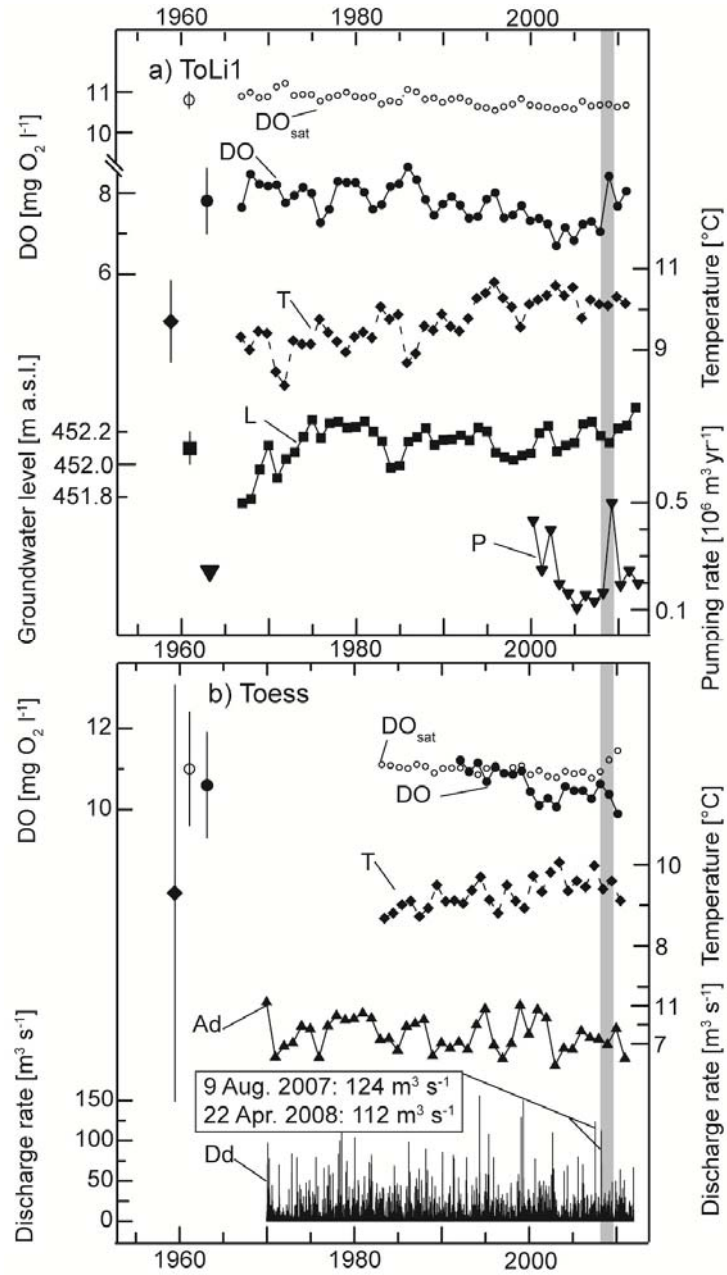
Figure 5.6: *ToLi* aquifer (*ToLi1*) and River Toess. (a) Annual mean DO concentration (DO), groundwater temperature (T), DO saturation concentration (DO$_{sat}$), groundwater level (L), and annual pumping rate (P) measured in pumping well *ToLi1* of the *ToLi* aquifer. (b) Annual mean DO concentration (DO), water temperature (T), DO saturation concentration (DO$_{sat}$), annual mean discharge (Ad), and daily mean discharge (Dd) of the River Toess. The symbols and vertical lines on the left-hand side of the panels illustrate the mean value of each time series and its amplitude as determined from a trigonometric regression. The shaded areas highlight the abrupt increase in groundwater DO concentration from 2008 to 2009.

Figure 5.7: *ToLi* aquifer (*ToLi2-ToLi5*) and *ToZe* aquifer. (a)-(d) Annual mean DO concentration (DO), groundwater temperature (T), DO saturation concentration (DO$_{sat}$), groundwater level (L), and annual pumping rate (P) measured in pumping wells *ToLi2-ToLi5* of the *ToLi* aquifer. (e) Annual mean DO concentration (DO), groundwater temperature (T), and DO saturation concentration (DO$_{sat}$) measured in the *ToZe* aquifer. The symbols and vertical lines on the left-hand side of each panel illustrate the mean value of each time series and its amplitude as determined from a trigonometric regression. The shaded areas highlight the abrupt increase in groundwater DO concentration from 2008 to 2009.

54

Table 5.3: Temporal trends. Temporal trends (1979-2005) in the annual mean values of (i) groundwater DO concentration, groundwater temperature, groundwater DO saturation concentration, and groundwater level; and (ii) river-water DO concentration, river-water temperature, river-water DO saturation concentration, and river discharge rate as determined by the Theil-Sen method (Theil, 1950; Sen, 1968). Tabulated values were tested for significance at the $p < 0.05$ level using the nonparametric Kendall τ statistic (Helsel and Hirsch, 1992). The lack of a significant trend (i.e., $p \geq 0.05$) is designated by "ns", and the lack of sufficient data by "-". Groundwater level at *EmSi* and DO concentrations in the rivers Emme and Toess were not available during the entire period 1979-2005 (Table 5.2). For comparison purposes, trends for *EmSi* and *ToLi* and for the rivers Emme and Toess were therefore also calculated for the period 1992-2005 (values in parentheses). No DO concentration or temperature measurements were available for G101 after 1984.

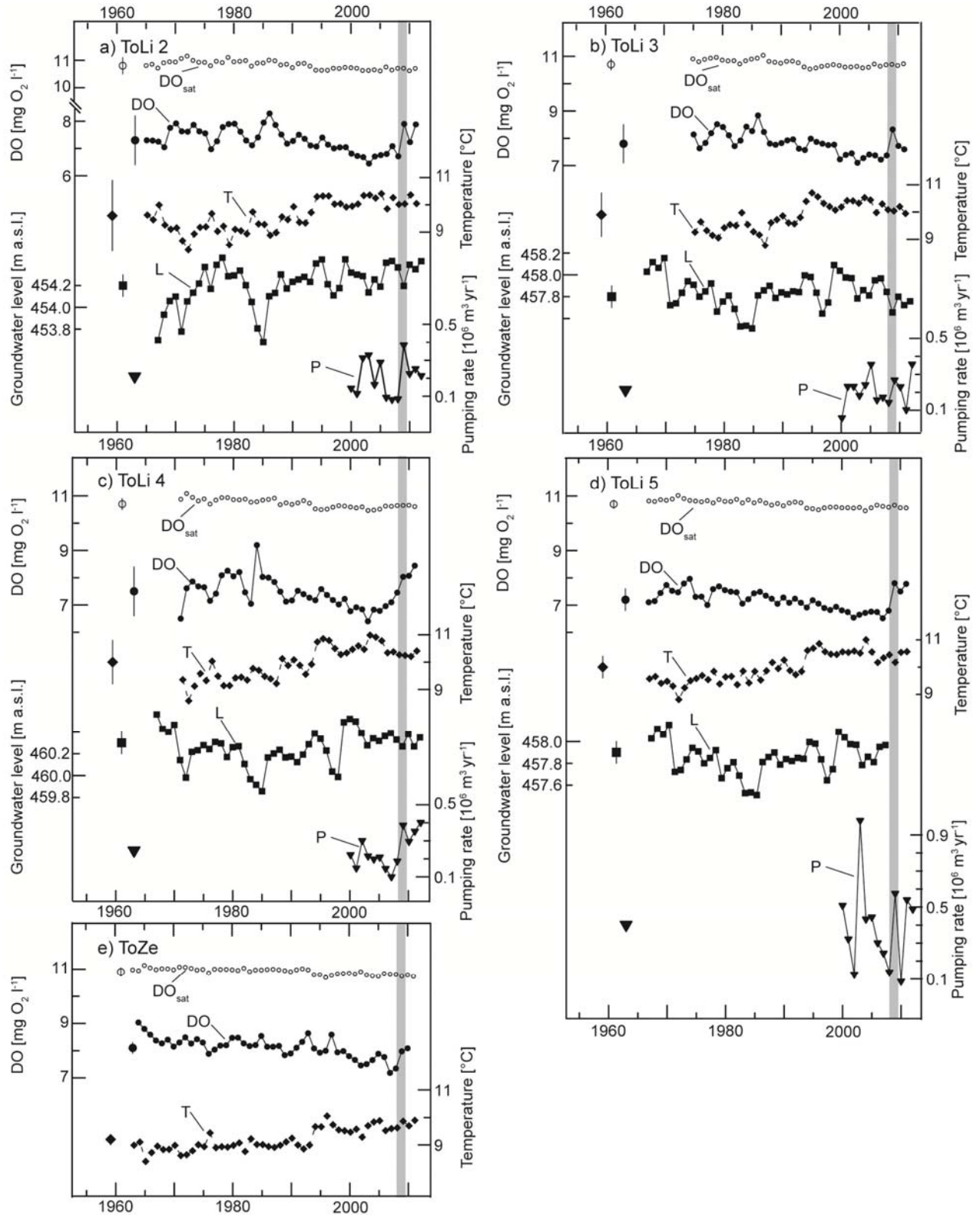| (i) Groundwater				
	DO [mg O_2 l^{-1} yr^{-1}] 1979-2005 (1992-2005)	Temperature [°C yr^{-1}] 1979-2005 (1992-2005)	DO saturation [mg O_2 l^{-1} yr^{-1}] 1979-2005 (1992-2005)	Groundwater level [cm yr^{-1}] 1979-2005 (1992-2005)
EmSi	ns (ns)	0.060 (0.036)	-0.016 (-0.010)	- (6.7)
AaKi	0.043	0.056	-0.013	-0.6
RhSe				
PW	-0.016	0.071	-0.017	ns
G10	ns	ns	ns	-
G11	ns	0.037	-0.009	-
G101	-	-	-	-
G101T	0.082	ns	ns	-
G19	ns	0.054	-0.013	-
G20	-0.048	0.045	-0.011	-
G21	-0.069	0.103	-0.025	-
G403	ns	0.055	-0.015	-
ToLi				
ToLi1	-0.045 (-0.053)	0.052 (0.051)	-0.013 (-0.013)	ns (ns)
ToLi2	-0.047 (-0.053)	0.058 (0.034)	-0.015 (-0.009)	ns (ns)
ToLi3	-0.041 (-0.052)	0.049 (ns)	-0.013 (ns)	1.0 (1.3)
ToLi4	-0.057 (-0.056)	0.062 (0.061)	-0.016 (-0.016)	1.0 (ns)
ToLi5	-0.037 (-0.042)	0.051 (ns)	-0.013 (ns)	1.0 (1.2)
ToZe	-0.028 (-0.064)	0.036 (ns)	-0.009 (ns)	- (-)

(ii) River water				
	DO [mg O_2 l^{-1} yr^{-1}] 1979-2005 (1992-2005)	Temperature [°C yr^{-1}] 1979-2005 (1992-2005)	DO saturation [mg O_2 l^{-1} yr^{-1}] 1979-2005 (1992-2005)	Discharge rate [m^3 s^{-1} yr^{-1}] 1979-2005 (1992-2005)
Emme	- (ns)	0.035 (ns)	-0.009 (ns)	ns (ns)
Aare	-0.021	0.049	-0.013	ns
Rhine	0.014	0.054	-0.013	ns
Toess	- (-0.064)	- (0.042)	- (ns)	ns (ns)

5.3.1.1 Long-term trends

Temporal trends in the DO data, calculated for the period 1979–2005 using the Theil-Sen method (Table 5.3), reveal a statistically significant ($p < 0.05$) long-term decrease in DO concentration at the *RhSe* (Fig. 5.4a), *ToLi* (Figs. 5.6a, 5.7a-d), and *ToZe* (Fig. 5.7e) pumping wells. The *ToLi* data (Fig. 5.6a, 5.7a-d) suggest that this long-term decreasing trend encompassed the entire *ToLi* aquifer. The *RhSe* piezometer data (Fig. 5.5), however, make it clear that the long-term behavior of the DO concentration within the *RhSe* aquifer can be very heterogeneous. The DO concentration at *EmSi* (Fig. 5.2b) underwent a long-term decrease from 1980 to 2000, but the trend for the period 1979-2005 was not significant because of a shift to higher DO concentrations after 2000. At *AaKi* (Fig. 5.3b), DO concentrations showed the opposite behavior, with a rise having occurred in the long term (Table 5.3). The similar rates of decline in DO concentration observed at the *EmSi*, *RhSe*, *ToLi*, and *ToZe* pumping wells between approximately 1980 and 2000 (Figs. 5.2b, 5.4a, 5.6a, 5.7) suggest that a common external forcing factor governs the long-term behavior of the groundwater DO concentrations. However, the contradictory results for *AaKi* and the heterogeneity of the results from the *RhSe* piezometers show that local aquifer properties are also likely to play an important determining role.

5.3.1.2 Abrupt changes

DO concentrations measured at *EmSi*, *AaKi*, *ToLi*, and *ToZe*, and in *RhSe* piezometers G10, G11, and G101T, underwent abrupt, episodic increases and decreases at various points in time. At *EmSi* and *AaKi*, DO concentrations increased strongly from 2001 to 2002, and at *ToLi* and *ToZe* from 2008 to 2009 (Figs. 5.2b, 5.3b, 5.6a, 5.7; grey shaded areas). In *RhSe* piezometers G10, G11, and G101T, a rapid, strong decrease in DO concentration from the early to the mid-1970s was followed by a multi-annual period of low DO concentration and a subsequent rapid recovery phase in the late 1970s and early 1980s (Fig. 5.5a,b,c; grey shaded areas). The simultaneous occurrence of the abrupt changes at *EmSi* and *AaKi* suggests, as for the temporal trends, a common external forcing factor. However, the occurrence of abrupt changes at different points in time in the other aquifers shows that common external forcing is not the whole story.

5.3.2 The spatial distribution of DO concentration in the *RhSe* and *ToLi* aquifers

In order to analyze the spatial distribution of DO concentration at *RhSe*, the measuring sites (pumping well and piezometers) were divided into two groups based on their perpendicular distance from the riverbank, and the mean DO concentrations measured at the sites were compared using Student's t-test. The mean DO concentration measured at sites G10, G11, G101, and G101T, located close to the riverbank (15-30 m), was 6.0 ± 2.2 mg O_2 l^{-1}, and that measured at sites PW, G19, G20, G21, G403, located much farther from the riverbank (520-2000 m), was 5.8 ± 0.4 mg O_2 l^{-1}. The difference between the two mean values (0.2 mg O_2 l^{-1}) was small and not statistically significant ($p = 0.93$). To exclude any effect of the excursion to low values in the 1970s that was especially evident at G10 (Fig. 5.5a), G11 (Fig. 5.5b), and G101T (Fig. 5.5c), the test was repeated using only the data from 1985 onward. Although the

difference was greater (1.3 mg O_2 l^{-1}), it was still not statistically significant (p = 0.18). The data thus show that the mean DO concentration does not decrease substantially with increasing distance from the riverbank.

Based on data from *ToLi3* and *ToLi4*, Beyerle et al. (1999) came to a similar conclusion for the *ToLi* aquifer. They found oxygen consumption to be 2.8 mg O_2 l^{-1}during passage through the hyporheic zone and 1.2 mg O_2 l^{-1} yr^{-1} in the interior of the aquifer using DO concentration measurements and ^{3}He-^{3}H groundwater ages. Groundwater ages at *ToLi3* and *ToLi4* were estimated to be 10 ± 3 months and 13 ± 3 months, respectively (Beyerle et al., 1999).

These findings indicate that, at least at *RhSe* and *ToLi*, oxygen consumption in the river-aquifer system occurs mainly or exclusively during infiltration; i.e., during passage through the hyporheic zone. Because of the similarity of the RBF systems analyzed in this study, we assume that this statement is also valid for aquifers *EmSi*, *AaKi*, and *ToZe*.

5.3.3 Hypotheses explaining the observed features

To explain the observed features of long-term trends and abrupt changes in the groundwater DO concentrations, we analyzed three hypotheses based on the available data:

1. Oxygen consumption rates in the hyporheic zone and within the aquifer were constant with time, and the long-term trends found in the groundwater DO concentrations resulted from long-term trends in the DO concentration in the losing river.

2. An increase in groundwater temperature led both to a decrease in physical solubility and to an increase in microbial activity in the hyporheic zone, which in turn led to a decrease in groundwater DO concentration.

3. Changes in hydrological conditions – i.e., changes in pumping rate, river discharge rate, or groundwater level – affected the groundwater DO concentration by altering the residence time of the water in the microbiologically active hyporheic zone.

5.3.3.1 The influence of the DO concentration in the losing river

At *ToLi* and *ToZe* the decreases in DO concentration during the 1990s (Figs. 5.6a, 5.7) appear to be associated with a simultaneous decrease in DO concentration in the River Toess (Fig. 5.6b). However, no increase in DO concentration in the River Toess was observed from 2008 to 2009 that might explain the abrupt increase in groundwater DO concentration that occurred at both *ToLi* and *ToZe* at this time (Figs. 5.6-5.7); in fact, the DO concentration in the River Toess decreased from 2008 to 2009 (Fig. 5.6b). At *EmSi*, *AaKi*, and *RhSe*, either no temporal trends in river water DO concentration were found, or any trends that were found were opposite in sign to the trends found in groundwater DO concentration (Table 5.3; Figs. 5.2-5.5). Significant (p < 0.05) correlations between the annual mean groundwater DO concentrations in the *RhSe*, *ToLi*, and *ToZe* aquifers and the annual mean DO concentrations in the respective losing rivers (with lags of 0 - 2 yr) were mostly positive (Table 5.4). These correlations suggest that in the short term, groundwater DO concentrations might be influenced to some extent by the DO concentration in the losing river. Taking into account the large distances between the river gauging sites and the infiltration sites, however, the correlations between river-water and groundwater DO concentrations should be interpreted with caution. Nevertheless, the comparison of features such as trends and abrupt changes in the time series of DO

concentration in the groundwater and in the losing river indicate that the long-term behavior of the DO concentration in groundwater is very unlikely to be governed primarily by the DO concentration in the losing river.

5.3.3.2 The influence of groundwater temperature

At all sites where the DO concentration exhibits a decreasing trend (*EmSi*, *RhSe*, *ToLi*, and *ToZe*; Figs. 5.2, 5.4-5.7; Table 5.3), both groundwater temperature and river-water temperature exhibit strong, increasing trends (Table 5.3). The trends in the computed groundwater DO saturation concentrations (Table 5.3) give an indication of how much the increase in groundwater temperature would reduce the physical solubility of oxygen. In the *RhSe* pumping well (Fig. 5.4a) the similarity of the temporal trend in groundwater DO concentration to that of the DO saturation concentration suggests that the decrease in this pumping well might be attributable to the reduction in physical solubility resulting from the higher temperatures, with the contribution of microbial oxygen consumption (responsible for the difference between the DO saturation concentration and the measured DO concentration) being constant. In *RhSe* piezometers G20 and G21, and in the pumping wells of the *ToLi* and *ToZe* aquifers, however, the decreasing trends in the DO concentration were greater than would be expected from trends in physical solubility alone (Table 5.3). This would imply that other effects – such as, presumably, enhanced microbial activity – were causing a further reduction in groundwater DO concentration. Further evidence supporting the temperature effect hypothesis is given by the significantly negative correlations ($p < 0.05$) between groundwater DO concentration and groundwater temperature at *EmSi*, *RhSe* (except piezometer G21), and *ToLi* (Table 5.4). Other results, on the other hand, suggest that this hypothesis might be too simplistic. For instance, at *AaKi* the strong, long-term increase in groundwater temperature that began in the late 1980s (Figura et al., 2011) did not lead to a corresponding decrease in DO concentration. Further, the abrupt, strong increases in DO concentration observed at *EmSi* and *AaKi* from 2001 to 2002, and at *ToLi* and *ToZe* from 2008 to 2009, did not coincide with any significant drops in groundwater temperature.

Despite the partially contradictory nature of the results, the hypothesis of a temperature-related decrease in groundwater DO cannot be rejected completely. Although the data do not unequivocally imply an increase in microbial activity, the strong warming observed in the aquifers (Table 5.3; Figura et al., 2011) suggests that groundwater temperature has likely contributed to the steady decrease in groundwater DO concentration. However, the presence of abrupt shifts in the groundwater DO concentration time-series that are unrelated to groundwater temperature implies that temperature-dependent physical and microbial processes are not the only processes to have a strong impact on groundwater DO concentration.

Table 5.4: Correlations between annual means of groundwater DO concentration and potential driving variables. Lag (from 0 to 2 yr) of the Spearman rank correlation coefficient between the time-series of the annual mean groundwater DO concentration and the time-series of the annual means of: DO concentration in the losing river; groundwater temperature; groundwater DO saturation concentration; groundwater level; discharge rate of the losing river; and groundwater pumping rate. The numbers listed are the lag in years (groundwater DO concentration lagging the potential driving variables) at which there is a positive (+) or negative (-) correlation significant at the $p < 0.05$ level or better. Prior to calculating the correlations, all time-series were detrended using the procedure of Cleveland et al. (1990). Significance levels are: $p < 0.05$ (*); $p < 0.01$ (**); $p < 0.001$ (***). The lack of any significant correlation at any lag from zero to 2 yr ($p > 0.05$) is denoted by "ns", and the lack of sufficient data by "-".

	River-water DO concentration	Groundwater temperature	Groundwater DO saturation	Groundwater level	River discharge rate	Groundwater pumping rate
EmSi	ns	0**(-), 1*(-)	0**(+), 1*(+)	ns	ns	ns
AaKi	ns	ns	ns	ns	ns	ns
RhSe						
PW	0***(+), 1***(+)	0*(-)	0*(+)	ns	ns	ns
G10	ns	ns	1*(+)	-	ns	-
G11	ns	ns	ns	-	ns	-
G101	ns	0*(-)	ns	-	ns	-
G101T	ns	0**(-)	0**(+)	-	ns	-
G19	1*(+)	ns	ns	-	0*(+), 1*(+),	-
G20	0*(+), 2*(-)	ns	ns	-	ns	-
G21	ns	0**(-)	0**(+)	-	ns	-
G403	0*(+), 1*(+)	ns	ns	-	0*(+)	-
ToLi						
ToLi1	2*(+)	0*(-)	ns	ns	ns	ns
ToLi2	1**(+)	0**(-), 1*(-)	ns	ns	ns	ns
ToLi3	1*(+)	0**(-)	ns	ns	ns	ns
ToLi4	1*(+)	0***(-), 1*(-)	ns	2*(+)	ns	ns
ToLi5	1*(+)	0*(-), 1*(-), 2*(-)	ns	ns	ns	ns
ToZe	ns	ns	ns	-	ns	-

5.3.3.3 The influence of hydrological variables

Temporal trends in river discharge rate and groundwater level are generally weak or absent (Table 5.3; no trends were calculated for pumping rate due to the scarcity of the data). Correlations between annual mean groundwater DO concentration and annual means of the pumping rate, river discharge rate, and groundwater level indicate no consistent relationship (Table 5.4). The results of trend and correlation analyses show that any influence that hydrological variables might have on the long-term evolution of the groundwater DO concentration is certainly not linear.

An event-based comparison of groundwater DO concentration with pumping rate revealed a remarkably strong association between the two in the *ToLi* aquifer. The strong rise in DO concentration from 2008 to 2009 in the *ToLi* aquifer coincided with the unusually high pumping rates registered in 2009 (Figs. 5.6a, 5.7a-d), which were the result of a large-scale pumping test held in this year. These unusually high pumping rates in 2009 most probably led to the faster infiltration of a larger-than-usual volume of river water, resulting in a strong increase in DO concentration. At *AaKi* also, the increase in DO concentration from 2001 to 2002 was accompanied by a slight increase in pumping rate (Fig. 5.3b). However, high pumping rates were not always accompanied by sudden increases in DO concentration. Pumping rates even higher than those in 2009 were observed at *ToLi3* in 2005 and at *ToLi5* in 2003, but these had no effect on DO concentration (Figs. 5.6a, 5.7a-d); and at *AaKi* pumping rates continued to increase after 2002, while groundwater DO concentration decreased (Fig. 5.3b). Furthermore, at *EmSi* the rise in DO concentration from 2001 to 2002 was seemingly not caused by a change in pumping rate (Fig. 5.2b), and in the *RhSe* aquifer the pumping rate seems to have had no effect on groundwater DO concentration (Fig 5.4a).

Abrupt increases in groundwater DO concentration that cannot be explained by high pumping rates can often be explained as the result of events of extremely high river discharge. At *EmSi*, *AaKi*, *ToLi*, and *ToZe*, sudden increases in groundwater DO concentration often coincided with, or immediately followed, such events. These findings are confirmed by the results of the intervention analysis (Table 5.5).

At *EmSi* the increase in groundwater DO concentration from 2001 to 2002 coincided with two years in which the annual mean discharge rate of the River Emme was unusually high (Fig. 5.2d). The synchronicity of peak DO concentration and peak discharge rate was especially evident in the fall of 2002 (Fig. 5.2c). Table 5.5 shows that an intervention model yielded the best fit with interventions in 1999, 2001, and 2002. The annual mean river discharge rates for these years were among the five highest values ever observed. The high river discharge rates in 1999, 2001, and 2002 (Fig. 5.2d) presumably led to an increase in the infiltration of river water, evidenced by a strong rise in groundwater level from 2001 to 2002 (Fig. 5.2b).

At *AaKi*, a relatively high annual mean discharge in 2002 (Fig. 5.3c) was observed, which, in combination with a slightly increased pumping rate (Fig. 5.3b), might have led to the increase in DO concentration from 2001 to 2002. The relatively high annual mean discharge of the River Aare in 2002 (Fig. 5.3c), though, did not affect groundwater DO concentration at *AaKi* in the same way as at *EmSi*, as there was no increase in groundwater level (Fig. 5.3b) and the abrupt rise in DO concentration was not confined to fall, but was observed in all seasons. However, the abrupt increase in groundwater DO concentration was preceded by three individual major discharge events: on 28 January 1999, 11 December 2000, and 18 November

2002. We assume that in this case, repeated, intense scouring of the riverbed reduced clogging and facilitated the infiltration of river water, resulting in an increase in groundwater DO concentration. The intervention model fits best with a single intervention in 2002 (Table 5.5), highlighting the discharge event in 2002 as a potential cause of the increase in DO concentration from 2001 to 2002.

As in the case of *AaKi* in 2002, the sudden increases in DO concentration in the *ToLi* and *ToZe* pumping wells in 2009 (Figs. 5.6a, 5.7) were preceded by major individual discharge events in 2007 (9 August) and 2008 (22 April) (Fig. 5.6b). The intervention model yields the lowest RMSD values for interventions in 2007 and 2008 based on daily mean discharge data (Table 5.5). The previously mentioned absence of abrupt increases in DO concentration at *ToLi3* in 2005 and *ToLi5* in 2003, despite pumping rates that exceeded those in 2009, is thus potentially a consequence of lower infiltration rates associated with a clogged riverbed. The scouring of the riverbed in 2007 and 2008 by the high discharge events that occurred in these years would have allowed the infiltration rate, and hence the groundwater DO concentration, to respond more sensitively to the increase in pumping rate from 2008 to 2009. The abrupt increase in DO concentration from 2008 to 2009 was therefore a consequence of the interplay of two factors: riverbed scouring resulting from high discharge events, and an increase in pumping rate.

Evidence of the potential effect of riverbed clogging on groundwater DO concentration is given by observations made in the *RhSe* aquifer in the 1970s and 1980s. In the 1970s, the operators of the *RhSe* pumping well discovered layers of zebra mussels (Dreissena polymorpha Pallas) up to 5 cm thick on the riverbed in the area between piezometers G10 and G101, where most of the infiltration of river water into the groundwater usually occurs, but diving expeditions showed that by the late 1980s this layer of zebra mussels had disappeared (Stahel, 1989). Clogging of the riverbed by the zebra mussels presumably led to a reduction in the rate of infiltration of river water, so that DO concentrations in the piezometers close to the river (G10, G11, and G101T) dropped significantly over a period of several years (Fig. 5.5a,b,c). The disappearance of this layer of mussels allowed the river water to infiltrate faster, leading to an increase in DO concentration in the late 1970s and early 1980s (Fig. 5.5a,b,c).

These results suggest that high pumping rates and high annual mean discharge rates lead to an increase in groundwater DO concentration by facilitating the infiltration of river water. Nevertheless, the examples of *AaKi* and *ToLi* indicate that this process does not occur on every occasion when high pumping rates or high annual mean river discharge rates prevail. It seems that the intermittent scouring and unclogging of the riverbed by individual extreme river discharge events might be a necessary condition that must be fulfilled before pumping rates and annual mean river discharge rates can affect the infiltration of river water and, as a consequence, the groundwater DO concentration. Riverbed clogging, by extending the residence time of the infiltrating river water in the microbiologically active hyporheic zone, might also explain the periods of decreasing DO concentration at *EmSi, RhSe, ToLi*, and *ToZe*.

Table 5.5: Results of the intervention analysis. Results of the intervention analysis model for groundwater DO concentration (eq. 5.2). The first term of eq. 5.2 (N_t) was modeled as an ARIMA model, the order of which is given in the first row. The second term of eq. 5.2 (m_t) is an exponential pulse function that represents the change in the mean caused by each intervention. Interventions were defined as having occurred in the five years containing the five highest values of annual mean discharge or daily mean discharge ("extreme events"). Allowing 1-5 interventions to take place, 31 combinations of years with an intervention are possible (see text). The years for which the inclusion of an intervention led to the best fit of the intervention model are highlighted in bold. The root mean square deviation (RMSD) shown is that between the measured DO concentration and the best-fit intervention model. The model was fitted using data from 1980 until the end of each DO time-series.

	EmSi	AaKi	ToLi1	ToLi2	ToLi3	ToLi4	ToLi5	ToZe
Order of ARIMA model for N_t	(1,0,0)	(1,1,1)	(1,0,2)	(1,0,0)	(1,0,0)	(1,0,0)	(1,0,0)	(1,0,0)
Annual mean discharge								
	2001	1992	1999	**1999**	1999	**1999**	**1999**	**1999**
	1999	1988	**1995**	**1995**	1995	**1995**	**1995**	**1995**
Years of "extreme events"	**2002**	1987	2001	2001	**2001**	**2001**	**2001**	**2001**
	1995	**2002**	1981	1981	1981	1981	1981	1981
	2007	1996	**2002**	**2002**	**2002**	**2002**	**2002**	**2002**
RMSD	0.16	0.21	0.24	0.30	0.35	0.59	0.22	0.23
Daily mean discharge								
	2005	1992	1994	1994	1994	1994	1994	1994
	2006	1999	1999	1999	1999	1999	1999	1999
Years of "extreme events"	**2004**	2001	1999	1999	1999	1999	1999	1999
	2007	1997	2007	**2007**	2007	**2007**	**2007**	**2007**
	1999	**2002**	**2008**	**2008**	**2008**	**2008**	**2008**	**2008**
RMSD	0.29	0.21	0.20	0.28	0.30	0.47	0.18	0.20

5.4 Conclusions

The time-series of groundwater DO concentration analyzed in this study all exhibited both long-term trends and abrupt changes. Of the three hypotheses considered as explanations for these two observed features, none could be excluded with certainty. The data indicate rather that these processes act as competing controls, which together determine the long-term behavior of the groundwater DO concentration. We regard the following explanation of the observed long-term trends and abrupt increases in the groundwater DO time-series as the most likely. During periods in which river water infiltration is not affected substantially by alterations in the hydraulic regime (such as high pumping rates, extremes in river discharge, or changes in the state of the riverbed), increasing groundwater temperatures result in decreasing groundwater DO concentrations because of both a decrease in the physical solubility of oxygen, and an increase in microbial activity in the hyporheic zone and in the groundwater (Chapelle, 1993; Greig et al., 2007; Sprenger et al., 2011; Diem et al., 2013). This may be compounded by a simultaneous decrease in DO concentrations in the losing river. Increased clogging of the riverbed might also reduce the rate of infiltration of river water through the hyporheic zone (Schälchli, 1992; Nogaro et al., 2010), resulting in a more rapid decrease in groundwater DO concentration (Nogaro et al., 2010). However, a combination of high pumping rates and high

annual mean river discharge rates can result in sudden increases in groundwater DO concentration (Mauclaire and Gibert, 1998), but this is likely only after the occurrence of individual, extreme river discharge events that are severe enough to scour the riverbed and free it from clogging (Schälchli, 1992).

Assuming air and river water temperatures will continue to increase both globally (Kundzewicz et al., 2007; Meehl et al., 2007) and in Switzerland (CH2011, 2011; FOEN, 2012) during the current century, DO concentrations in the aquifers analyzed in this study are likely to exhibit a continued tendency to decrease gradually in the long term. This decreasing tendency will be countered by the effect of an increase in the frequency of high discharge events in the losing rivers, which will probably result in intermittent scouring and unclogging of the riverbeds, followed by increased infiltration and abrupt increases in DO concentration. As a consequence, groundwater DO concentrations are unlikely to undergo an uninterrupted, steady decrease. Long-term hypoxia will therefore probably not occur in the type of aquifer analyzed in this study. Nevertheless, we assume that the risk of occurrence of extreme situations, such as documented by Hoehn and Scholtis (2011) for the summer of 2003, will increase. The risk of groundwater hypoxia will be higher if future hot, dry summers are preceded by several years with no discharge events intense enough to scour the riverbed sufficiently to reduce riverbed clogging.

<div style="text-align: right; font-size: 3em;">6</div>

Synthesis and Outlook

A review of the relevant literature suggests that groundwater will be affected by changing climatic conditions (Bates et al., 2008; Green et al., 2011; Taylor et al., 2013). However, as a consequence of the paucity of relevant long-term data there are still many open questions regarding the potential impact of climate change on groundwater quality (Aureli and Taniguchi, 2006; Dragoni and Sukhija, 2008; Green et al., 2011). A similar conclusion can be drawn from the report by BUWAL (2004) on the impact of the extraordinarily hot, dry summer of 2003 on water resources in Switzerland. Although this report did conclude that drinking-water production in Switzerland encountered no substantial problems related to groundwater quantity or quality during this period, it also stated that the full extent of the impact of the summer of 2003 on groundwater quality might not have been realized because of the lack of relevant long-term data.

Based on long-term data recently collected from Swiss aquifers (Schürch, 2011) the present work succeeded firstly in showing how groundwater temperature and DO concentration in aquifers recharged by RBF have reacted to changes in climatic conditions in the past 30 – 40 years, and secondly in estimating how these two variables - which are both important determinants of groundwater quality - are likely to change in the future. The study has shown that groundwater temperature at RBF sites has increased strongly in the past and suggests that it will continue to do so in the future. Such a warming will, under certain conditions, have a negative effect on groundwater DO concentrations, and consequently on groundwater quality, at such sites. In addition, this work highlights the general utility of historical data in environmental research. Such data – even when, as in this work, they are available only at low sampling frequency – can be extremely useful in identifying features in environmental systems, such as long-term trends and abrupt shifts, that might not be detectable in more detailed but temporally limited case-studies.

Preliminary studies of available long-term groundwater data in Switzerland (Figura, 2009) and similar studies in Austria (Schartner and Kralik, 2011) have shown that groundwater temperatures have increased in the past, possibly in response to increases in air temperature. In this thesis, an analysis of groundwater temperatures measured in the pumping wells of five aquifers recharged by RBF not only confirmed that the groundwater temperature at these sites has increased particularly strongly in the recent past, but also showed that much of this

warming took place in response to the late 1980s climate regime shift (CRS) around 1987/88. The late 1980s CRS, which is associated with a shift to a strong positive phase in the Arctic Oscillation, caused an abrupt, strong increase in air temperature that was transmitted through the losing rivers to the groundwater. While the effect of the late 1980s CRS on river-water temperature was immediate and confined mainly to spring and summer, its effect on groundwater temperature was also observed in other seasons because the climatic signal in groundwater is damped and delayed. The current study showed further that the reaction of the groundwater temperature to the late 1980s CRS differed among the aquifers. Whereas in two aquifers groundwater temperature remained statistically stationary after the late 1980s CRS, in the other three aquifers it continued to increase. Although the reaction of groundwater temperatures to the late 1980s CRS was heterogeneous, it can be concluded that groundwater temperature at RBF sites responds strongly to large-scale climatic phenomena such as the Arctic Oscillation.

Forecasts of groundwater temperature were calculated for four aquifers recharged by RBF and three aquifers recharged by the percolation of precipitation only. With respect to the reference period 1980-2009, groundwater temperature in three of the aquifers recharged by RBF are predicted to increase by 1.0 to 3.5 K by the end of this century, depending on the assumed greenhouse-gas emissions scenario. This suggests that groundwater at RBF sites will undergo substantial warming approximately in parallel with climate change. In the aquifers recharged by the percolation of precipitation, and in the fourth aquifer recharged by RBF, the mean predicted increase was approximately 1 K. The results of the study further showed that the performance of the two linear regression models used for the predictions depends strongly on the length and variability of the training data available for the calibration of the models. In particular, the models performed considerably better when the period of the training data included the late 1980s CRS. However, the time-series of the aquifers recharged by the percolation of precipitation and of the fourth aquifer recharged by RBF started only in 1989, so it is not clear whether the predicted small increase is the consequence of a weak response to climatic forcing or – more likely - the result of a poor fit of the models because of the shortness of the time-series.

The analysis of groundwater DO time-series at RBF sites suggests that periods of decreasing groundwater DO concentration observed in the past were associated with the warming of the groundwater and of the losing rivers. However, changes in hydrological conditions – for instance in the groundwater pumping rate or in the annual mean river-discharge rate – as well as individual extreme river-discharge events that were able to unclog the riverbed, resulted in sudden increases in groundwater DO concentration. These sudden increases were presumably the consequence of a larger-than-usual and faster infiltration of highly oxygenated river water into the aquifer. Although the runoff regimes of Swiss rivers are expected to shift seasonally in the future, annual mean discharge rates will not undergo substantial change. However, an increase in the frequency of extreme discharge events is possible (FOEN, 2012). Any potential long-term decrease in DO concentrations that might result from the warming of groundwater and river-water is therefore likely to be interrupted regularly by sudden, abrupt increases that will prevent the groundwater DO concentrations from decreasing continuously.

One big concern about the direct impact of climate change on groundwater quality at RBF sites is that a decrease in DO concentration in response to warming might lead to anoxia, and

hence to the occurrence of reducing conditions (Sprenger et al., 2011). This, in turn, might result in the dissolution of manganese and iron (hydr)oxides in the groundwater. The precipitation of iron and manganese after re-oxidation in the pumping wells can cause them to clog, possibly posing problems in the production of drinking water. As mentioned above, the results of this work suggest that permanent groundwater anoxia is improbable. Nevertheless, climate model projections indicate that hot, dry periods in summer are likely to become more frequent and longer (Schär et al., 2004; CH2011, 2011; FOEN, 2012). The risk of encountering anoxic and reducing conditions similar to those observed in the summer of 2003 (Rohns et al., 2006; Hoehn and Scholtis, 2011; A. Scholtis, unpublished data) will therefore in my view be clearly higher by the end of the century. Such negative conditions are particularly likely to occur after multi-annual periods of generally low river discharge with no discharge events severe enough to unclog the riverbeds.

In a review article, Sprenger et al. (2011) discussed the susceptibility of RBF systems to climate change. The work in this thesis confirmed that groundwater quality at RBF sites is likely to be affected negatively by the increases in groundwater temperature and decreases in DO concentration which are expected to take place as a result of climate warming. However, some issues could not be addressed in this work, leaving some open questions. This is particularly true with respect to the hypotheses on the processes assumed to govern groundwater DO concentration introduced in Chapter 5. These hypotheses need to be examined in detail, which would require additional field data. To further examine the impacts of climate change on groundwater quality at RBF sites in Switzerland, I would recommend the following research and monitoring strategies.

Further research. The majority of questions still open concern the processes responsible for the long-term behavior of the groundwater DO concentration. The available data allowed only a subset of potentially relevant processes to be analyzed. There are, however, others. Diem et al. (2013), for example, showed that microbial respiration in the hyporheic zone increased after flood events because of the input of natural organic matter (NOM). In this work, information about NOM might be the most crucial data missing for the description of DO because of the importance of the availability of organic matter for microbial respiration. It is also not clear how important the input of oxygen through the unsaturated zone is for the groundwater DO concentration. With regard to the input of oxygen through the unsaturated zone, the importance of "excess air" processes for groundwater DO concentration needs to be analyzed in more detail. Most importantly, the hypothesis that clogging of the riverbed plays a crucial role for groundwater DO concentration by affecting the residence time of the infiltrating river water in the hyporheic zone needs to be verified or falsified by field observations. I would therefore highly recommend designing field studies to evaluate the impact of hydrological conditions (e.g., river discharge, pumping amount, clogging of the riverbed) and NOM input on respiration in the hyporheic zone. Some relevant studies already exist (e.g., Brunke and Gonser, 1997; Malard and Hervant, 1999; Diem et al., 2013). However, these previous studies were conducted on relatively small spatial and short temporal scales. To upgrade future studies on processes in the hyporheic zone and in the unsaturated zone both spatially and temporally, they should be carried out simultaneously, and the combined results related to observations in the pumping well. Such an integrated analysis could be achieved by conducting future field studies at sites

where long-term data already exist and where monitoring, as described below, is being conducted.

Further research based on the findings of this thesis and of potential future studies might focus on evaluating the practical implications of the evolution of DO concentration at RBF sites. The conditions under which a change in DO concentration would complicate the operation and maintenance of pumping wells need to be evaluated in detail. An additional task consists of setting the impact of climate change on groundwater DO concentration in relation to other impacts of global change on groundwater quality; e.g., a change in the input of pollutants due to altered recharge conditions and increased population (Green et al., 2011).

Regarding groundwater temperature at RBF sites, it seems certain that groundwater will warm substantially in the future. However, taking into account the fact that groundwater is often used for heating or cooling purposes (Lee and Hahn, 2005; Shin et al., 2010; Epting and Huggenberger, 2013), detailed knowledge about future groundwater temperature is essential. Therefore, more detailed and less uncertain predictions of future groundwater temperature might be necessary, particularly with regard to seasonal variability. Future studies need to assess whether empirical models can provide adequate forecasts of groundwater temperature, or whether numerical models are to be preferred. I would recommend comparing the linear regression models used in this work, and more elaborate empirical models, with numerical groundwater flow and heat-transport models. Such an approach would allow better determination of the impact of hydrological conditions on groundwater temperature. A further open question with respect to groundwater temperature remains for those sites where the linear regression models failed to model groundwater temperature adequately. I believe that the data available from these sites would allow a better modeling of temperature than was achieved in this work. However, the development of more adequate statistical temperature models for these aquifers would necessitate quite a considerable amount of additional work.

The study on the groundwater temperature regime shift presented in Chapter 3 also left an open question. It is not clear why groundwater temperature in the 1990s continued to increase at three sites while remaining statistically stationary at the other two sites. The possible reasons for this phenomenon remain to be investigated. One possibility is that the aquifers at which groundwater temperature continued to increase in the 1990s contain a large proportion of groundwater with a long residence time, which could have delayed the climatic signal for several years. Another explanation could perhaps be the alteration of recharge and flow properties at certain sites related to the late 1980s regime shift.

Not in direct relation to this work, but with respect to the data collected in the run-up to this project (Schürch, 2011), I would highly recommend analyzing the available time-series on groundwater quantity. Several dozen time-series on spring discharge, groundwater level, and – in some cases – groundwater pumping rates exist that are 30 – 100 yr long. Analyzing these data with the statistical methods used in this work or with numerical groundwater models would allow the potential impact of climate change on groundwater quantity in Switzerland to be determined.

Monitoring. To identify critical conditions at RBF sites, I would recommend that detailed monitoring be conducted, especially at sites where low oxygen concentrations have been observed in the past, and specifically at RBF sites where annual mean groundwater DO

concentrations are < 5 mg O_2 l^{-1} or where minimum concentrations have been close to or below 2 mg O_2 l^{-1}. Taking into account the findings discussed above the following variables at least should be monitored:

- River: discharge rate, water level, water temperature, DO concentration, NOM.
- Groundwater: water level, temperature, DO concentration, NOM.
- Pumping well: pumping rate, groundwater temperature, groundwater DO concentration.

Ideally, the groundwater monitoring should be conducted along the pathway of the infiltrating river water to the pumping well to determine the dynamics of DO during groundwater transport. If monitoring along a transect is not possible, measurements should at least be conducted in the pumping well. For the empirical assessment of long-term changes, high-frequency monitoring is not necessary. However, with the rapid growth in digital storage capacities, such high-frequency monitoring (perhaps every 10 - 15 minutes) has become easier and could provide interesting data which might allow processes affecting groundwater DO concentration to be identified that are not identifiable based only on monthly measurements, e.g., the input of oxygen due to "excess air" after abrupt rises in groundwater level (Mächler et al., 2013). Nevertheless, if financial resources do not allow such high-frequency sampling, monitoring should certainly be carried out at monthly intervals at least. During extreme events such as heat waves, droughts, and floods, the measurement frequency should be temporarily increased. In addition, to identify changes in redox conditions, I would highly recommend the measurement of other redox-sensitive variables such as nitrate, iron, manganese, and sulfate at monthly resolution or (especially during extremely hot and dry periods) higher. At sites where such monitoring already exists, it should be ensured that the data acquired are not only recorded but are stored centrally and analyzed regularly. Also, at sites that will potentially be used for drinking-water production, such monitoring should start as early as possible, even before the construction of new drinking-water production wells.

Appendix A

Data processing and statistical methods

This section summarizes the statistical methods most commonly used in this work. Section A.1 is based on the auxiliary material published as a supplement to Figura et al. (2011), and Section A.4 is a slightly modified version of part of this auxiliary material.

A.1   Outlier removal and interpolation of missing values

Potential outliers were first identified by visual inspection. Then the mean and standard deviation of the data within a 5-yr window centered on the suspect value were calculated. If the suspect value deviated by more than 3 standard deviations from the 5-yr mean, it was defined as an outlier and deleted from the time-series. The grey area in Fig. A1, which represents the band of 3 times the 5-yr running standard deviation around the 5-yr running mean, illustrates this approach exemplarily.

The temporal resolution of the historical measured data used in this work was not always the same. While groundwater data were in most cases available at the comparatively coarse resolution of one spot measurement per month, river data were often available as daily means. To make the data better comparable, all data were interpolated to daily resolution using cubic spline interpolation. Cubic spline interpolation is a method of interpolating gaps between data points using piecewise cubic polynomials (called splines) which are forced to pass through defined points, called "knots", in this case through the measured values, such that the polynomials and their first and second derivatives are continuous at the knots (Eubank, 1988). The time-series of interpolated daily values were then averaged to yield time-series of monthly means. Fig. A2 illustrates this approach. However, gaps in the measured data that exceeded five months (in Chapter 3) or three months (in Chapter 5) were interpolated differently (also shown in Fig. A2). In this case a cubic regression model (eq. A1) was fitted to the monthly means. The residuals from this model were then averaged for each month and added to the cubic regression model to obtain a series of monthly mean values (eq. A2).

$$T_{cubic,k} = \beta_0 + \beta_1 k + \beta_2 k^2 + \beta_3 k^3 \qquad (A1)$$

$$T_{interpol.,k} = T_{cubic} + \gamma_m \qquad (A2)$$

where $T_{cubic,k}$ is the monthly mean temperature in month k as modeled by the cubic regression; $T_{interpol.,k}$ is obtained by adding the averaged deviation of the measured data from the cubic regression model in month m, γ_m, to the value of the cubic regression model; and k is an integer from 1 to n (where n = total number of months in the time-series); β_0, β_1, β_2, and β_3 are the regression coefficients.
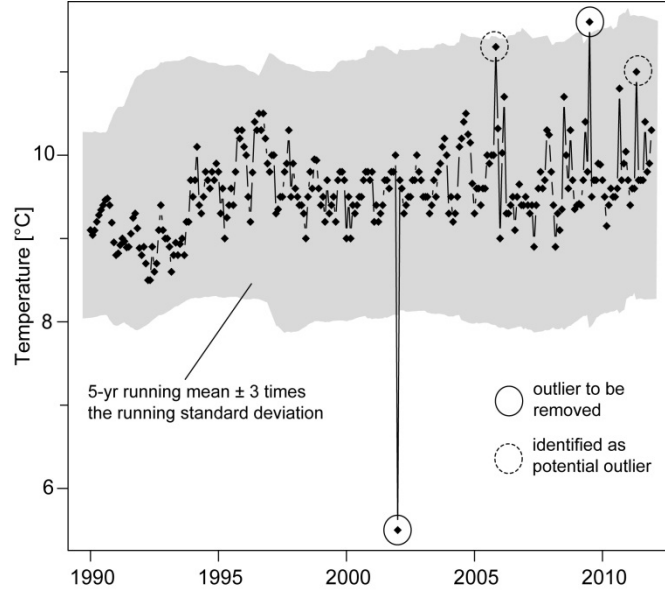

Figure A1: Temperature time-series measured in the pumping well of the *ToZe* aquifer. The grey area highlights the band of 3 times the 5-yr running standard deviation around the 5-yr running mean. Potential outliers that lay outside this band were defined as outliers and removed (solid-line circles). Potential outliers that lay inside the band were not defined as outliers and were retained in the time-series (dashed-line circles).
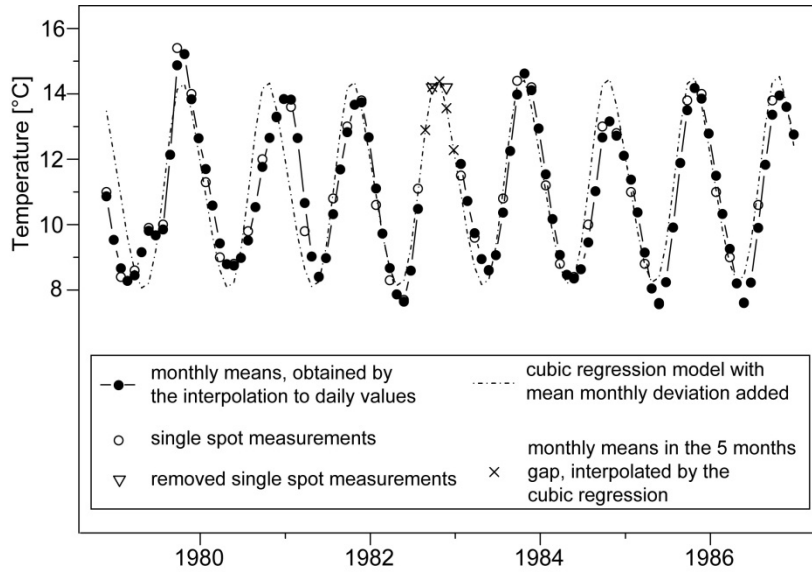
Figure A2: Illustration of the interpolation method used. Individual spot measurements (open circles) were first interpolated to yield time-series of daily values, which were then averaged to obtain monthly means (full circles). Gaps longer than three months were interpolated with a cubic regression model (dashed line; eq. A2, see text). To illustrate the interpolation with the cubic regression model, two individual spot measurements were removed (triangles) resulting in a gap of 5 months. The 5 values resulting from the interpolation of this gap with the cubic regression model are shown as crosses.

A.2   Removal of trend and seasonality

The removal of trend and seasonality was carried out using the seasonal-trend decomposition procedure of Cleveland et al. (1990) as implemented in the function *stl* in the statistical software *R* (R Development Core Team, 2011). This procedure is based on locally weighted regression scatter-plot smoothing, or *Loess*. For every data point $y(t)$, where t is time, *Loess* fits a weighted quadratic regression to the data within a predefined window around $y(t)$ (in this work the size of the window was set to 13 months). The data within the window are weighted based on their distance from $y(t)$, with the data farthest from $y(t)$ having the lowest weight. From each of these regressions, $\hat{y}(t)$, the modeled value of $y(t)$, is extracted, and the combination of all $\hat{y}(t)$ results in a smoothed time-series of monthly means which represents the seasonal component. The trend component is obtained by removing the seasonal component from the original time-series. The trend component is then again smoothed using *Loess* (here with a time window of 61 months). The mean value of the seasonal component is subtracted from the seasonal component and added to the trend component. Fig. A3 shows the output of the *stl* function for the example of the groundwater temperature time-series from the *Seewerben* aquifer.
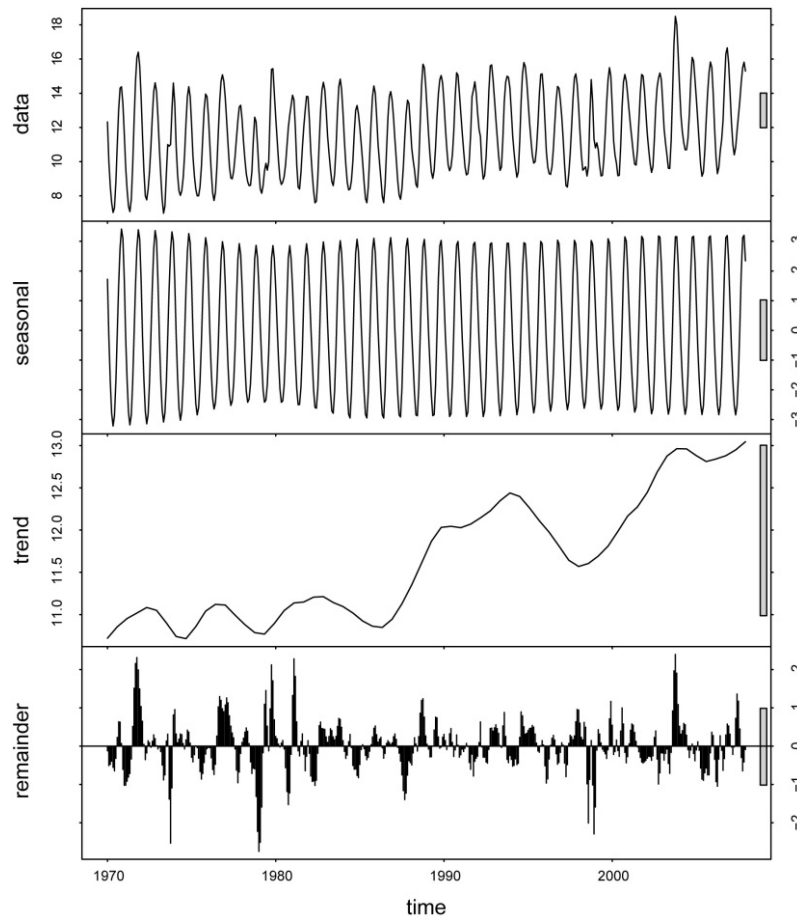
Figure A3: Output of the *stl* function (see text) for groundwater temperature of the *Seewerben* aquifer. The figure shows the original data (top panel), the seasonal component (second panel), the trend component (third panel), and the residuals obtained by subtracting the seasonal and trend components from the original data (bottom panel). Note that the y-axis scales in the four panels are not the same: as an aid to comparison, the grey bars on the right-hand side of each panel indicate a temperature difference of 2 K.

A.3 Cross-correlations

The cross-correlation function between two time-series X and Y is described by:

$$r_{XY}(k) = \frac{1}{n-2k} \frac{\sum_{i=k+1}^{n-k}[X(t_i)-\bar{X}](Y(t_{i+k})-\bar{Y})}{s_X s_Y} \tag{A3}$$

where Y (here: groundwater temperature) lags X (here: river-water temperature) by k time-steps (here: months), $r_{XY}(k)$ is the Pearson correlation coefficient between X and Y; n is the number of points in the time-series (here: the number of months); t is time; and s_X and s_Y are the standard deviations of X and Y, respectively. In addition, a standard deviation for r_{XY} can be calculated (formula not shown here) which, under the assumption that r_{XY} is normally distributed, makes it possible to test the statistical significance of r_{XY}.

Fig. A4 shows an example of the cross-correlation function between a time-series of monthly mean groundwater temperatures and a time-series of monthly mean river-water temperatures, with the groundwater temperature lagging the river-water temperature.

Instead of parametric Pearson correlation coefficients, nonparametric Spearman rank correlation coefficients can be calculated. To accomplish this, the two time-series are first ranked by value. The formula for calculating the Spearman rank correlation coefficient is the same as eq. A3, but instead of using the values of the time-series for the calculation, the ranks of the time-series values are used. Compared to the Pearson correlation, Spearman rank correlations are better suited for correlating two data series that are not strictly linearly related.
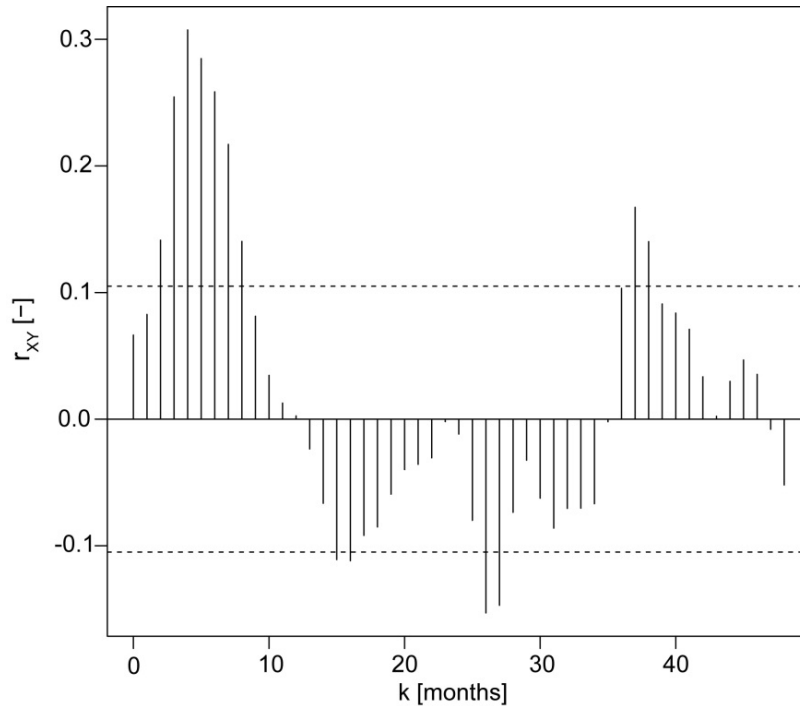
Figure A4: Cross-correlation function $r_{XY}(k)$ between monthly mean time-series of the water temperature of the River Rhine (X) and the groundwater temperature of the *Seewerben* aquifer (Y), with the groundwater temperature lagging the river-water temperature by $k = 0 \dots 48$ months. The horizontal dashed lines show an approximate value $(\frac{2}{\sqrt{n}})$, above which (or - for negative correlations - below which) the correlations can be assumed to be significant at the 95% significance level.

A.4 Regime-shift and change-point tests

In this section we provide a short summary of the three statistical tests used in Chapter 3 to identify abrupt changes in the temperature time-series, here denoted y_i, i = 1,...,n, where n is the length of the time-series. For detailed information on the tests, the reader is referred to the original literature, whose notation we use here as far as possible.

A.4.1. Rodionov regime-shift test (STARS)

The sequential t-test analysis of regime shifts (STARS) developed by Rodionov (2004) is a parametric test to identify abrupt shifts. The value of *diff* (eq. A4) indicates the difference between two subsequent regimes that "would be statistically significant according to the Student's t-test":

$$diff = t_{2l-2,p}\sqrt{2\sigma_l^2} \qquad (A4)$$

where σ_l^2 is the average variance for all running intervals with length l, and $t_{2l-2,\,p}$ is the value of the t-distribution with $2l$-2 degrees of freedom at a specified probability level p. As an example, we denote the average of y_1 to y_l as y_{R1}. Starting from $l+1$, we check whether the value y_i exceeds $y_{R1}\pm diff$. If it does not, y_i is integrated into y_{R1}. If y_i does exceed $y_{R1}\pm diff$, the year of the value of y_i is considered as a potential starting point j of a new regime. For this potential regime shift point j a Regime Shift Index (RSI) is calculated as in eq. A5.

$$RSI_{i,j} = \sum_{i=j}^{j+m}\frac{y_{i*}}{l\sigma_l}, m = 0, 1, ..., l-1 \qquad (A5)$$

where $y_i* = y_i - y_{R2}$ if the shift is positive and $y_i* = y_{R2} - y_i$ if it is negative (with y_{R2} denoting the average from y_{j+1} to y_{j+l-1}). If at any time from $i = j+1$ to $i = j+l-1$ the RSI becomes negative, j is rejected as a potential regime shift point. The value y at point j would then be taken to update y_{R1}. If every potential regime shift point was rejected, y_{R1} would be the average of all values y_i. A positive value for the RSI indicates a significant regime shift point. In this case, we calculate the new regime y_{R2} and search the next regime starting from $i = j+l$ with y_{R2} as the new base. As a consequence, the difference between two subsequent regimes is significant at least at the chosen significance level p. Application of Student's t-test to the mean values of the regimes identified returns actual p-values. In the study in Chapter 3 we chose $l = 10$ yr, because this is approximately half the length of the time-series to be analyzed, and set $p = 0.05$. The application of Student's t-test revealed that the actual p-values for the differences between subsequent regimes were all at least 0.01.

A.4.2. Pettitt change-point test

The Pettitt change-point test (Pettitt, 1979) is a nonparametric test, the results of which are calculated as in eq. A6. For each data point the Pettitt change-point test cumulatively sums the sign function calculated with all following data points.

$$U_{t,T} = \sum_{i=1}^{t}\sum_{j=t+1}^{T} Sgn(y_i - y_j) \qquad (A6)$$

where *Sgn* denotes the sign function and y is the data. A change-point K is found at $K=|max(U_{t,\,T})|$. The symbol t stands for the time from 1 to T. Change-points in the positive direction are found at $K^-=-min(U_{t,\,T})$, and in the negative direction at $K^+=max(U_{t,\,T})$. The

significance level is determined approximately by $p=2e^{(-6K^2/(T^2+T^3))}$. An important characteristic of the Pettitt test is that its structure allows only one change-point to be detected.

A.4.3. Barry and Hartigan change-point test

Barry and Hartigan (1993) use a Bayesian approach to the change-point problem. In their algorithm, a partition $\rho = (U_1, U_2, ..., U_n)$ is used, where $U_i = 1$ indicates a change-point at position $i + 1$ and $U_i = 0$ denotes the absence of a change-point. The conditional probability p for a change-point at $i+1$ is given by eq. A7. For each point in time i, a value for U_i is drawn from a conditional distribution for U_i with a Markov Chain Monte Carlo simulation. The conditional distribution is given by eq. A8. For every point in time, the algorithm returns a posterior probability for the occurrence of a change-point. The Barry and Hartigan change-point test was performed in the statistical software R (R Development Core Team, 2011) using the implemented package bcp (Erdman and Emerson, 2007). The relevant equations are:

$$\frac{p_i}{1-p_i} = \frac{P(U_i=1|Y,U_j,j\neq i)}{P(U_i=0|Y,U_j,j\neq i)} \tag{A7}$$

$$= \left(\frac{W_0}{W_1}\right)^{\frac{n-b-2}{2}} \cdot \left(\frac{B_0}{B_1}\right)^{\frac{b+1}{2}} \cdot \sqrt{\frac{B_1}{W_1}} \cdot \frac{[\int_0^{\frac{B_1\lambda/W_1}{1+B_1\lambda/W_1}} p^{(b+2)/2}(1-p)^{(n-b-3)/2}dp][\int_0^\gamma p^b(1-p)^{n-b-1}dp]}{[\int_0^{\frac{B_0\lambda/W_0}{1+B_0\lambda/W_0}} \frac{w^{(b-1)/2}}{(W_0+B_0w)^{(n-1)/2}}dw][\int_0^\gamma p^{b-1}(1-p)^{n-b}dp]} \tag{A8}$$

where W_0 and W_1 are the within-block sum of squares and B_0 and B_1 the between-block sum of squares for $U_i = 0$ and $U_i = 1$, respectively. Y is the data and b is the number of blocks when $U_i = 0$. The parameters γ and λ are tuning parameters for which initial values must be given. In this study, γ was set to 0.2 as suggested by Barry and Hartigan (1993). The starting value of λ was set equal to the variance of the linearly detrended time series.

A.5   Trend tests

In Chapter 3, trend tests were performed by testing the slope of the linear regression for significance and in chapter 5 by assessing the statistical significance of the Theil-Sen trend (Theil, 1950; Sen, 1968) with the Kendall τ statistic (e.g., Helsel and Hirsch, 1992).

A linear regression is fitted to a data series by minimizing the mean squared deviation of the measured values from the values modeled by the linear regression (eq. A9).

$$y_t = \alpha + \beta t + \varepsilon_t \tag{A9}$$

where y_t is a measurement at time t, α and β are the intercept and the slope of the model, respectively, and ε_t is the error term at t. The parameter estimation also returns a standard error for the slope which enables the statistical significance of the slope to be tested under the assumption that the data are independently and normally distributed (e.g., Helsel and Hirsch, 1992).

The Theil-Sen trend estimator is nonparametric, which means that no assumption of a parametric model, such as that of eq. A9, is made. The Theil-Sen estimator is described by the median of the slopes of all straight lines connecting all pairs of data points (eq. A10).

$$\beta = median \frac{(y_j - y_i)}{(t_j - t_i)}, i = 1, 2, \ldots, n-1, \ j = 2, 3, \ldots, n \qquad \text{(A10)}$$

To assess the statistical significance of the trend, the ratio S of the number of all positive (or negative) slopes to the total number of slopes is compared with the respective value of Kendall's τ (e.g. Helsel and Hirsch, 1992).

A.6 ARIMA and ARIMA intervention models

Auto-regressive moving-average (ARMA) models provide a method to model a stationary time-series Y (Box and Jenkins, 1970). ARMA models consist of two polynomial terms – an auto-regressive (AR) and a moving-average (MA) term – represented by the first and second terms, respectively, of eq. A11. If the first difference of Y is used for the combined AR and MA model (ARMA), the model is called an auto-regressive integrated moving-average (ARIMA) model. Eq. A11 shows the formulas for the ARMA(p,q) model of a detrended time-series.

$$Y_t = \sum_{i=1}^{p} \varphi_i Y_{t-i} + \sum_{i=1}^{q} \theta_i \varepsilon_{t-i} + \varepsilon_t \qquad \text{(A11)}$$

where ε_t is a white noise error term; t is time; p and q are the orders of the AR and MA models, respectively; and φ and θ are parameters to be estimated. The AR(p) model thus models the value of time series Y at time t with its p preceding values, and MA(q) is a moving average of the q preceding white-noise error terms.

In Chapter 5, ARIMA intervention models (Box and Tiao, 1975; Cryer and Chan, 2008) were used. Such models are intended to model time-series that have undergone an intervention. The basic model is:

$$Y_t = N_t + m_t \qquad \text{(A12)}$$

where N_t is an ARIMA model as described above and m_t is a function that represents the change in mean caused by the intervention at time t. If there is no intervention at time t, $m_t = 0$. If there is an intervention at time t, then m_t is represented by an AR(1) model (as in Chapter 5):

$$m_t = \delta m_{t-1} + \varpi P_t \qquad \text{(A13)}$$

where δ and ϖ are parameters to be estimated and P_t is the value of the binomial intervention time-series at time t. $P_t = 1$ if an intervention takes place at point t and $P_t = 0$ otherwise. Because $P_t = 0$ at times greater than t, m_t becomes an exponentially decaying pulse function after the occurrence of the intervention. Fig. A5 illustrates the intervention model for the example of a time-series of annual mean dissolved oxygen (DO) concentration from the *EmSi* aquifer.
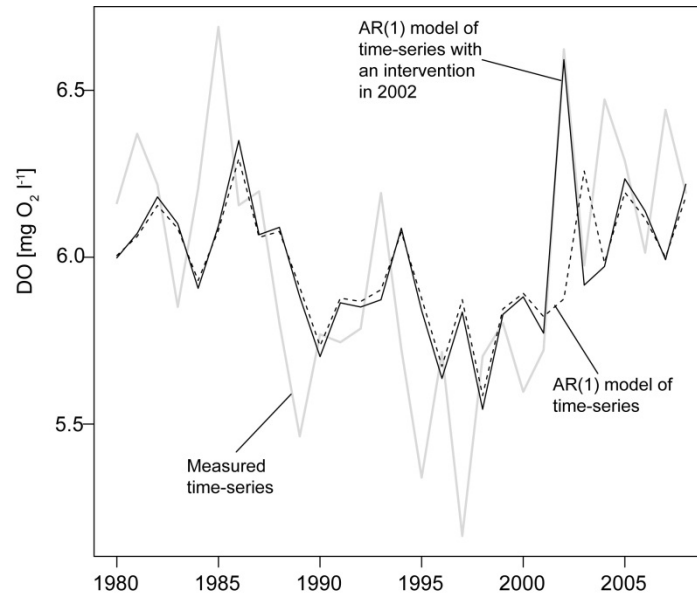
Figure A5: Annual mean time-series of groundwater DO concentration in the *EmSi* aquifer (grey line), AR(1) model of the annual mean time-series (dashed black line) and AR(1) model of the time-series with an intervention in 2002 (full black line). Due to slight differences in the parameter estimation the AR(1) model without an intervention and the AR(1) model with an intervention are not exactly the same before the intervention takes place in 2002.

Appendix B

Supplementary information to the article "Regime shift in groundwater temperature triggered by the Arctic Oscillation"

This section, which describes the data on which Chapter 3 is based, was published as part of the auxiliary material of Figura et al. (2011).

B.1 Groundwater temperature data

Fig. B1 shows the locations of the pumping wells where groundwater temperatures were measured and Table B1 summarizes some basic information about the aquifers and the temperature time-series. The aquifers analyzed in this study are alluvial valley-fill aquifers in alpine and perialpine valleys. In Switzerland, groundwater in such aquifers is known to be recharged predominantly by river-bank infiltration (Tripet, 2005), implying that river-bank infiltration is likely to be the dominant recharge mechanism for the aquifers analyzed in our study. Specific local information indicating that this is so for each aquifer individually is given for RhSe by Kempf et al. (1986), Trüeb (1971), and Wagner et al. (2001); for RhNe by Kempf et al. (1986) and Wagner et al. (2001); for EmSi by Arbenz et al. (1925); for AaKi by Kellerhals et al. (1981); and for *ToLi* by Kempf et al. (1986) and Mattle et al. (2001). Groundwater temperature time-series for aquifers *RhSe*, *RhNe*, *EmSi*, and *AaKi* were available from one pumping well per aquifer. Groundwater temperature time-series from aquifer *ToLi* were available from the five individual pumping wells *ToLi1-ToLi5* (Table B1, Fig. B1). The five wells lie within 2 km of one another and their temperature time-series show a very similar temporal structure. Their mean temperatures differed little from one another, ranging from 9.7 °C to 10.1 °C (1975-2007). The pairwise correlation coefficients (r) between time-series of the linearly detrended annual mean are all statistically significant ($p < 0.01$), with the proportion

of shared variance (r^2) ranging from 67% to 90%. The correlation coefficients between the monthly mean series are also all statistically significant ($p < 0.01$), with r^2 ranging from 40% to 75%. For the analysis described here, one mean time-series was therefore constructed for aquifer *ToLi* by taking the simple arithmetic mean of the temperature time-series from the five wells. The correlation coefficients of each individual time-series with the constructed mean time-series were statistically significant ($p < 0.01$) in all cases, with r^2 ranging from 65% to 88% for the annual time-series and from 64% to 87% for the monthly time-series.
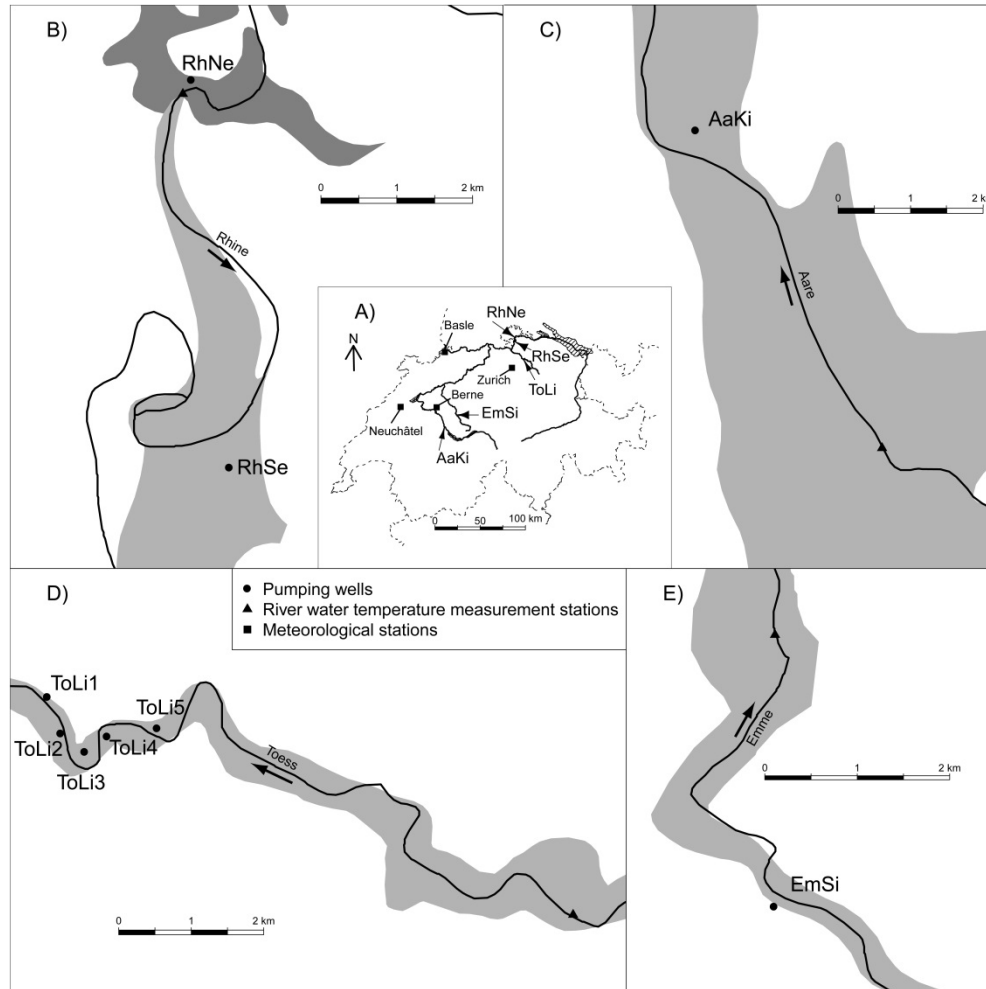

Figure B1: Maps showing the extent of the aquifers and locations of the pumping stations. (A) Map of Switzerland showing the losing rivers, the locations of the aquifers (arrows) and the Swiss Meteorological Office stations (squares). (B-D) Locations of the pumping wells (dots) and of the river temperature measurement stations (triangles). The shaded areas show the extent of the five aquifers. In panel B, the darker shading represents the *RhNe* aquifer and the lighter shading the *RhSe* aquifer.

B.2 River temperature data

For three of the four losing rivers that feed the aquifers (Rh, Em, and Aa), daily water temperature data were available from 1976-2007 or longer. For the fourth river (To), monthly mean water temperature data were available only from 1984-2007. For the analysis, the water temperature data were aggregated to obtain monthly and annual means. All river temperature measurements were made within 10 km of the respective groundwater pumping stations (Fig. B1).

B.3   Air temperature data

The regional air temperature time-series was constructed as the mean of the air temperature measured at the Swiss Meteorological Office stations at Zurich, Berne, Basle, and Neuchâtel (Fig. B1). This averaged time-series is known to yield a good estimate of the regional air temperature for the Swiss Plateau (Livingstone and Lotter, 1998).

Table B1: Groundwater measurement sites and temperature data. Individual groundwater temperature measurement sites, listing elevation, name of the losing river, closest distance to the riverbank, depth of the groundwater table, current pumping rates, periods of available data, number of measurements per year, and periods of missing data exceeding 5 months for which the cubic regression model was used for interpolation purposes rather than a cubic spline.

Site	Elevation [m a.s.l.]	Rivers	Distance to river bank [m]	Depth of groundwater table [m]	Current pumping rate [m³/d]	Period of available data	Measurements per year	Cubic egression model used
Seewerben (*RhSe*)	381	Rhine	450	27.7	4300	1957-2007	6-12	-
Neuhausen (*RhNe*)	361	Rhine	170	0.7	3500	1970-2007	~40	Mar. 1981 - June 1981
Signau (*EmSi*)	683	Emme	220	2.0	25000	1978-2000	12	-
Kiesen (*AaKi*)	541	Aare	340	4.0	65000	1968-2000	12	Jan. 1979 - Dec. 1979
Linsental (*ToLi*)								
ToLi1	461	Toess	60	2.7	1000	1968-2007	4-12	-
ToLi2	457	Toess	60	2.6	1000	1966-2007	4-12	Nov. 1996 - July 1997
ToLi3	454	Toess	260	1.9	1000	1975-2007	4-12	-
ToLi4	464	Toess	160	3.4	1000	1972-2007	4-12	-
ToLi5	470	Toess	140	2.2	1000	1967-2007	4-12	Nov. 2001 - June 2002

Appendix C

Further publications

This chapter lists alphabetically further publications that emerged during the work on the PhD thesis or publications to which I contributed during the PhD thesis.

Brennwald, M. S., N. Vogel, S. Figura, M. K. Vollmer, R. Langenfelds, L. P. Steele, C. Maden, and R. Kipfer (2013), Concentrations and isotope ratios of helium and other noble gases in the Earth's atmosphere during 1978–2011. *Earth and Planetary Science Letters*, *366*, **27-37.**
M. S. Brennwald analyzed the ^{3}He/^{4}He ratio in several air samples from the Cape Grim Air Archive. I contributed to this work by calculating the trends in the data and their statistical significance.

Figura, S., D. M. Livingstone, R. Kipfer, and E. Hoehn (2013b), Klima und Grundwasser: Rückblicke und Vorhersagen von Temperatur und Sauerstoff mittels historischer Aufzeichnungen. *Aqua & Gas*, *7/8*, **28-33 (in German).**
Aqua & Gas (formerly gwa) is a non-peer-reviewed journal published by the Swiss Society of the Gas and Water Industry (SVGW) and is intended for a technical readership. The article summarizes the findings of Chapters 3-5.

Rössler, O., N. Addor, L. Bernhard, S. Figura, N. Köplin, D. M. Livingstone, B. Schädler, R. Seibert, R. Weingartner (in revision), Water, in: *CH2014 Impacts – Impacts of Climate Change on Switzerland*, **edited by C. Raible and K. Strassmann,** to be published by the Oeschger Center for Climate Change Research (OCCR), the Swiss Federal Office for the

Environment (FOEN), the Swiss Federal Office of Meteorology and Climatology (MeteoSwiss), and the Swiss National Center of Competence in Research on Climate (NCCR).

(http://www.oeschger.unibe.ch/research/projects/ch2014/index_en.html)

In this article, the major findings of the temperature projections presented in Chapter 3 of this work are summarized. The *CH2014 Impacts* report will publish the results of various impact studies that are based on the *CH2011* (2011) climate projections for Switzerland. It will be published in early 2014.

Scheiwiller, S., S. Figura, E. Hoehn, and P. Haldimann (2013), Klimaänderung und Karstquellenertrag: Zeitreihenanalyse des Ertrags der Pertusio-Quelle (TI) und Ursprung-Quelle (NW). Aqua & Gas, 7/8, 14-20 (in German).

In her M.S. thesis, S. Scheiwiller analyzed the discharge time-series of two alpine springs with regard to the potential impacts of climatic forcing and climate change. I supported S. Schweiwiller in the statistical analysis of the data and E. Hoehn in the writing of the article.

Vogel, N., Y. Scheidegger, M. S. Brennwald, D. Fleitmann, S. Figura, R. Wieler, and R. Kipfer (2013), Stalagmite water content as a proxy for drip water supply in tropical and subtropical areas. Climate of the Past, 9, 1-12, doi:10.5194/cp-9-1-2013.

N. Vogel analyzed the water content of three stalagmites and related it to the concentrations of $\delta^{18}O$ in the stalagmite's calcite. I contributed to this work by conducting the statistical analysis of the data. The analysis included application of the Rodionov regime-shift test (Rodionov, 2004), which was used to identify the simultaneous shift in stalagmite water content and calcite $\delta^{18}O$ concentrations, highlighting the relationship between these two variables.

References

Akaike, H. (1974), A new look at the statistical model identification, *IEEE T. Automat. Contr., 19*(6), 716–723.

Alheit, J., C. Möllmann, J. Dutz, G. Kornilovs, P. Loewe, V. Mohrholz, and N. Wasmund (2005), Synchronous ecological regime shifts in the central Baltic and the North Sea in the late 1980s, *ICES J. Mar. Sc., 62*(7), 1205-1215.

Anderson, M. P. (2005), Heat as a ground water tracer, *Ground Water, 43*(6), 951-968.

Anneville, O., S. Souissi, S. Gammeter, and D. Straile (2004), Seasonal and inter-annual scales of variability in phytoplankton assemblages: Comparison of phytoplankton dynamics in three peri-alpine lakes over a period of 28 years, *Freshw. Biol., 49*(1), 98-115.

Arbenz, P., J. Freiburghaus, and H. Peter (1925), *Expertenbericht zu Handen der Baudirektion des Kantons Bern betreffend Wasserableitung aus dem Emmental durch die Stadt Bern*, Rutishauser, Bern, Switzerland.

Aureli, A., and M. Taniguchi (2006), *Groundwater assessment under the pressures of humanity and climate changes – GRAPHIC*, in GRAPHIC Series, *1*, United Nations Educational, Scientific, and Cultural Organization, Paris, France.

Barry, D., and J. A. Hartigan (1993), A Bayesian analysis for change point problems, *J. Am. Stat. Ass., 88*(421), 309-319.

Baker J. M., and D. G. Baker (2002) Long-term ground heat flux and heat storage at a mid-latitude site, *Climatic Change, 54*, 295-303.

Bates, B. C., Z. W. Kundzewicz, S. Wu, and J. P. Palutikof (2008), Climate Change and Water. Technical Paper of the Intergovernmental Panel on Climate Change, IPCC Secr., Geneva, Switzerland.

Beyerle, U., W. Aeschbach-Hertig, M. Hofer, D. M. Imboden, H. Baur, and R. Kipfer (1999), Infiltration of river water to a shallow aquifer investigated with ^{3}H/^{3}He, noble gases and CFCs, *J. Hydrol.*, *220*, 169-185.

Blau, R. V., and F. Muchenberger (1997), Nutzungs-, Schutz- und Überwachungskonzept für die Grundwasserleiter des obersten Emmentals, zwischen Emmenmatt, Langnau und Eggiwil - Synthesebericht*, in Grundlagen für Schutz und Bewirtschaftung der Grundwasser des Kantons Bern,* Geotechnisches Institut AG, Bern, Switzerland.

Boulton, A. J., S. Findlay, P. Marmonier, E. H. Stanley, and H. M. Valett (1998), The functional significance of the hyporheic zone in streams and rivers, *Annu. Rev. Ecol. Syst.*, *29*, 59-81.

Bourg, C. M., and C. Bertin (1993), Biogeochemical processes during the infiltration of river water into an alluvial aquifer, *Environ. Sc. Technol.*, *27*, 661-666.

Box, G.E.P., and G. M. Jenkins (1970) *Time series analysis - Forecasting and control*, Holden Day, San Francisco, CA.

Box, G. E. P., and G. Tiao (1975). Intervention analysis with applications to economic and environmental problems, *J. Am. Stat. Assoc.*, *70*, 70-79.

Bouwer, H. (1978), *Groundwater hydrology*, McGraw-Hill, New York, NY.

Brennwald, M. S., N. Vogel, S. Figura, M. K. Vollmer, R. Langenfelds, L. P. Steele, C. Maden, and R. Kipfer (2013), Concentrations and isotope ratios of helium and other noble gases in the Earth's atmosphere during 1978–2011, *Earth Planet. Sc. Lett.*, *366*, 27-37.

Brunke, M., and T. Gonser (1997), The ecological significance of exchange processes between rivers and groundwater, *Freshwater Biol.*, *37*, 1-33.

BUWAL, Bundesamt für Umwelt, Wald und Landschaft, Bundesamt für Wasser und Geologie (BWG), and Bundesamt für Meteorologie und Klimatologie (Meteo Schweiz) (2004) *Auswirkungen des Hitzesommers 2003 auf die Gewässer*, in Schriftenreihe Umwelt, *369*, Bundesamt für Umwelt, Wald und Landschaft (ed.), Bern, Switzerland.

Bührer, H. (1975), Computerprogramm zur Bekanntgabe aktueller Seedaten, *Schweiz. Z. Hydrol.*, *37*, 332-346.

Caissie, D. (2006), The thermal regime of rivers: a review, *Freshwater Biol.*, *51*, 1389-1406.

Chapelle, F. H. (1993), *Groundwater microbiology and geochemistry*, J. Wiley, New York, NY.

CH2011 (2011), Swiss climate change scenarios CH2011, publ. by C2SM, MeteoSwiss, ETH, NCCR Climate, and OcCC, Zurich, Switzerland.

Cleveland, R. B., W. S. Cleveland, J. E. McRae, and I. Terpening (1990), STL: A seasonal-trend decomposition procedure based on Loess, *J. Official Stat.*, *6*, 3-73.

Connor, R., J.-M. Faurès, J. Kuylenstierna, J. Margat, P. Steduto, D. Vallée, and W. van der Hoek (2009), *Evolution of water use*, in The United Nations World Water Development Report 3: Water in a Changing World, pp. 96–126, World Water Assess. Programme, UNESCO, Paris.

Constantz, J., C. L. Thomas, and G. Zellweger (1994), Influence of diurnal variations in stream temperature on streamflow loss and groundwater recharge, *Water Resour. Res.*, *30*(12), 3253-3264.

Conversi, A., S. F. Umani, T. Peluso, J. C. Molinero, A. Santojanni, and M. Edwards (2010), The Mediterranean Sea regime shift at the end of the 1980s, and intriguing parallelisms with other European Basins, *PLOS ONE*, *5*(5), doi:10.1371/journal.pone.0010633.

Cryer, J. D., and K.-S. Chan (2008), Time series regression models, in *Time series analysis: with applications in R*, edited by J. D. Cryer and K.-S. Chan, pp. 249-276, Springer, New York, NY.

Diem, S., M. Rudolf von Rohr, J. G. Hering, H.-P. E. Kohler, M. Schirmer, U. von Gunten (2013), NOM degradation during river infiltration: Effects of the climate variables temperature and discharge, *Water Res.*, *47*(17), 6585-6595.

Dragoni, W., and B. S. Sukhija (2008), Climate change and groundwater: a short review, in: *Climate change and groundwater: a short review*, edited by W. Dragoni and B. S. Sukhija, pp. 1–12, Geological Society Special Publications, *288*, London, UK.

Eckert, P., R. Lamberts, and C. Wagner (2008) The impact of climate change on drinking water supply by riverbank filtration, *Wat. Sci. Technol. Wat. Supply*, *8*(3), 319-324.

Epting, J., and P. Huggenberger (2013), Unraveling the heat island effect observed in urban groundwater bodies – Definition of a potential natural state, *J. Hydrol*, *501*, 193-204.

Erdman, C., and J. W. Emerson (2007), bcp: An R package for performing a bayesian analysis of change point problems, *J. Stat. Softw.*, *23*(3), 1-13.

Eubank, R. L. (1988), *Spline smoothing and nonparametric regression*, Dekker, New York, NY.

Ferguson, G., A. D. Woodbury (2007), Urban heat island in the subsurface, *Geophys. Res. Lett.*, *34*, L23713, doi:10.1029/2007GL032324.

Figura, S. (2009), Response of Swiss groundwaters to climatic forcing and climate change. A preliminary analysis of the available historical instrumental records, Master thesis, ETH Zürich.

Figura, S., D. M. Livingstone, E. Hoehn, and R. Kipfer (2011), Regime shift in groundwater temperature triggered by the Arctic Oscillation, *Geophys. Res. Lett.*, *38*(23), L23401, DOI: 10.1029/2011GL049749.

Figura, S., D. M. Livingstone, and R. Kipfer (2013a), Competing controls on groundwater oxygen concentrations revealed in multidecadal time-series from riverbank filtration sites, *Water Resour. Res.*, *49*(11), 7411-7426.

Figura, S., D. M. Livingstone, R. Kipfer, and E. Hoehn (2013b), Klima und Grundwasser: Rückblicke und Vorhersagen von Temperatur und Sauerstoff mittels historischer Aufzeichnungen, *Aqua & Gas*, *7/8*, 28-33.

Findlay, S., (1995), Importance of Surface-Subsurface Exchange in Stream Ecosystems: The Hyporheic Zone, *Limnol. Oceanogr.*, *40*(1), 159-164.

FOEN (2012), Effects of climate change on water resources and watercourses. Synthesis report on the "Climate Change and Hydrology in Switzerland (CCHydro)" project, in *Umwelt-Wissen*, *1217*, Federal Office for the Environment (ed.), Bern, Switzerland.

FOPH (2003), Schweizerisches Lebensmittelbuch, Kapitel 27A Trinkwasser, Federal Office of Public Health, Bern, Switzerland.

Freeze, R. A., and J. A. Cherry (1979), *Groundwater*, Prentice-Hall, Inc., Englewood Cliffs, NJ.

Green, T. R., M. Taniguchi, H. Kooi, J. J. Gurdak, D. M. Allen, K. M. Hiscock, H. Treidel, and A. Aureli (2011), Beneath the surface of global change: Impacts of climate change on groundwater, *J. Hydrol.*, *405*(3-4), 532-560.

Gerten, D., and R. Adrian (2000), Climate-driven changes in spring plankton dynamics and the sensitivity of shallow polymictic lakes to the North Atlantic Oscillation, *Limnol. Oceanogr.*, *45*(5), 1058-1066.

Greig, S. M., D. A. Sear, and P. A. Carling (2007), A review of factors influencing the availability of dissolved oxygen to incubating salmonid embryos, *Hydrol. Process.*, *21*, 323-334.

Gunawardhana, L. N., and S. Kazama (2011), Climate change impacts on groundwater temperature change in the Sendai plain, Japan, *Hydrol. Process.*, *25*(17), 2665-2678.

Gunawardhana, L. N., and S. Kazama (2012), Statistical and numerical analysis of climate variability on aquifer water levels and groundwater temperatures: The impacts of climate change on aquifer thermal regimes, *Global Planet. Change*, 86-87, 66-78.

Gunawardhana, L. N., S. Kazama, and S. Kawagoe (2011), Impact of urbanization and climate change on aquifer thermal regimes, *Water Resour. Manag.*, *25*(13), 3247-3276.

Gurdak, J. J., R. T. Hanson, P. B. McMahon, B. W. Bruce, J. E. McCray, G. D. Thyne, and R. C. Reedy (2007), Climate variability controls on unsaturated water and chemical movement, High Plains Aquifer, USA, *Vadose Zone J.*, *6*(2), 533-547.

Gutsalo, R. K. (1971), Radiolysis of water as the source of free oxygen in the underground hydrosphere, *Geochem. Int.*, *8*, 897-903.

Hanson, R. T., M. D. Dettinger, and M. W. Newhouse (2006), Relations between climatic variability and hydrologic time series from four alluvial basins across the southwestern United States, *Hydrogeol. J.*, *14*(7), 1122-1146.

Hare, S. R., and N. J. Mantua (2000), Empirical evidence for North Pacific regime shifts in 1977 and 1989, *Progr. Oceanogr.*, *47*(2-4), 103-145.

Hari, R. E., D. M. Livingstone, R. Siber, P. Burkhardt-Holm, and H. Güttinger (2006), Consequences of climatic change for water temperature and brown trout populations in Alpine rivers and streams, *Glob. Change Biol.*, *12*(1), 10-26.

Helsel, D. R., and R. M. Hirsch (1992), *Statistical methods in water resources*, Elsevier, Amsterdam, Netherlands.

Hoehn, E., and A. Scholtis (2011), Exchange between a river and groundwater, assessed with hydrochemical data, *Hydrol. Earth Syst. Sci.*, *15*, 983-988.

Holman, I. P., M. Rivas-Casado, J. P. Bloomfield, and J. J. Gurdak (2011), Identifying non-stationary groundwater level response to North Atlantic ocean-atmosphere teleconnection patterns using wavelet coherence, *Hydrogeol. J.*, doi: 10.1007/*S1*0040-011-0755-9.

Hunt, H., J. Schubert, and C. Ray (2002), Operation and maintenance considerations, in *Riverbank filtration: improving source-water quality*, Water science and technology library, *43*, edited by C. Ray et al., pp. 61-70, Kluwer Academic Publishers, Dordrecht, Netherlands.

Jäckli, H. (1968), *Die Grundwasservorkommen des Kantons Aargau*, in Mitteilungen aus dem geologischen Institut der Eidg. Technischen Hochschule und der Universität Zürich, *101*, Zürich, Switzerland.

Kellerhals, P., C. Haefeli, and B. Tröhler (1981), Hydrogeologie Aaretal, zwischen Thun und Bern, in *Grundlagen für Schutz und Bewirtschaftung der Grundwasser des Kantons Bern,* Wasser- und Energiewirtschaftsamt des Kantons Bern, Bern, Switzerland.

Kempf, T., M. Freimoser, P. Haldimann, V. Longo, E. Müller, C. Schindler, G. Styger, and L. Wyssling (1986), Die Grundwasservorkommen im Kanton Zürich, in *Beiträge zur Geologie der Schweiz,* Geotechnische Serie*, 69*, Kümmerly & Frey, Bern, Switzerland.

Kohfahl, C., G. Massmann, and A. Pekdeger (2009), Sources of oxygen flux in groundwater during induced bank filtration at a site in Berlin, Germany, *Hydrogeol. J.*, *17*, 571-578.

Kundzewicz, Z. W., L. J. Mata, N. W. Arnell, P. Döll, P. Kabat, B. Jiménez, K. A. Miller, T. Oki, Z. Sen, and I. A. Shiklomanov (2007), Freshwater resources and their management, in *Climate Change 2007: Impacts, Adaptation and Vulnerability*. Contribution of Working Group II to the Fourth Assessment Report of the Intergovernmental Panel on Climate Change (M. L. Parry, O. F. Canziani, J. P. Palutikof, P. J. van der Linden and C. E. Hanson, eds.). Cambridge University Press, Cambridge, UK, pp. 173-210.

Kurylyk, B. L., C.P.-A. Bourque, and K.T.B. MacQuarrie (2013), Potential surface temperature and shallow groundwater temperature response to climate change: an example from a small forested catchment in east-central New Brunswick (Canada), *Hydrol. Earth Syst. Sci.*, *17*, 2701-2716.

Kurylyk, B. L., and K. T. B. MacQuarrie (2013), A new analytical solution for assessing climate change impacts on subsurface temperature, *Hydrol. Process.*, doi: 10.1002/hyp.9861.

Lee, J.-Y., and J.-S. Hahn (2005), Characterization of groundwater temperature obtained from the Korean national groundwater monitoring stations: Implications for heat pumps, *J. Hydrol.*, *329*, 514-526.

Livingstone, D. M., and A. F. Lotter (1998), The relationship between air and water temperatures in lakes of the Swiss Plateau: A case study with palaeolimnological implications, *J. Paleolimnol.*, *19*(2), 181-198.

Livingstone, D. M. (2003) Impact of secular climate change on the thermal structure of a large temperate Central European lake, *Clim. Change*, *57*(1-2), 205-225.

Malard, F., and F. Hervant (1999), Oxygen supply and the adaptations of animals in groundwater, *Freshwater Biol.*, *41*, 1-30.

Mattle, N., W. Kinzelbach, U. Beyerle, P. Huggenberger, and H. H. Loosli (2001), Exploring an aquifer system by integrating hydraulic, hydrogeologic and environmental tracer data in a three-dimensional hydrodynamic transport model, *J. Hydrol., 242,* 183-196.

Mauclaire, L., and J. Gibert (1998), Effects of pumping and floods on groundwater quality: a case study of the Grand Gravier well field (Rhône, France), *Hydrobiologia*, *389*, 141-151.

Mächler, L, M. S. Brennwald, and R. Kipfer (2013), Argon concentration time-series as a tool to study groundwater gas dynamics in the hyporheic zone, *Environ. Science and Technol.*, *47*(13), 7060-7066.

Meehl, G. A., T.F. Stocker, W. D. Collins, P. Friedlingstein, A. T. Gaye, J. M. Gregory, A. Kitoh, R. Knutti, J. M. Murphy, A. Noda, S. C. B. Raper, I. G. Watterson, A. J. Weaver, and Z.-C. Zhao (2007) Global Climate Projections, in *Climate Change 2007: The Physical Science Basis*. Contribution of Working Group I to the Fourth Assessment Report of the Intergovernmental Panel on Climate Change (Solomon, S., D. Qin, M. Manning, Z. Chen, M. Marquis, K. B. Averyt, M. Tignor, and H.L. Miller, eds.). Cambridge University Press, Cambridge, UK, and New York, NY, USA, pp. 748-846.

Metsaranta, J. M., and V. J. Lieffers (2010), Patterns of inter-annual variation in the size asymmetry of growth in Pinus banksiana, *Oecol.*, *163*(3), 737-745.

Moriasi D. N., J. G. Arnold, M.W. Van Liew, R. L. Bingner, R. D. Harmel, t. L. and Veith (2007), Model evaluation guidelines for systematic quantification of accuracy in watershed simulations, *T. ASABE*, 50, 885-900.

Nogaro, G., T. Datry, F. Mermillod-Blondin, S. Descloux, and B. Montuelle (2010), Influence of streambed sediment clogging on microbial processes in the hyporheic zone, *Freshwater Biol.*, *55*, 1288-1302.

Parsons, M. L. (1970), Groundwater thermal regime in a glacial complex, *Water Resour. Res.*, *6*(6), 1701–1720.

Pettitt, A. N. (1979), A non-parametric approach to the change-point problem, *Appl. Stat.*, *28*(2), 126-135.

Ray, C., J. Schubert, R. B. Linsky, and G. Melin (2002), Introduction, in *Riverbank filtration: improving source-water quality*, Water science and technology library, *43*, edited by C. Ray et al., pp. 1-18, Kluwer Academic Publishers, Dordrecht, Netherlands.

R Development Core Team (2011), R: A language and environment for statistical computing, *R Foundation for Statistical Computing*, Vienna, Austria.

Refsgaard, J. C., T. H. Christensen, and H. C. Ammentorp (1988), A proposal for an unsaturated zone oxygen transport and consumption model, in *Proceedings of the International Conference on Water Quality Modelling in the Inland Natural Environment*, edited by J. Stanbury, 199-210, The Fluid Engineering Centre, Bedford, UK.

Reid, P. C., M. De Fatima Borges, and E. Svendsen (2001), A regime shift in the North Sea circa 1988 linked to changes in the North Sea horse mackerel fishery, *Fish. Res.*, *50*(1-2), 163-171.

Rohns H.-P., C. Forner, P. Eckert and R. Irmscher (2006), Efficiency of riverbank filtration considering the removal of pathogenic microorganisms of the River Rhine, in *Recent Progress in Slow Sand and Alternative Biofiltration Processes*, edited by R. Gimbel et al., pp. 539-546, IWA Publishing, London, UK.

Rodionov, S. N. (2004), A sequential algorithm for testing climate regime shifts, *Geophys. Res. Lett.*, *31*(9), L09204, doi: 194 10.1029/2004GL019448.

Rodionov, S. N., and J. E. Overland (2005), Application of a sequential regime shift detection method to the Bering Sea ecosystem, *ICES J. Mar. Sc.*, *62*, doi:10.1016/j.icesjms.2005.01.013.

Schartner, C., and M. Kralik (2011), Trends der Grundwassertemperatur: Untersuchungen der Daten der Überwachung des Gewässerzustandes in Österreich, *Report 0328*, Umweltbundesamt, Vienna, Austria.

Schälchli, U. (1992), The clogging of coarse gravel river beds by fine sediment, *Hydrobiolgia*, *235/236*, 189-197.

Schär, C., P. L. Vidale, D. Lüthi, C. Frei, C. Häberli, M. A. Liniger, and C. Appenzeller (2004), The role of increasing temperature variability in European summer heatwaves, *Nature, 427*, 332–336.

Scheiwiller, S., S. Figura, E. Hoehn, and P. Haldimann (2013), Klimaänderung und Karstquellenertrag: Zeitreihenanalyse des Ertrags der Pertusio-Quelle (TI) und Ursprung-Quelle (NW). *Aqua & Gas*, *7/8*, 14-20.

Schijven, J. V., and A. M. de Roda Husman (2005), Effect of climate changes on waterborne disease in The Netherlands, *Water Sci. Technol.*, *51*(5), 79-87.

Schürch, M. (2011), Auswirkungen des Klimawandels auf das Grundwasser. Erster Bericht der Arbeitsgruppe „Klima und Grundwasser", *gwa*, *3*, 177-182.

Sen, P. K. (1968), Estimates of the regression coefficient based on Kendall's τ, *J. Am. Stat. Assoc.*, *63*, 1379-1389.

Shin, J., K.-H. Kim, K.-K. Lee, and H.-S. Kim (2010), Assessing temperature of riverbank filtrate water for geothermal energy utilization, *Energy*, *35*, 2430-2439.

Sprenger, C., G. Lorenzen, J. Hülshoff, G. Grützmacher, M. Ronghang, and A. Pekdeger (2011), Vulnerability of bank filtration systems to climate change, *Sci. Tot. Environ.*, *409*(4), 655-663.

Stahel, W. (1989), Rheinsohleuntersuchungen im Kraftwerkstau Rheinau, in *Kraftwerk Rheinau, Grundwasserverhältnisse. Bericht der Grundwasserkommission über die Untersuchungen im Zusammenhang mit der Erstellung des Kraftwerks*, edited by P. Giger et al. (1990), Tech. Rep., Zürich, Switzerland.

SVGW (2008), Infoblatt TWI 12. Schweizerischer Verein des Gas- und Wasserfachs, Zürich, Switzerland.

Taniguchi, M., J. Shimada, T. Tanaka, I. Kayane, Y. Sakura, Y. Shimano, S. Dapaah-Siakwan, and S. Kawashima (1999), Disturbances of temperature-depth profiles due to surface climate change and subsurface water flow: 1. An effect of linear increase in surface temperature caused by global warming and urbanization in the Tokyo metropolitan area, Japan, *Water Resour. Res. 35*(5), 1507–1517.

Taniguchi, M., T. Uemura, and K. Jago-on (2007), Combined effects of urbanization and global warming on subsurface temperature in four Asian cities, *Vadose Zone J.*, *6*(3), 591-596.

Taylor, C. A., and H. G. Stefan (2009), Shallow groundwater temperature response to climate change and urbanization, *J. Hydrol.*, *375*(3-4), 601-612.

Taylor, R. G., B. Scanlon, P. Döll, M. Rodell, R. van Beek, Y. Wada, L. Longuevergnem M. Leblanc, J. S. Famiglietti, M. Edmunds, L. Konikow, T. R. Green, J. Chen, M. Taniguchi, M. F. P. Bierkens, A. MacDonald, Y. Fan, R. M. Maxwell, Y. Yechieli, J. J. Gurdak, D. M. Allen, M. Shamsudduha, K. Hiscock, P. J.-F. Yeh, I. Holman, and H. Treidel (2013), Ground water and climate change, *Nature Clim. Change*, *3*(4), 322-329.

Temnerud, J., and G. A. Weyhenmeyer (2008), Abrupt changes in air temperature and precipitation: Do they matter for water chemistry?, *Glob. Biogeochem. Cycl.*, *22*(2), doi:10.1029/GB003023.

Theil, H. (1950), A rank-invariant method of linear and polynomial regression analysis I-III, *Nederl. Akad. Wetensch. Proc., 53*, 386-1412.

Tian, Y., H. Kidokoro, T. Watanabe, and N. Iguchi (2008), The late 1980s regime shift in the ecosystem of Tsushima warm current in the Japan/East Sea: Evidence from historical data and possible mechanisms, *Progr. Oceanogr., 77*(2-3), 127-145.

Tripet, J.-P. (2005), Grundwasser, in *Hydrologie der Schweiz - Ausgewählte Aspekte und Resultate*, edited by M. Spreafico, and R. Weingartner, pp. 79-136, Berichte des BWG, Serie Wasser, *7*, Bern, Switzerland.

Trüeb, E. U. (1971), Betrachtungen über die Veränderung des Sauerstoffgehalts im Grundwasser als Folge von Flussstau und Temperaturerhöhung des Flusswassers, *gwf - Wasser/Abwasser*, *9*, 433-436.

Vogel, N., Y. Scheidegger, M. S. Brennwald, D. Fleitmann, S. Figura, R. Wieler, and R. Kipfer (2013), Stalagmite water content as a proxy for drip water supply in tropical and subtropical areas, *Clim. Past*, *9*, 1-12, doi:10.5194/cp-9-1-2013.

von Gunten, H. R., G. Karametaxas, U. Krähenbühl, M. Kuslys, R. Giovanoli, E. Hoehn, and R. Keil (1991), Seasonal biogeochemical cycles in riverborne groundwater, *Geochem. Cosmochem. Acta*, *55*(12), 3597-3609.

Wagner, U., P. Huggenberger, W. Kanz, D. Schaub, M. Thater, and J. Reich (2001), *INTERREG II: Erkundung der Grundwasserleiter und Böden im Hochrheintal zwischen Schaffhausen und Basel*, Waldshut, Germany.

Webb B. W. (1996), Trends in stream and river temperature, *Hydrol. Process.*, *10*, 205-226.

White, D. S. (1993), Perspectives on defining and delineating hyporheic zones, *J. N. Am. Benthol. Soc.*, *12*, 61-69.

Woessner, W. W. (2000), Stream and fluvial plain ground water interactions: rescaling hydrogeological thought, *Ground Water*, *38*(3), 423-429.

Curriculum vitae
Simon Figura
born 26 September 1984 in Schlieren/ZH
citizen of Switzerland and Italy

Education

PhD student in Environmental Science (2/2010-11/2013)
Eawag – Swiss Federal Institute of Aquatic Science and Technology, and
ETH Zurich – Federal Institute of Technology
Thesis conducted in the framework of the National Research Programme 61
on Sustainable Water Management.

MSc in Statistics, specialisation: Applied statistics (9/2007-10/2009)
ETH Zurich, Department of Mathematics
Thesis title: Response of Swiss groundwaters to climatic forcing and climate
change - a preliminary analysis of the available historical instrumental records.
Thesis advisor: Prof. Dr. Rolf Kipfer

BSc in Environmental Science, specialisation: Aquatic Systems (9/2004-8/2007)
ETH Zurich, Department of Environmental Systems Science
Two Theses, in natural and social science
Natural science thesis: Comparison of growth response of *Silene dioica*
and *S. latifolia* to two different temperature regimes. (in german)
Thesis advisor: Prof. Dr. Sophie Karrenberg
Social science thesis: IMF and democratization. (in german)
Thesis advisor: Prof. Dr. Axel Dreher

High School, *Matura* (8/1997-9/2003)
Gymnasium Hohe Promenade, Zurich

Primary school (8/1991-8/1997)
Dietikon

Professional Experience

Corris AG, *Fundraising agency for NGOs, Zurich*
(2/2004-12/2009, part-time during undergraduate studies)
Call center supervisor and assistant to the head of the call center.
Operational management: supervision and training of 10-20 call agents;
internal analyses for the optimisation of processes; analyses for customers and
monthly billing; controlling of campaigns; controlling of wages and bonuses of
call agents.